



**ΕΘΝΙΚΟ ΚΑΙ ΚΑΠΟΔΙΣΤΡΙΑΚΟ ΠΑΝΕΠΙΣΤΗΜΙΟ
ΑΘΗΝΩΝ**

**ΤΜΗΜΑ ΒΙΟΛΟΓΙΑΣ
ΤΟΜΕΑΣ ΒΟΤΑΝΙΚΗΣ**

**Μεταπτυχιακό Δίπλωμα Ειδίκευσης
“Μικροβιακή Βιοτεχνολογία”**

**«Διερεύνηση του ρόλου των σιδηροφορέων στη βιοχειραγώγηση
φυτικών συστημάτων»**

Συνεπιβλέποντες Καθηγητές

Γιώργος Διαλλινάς, Καθηγητής

Νικόλαος Σκανδάλης, Αναπληρωτής Καθηγητής

ΜΑΡΙΛΕΝΑ ΚΟΥΚΟΥΝΙΑ

ΑΜ: 248006

ΑΘΗΝΑ 2017



**NATIONAL AND KAPODISTRIAN UNIVERSITY OF
ATHENS**

FACULTY OF BIOLOGY

DEPARTMENT OF BOTANY

Master Degree

“Microbial Biotechnology”

**«Investigation of the role of siderophores in biomanipulation of
plant systems»**

Co-supervisors

George Diallinas, Professor

Nicholas Skandalis, Association Professor

MARILENA KOUKOUNIA

RN: 248006

AΘHNA 2017



**ΕΘΝΙΚΟ ΚΑΙ ΚΑΠΟΔΙΣΤΡΙΑΚΟ ΠΑΝΕΠΙΣΤΗΜΙΟ
ΑΘΗΝΩΝ
ΤΜΗΜΑ ΒΙΟΛΟΓΙΑΣ
ΤΟΜΕΑΣ ΒΟΤΑΝΙΚΗΣ**

**Μεταπτυχιακό Δίπλωμα Ειδίκευσης
“Μικροβιακή Βιοτεχνολογία”**

**«Διερεύνηση του ρόλου των σιδηροφορέων στη βιοχειραγώγηση
φυτικών συστημάτων»**

Συνεπιβλέποντες Καθηγητές

Γιώργος Διαλλινάς, Καθηγητής

Νικόλαος Σκανδάλης, Αναπληρωτής Καθηγητής

ΜΑΡΙΛΕΝΑ ΚΟΥΚΟΥΝΙΑ

ΑΜ: 248006

ΑΘΗΝΑ 2017



**NATIONAL AND KAPODISTRIAN UNIVERSITY OF
ATHENS**

**FACULTY OF BIOLOGY
DEPARTMENT OF BOTANY**

**Master Degree
“Microbial Biotechnology”**

**«Investigation of the role of siderophores in biomanipulation of
plant systems»**

Co-supervisors

George Diallinas, Professor

Nicholas Skandalis, Association Professor

MARILENA KOUKOUNIA

RN: 248006

ΑΘΗΝΑ 2017

Η παρούσα Διπλωματική Εργασία δεν θα μπορούσε να πραγματοποιηθεί χωρίς την αμέριστη βοήθεια του Δρ. Νικόλα Σκανδάλη που ήταν πάντα δίπλα μου δίνοντάς μου καθημερινά τροφή για σκέψη, μια διορατική ματιά στην εξήγηση των αποτελεσμάτων και δείχνοντάς μου εμπιστοσύνη ότι θα τα καταφέρω. Στον Δρ. Γιάννη Θεολογίδη που αφιέρωσε χρόνο για την πραγματοποίηση της στατιστικής ανάλυσης των αποτελεσμάτων, στην βοήθεια που μου προσέφερε τις στιγμές που είχα φτάσει σε αδιέξοδο πειραματικά καθώς και στην καθημερινή ψυχαγωγία και εμπύχωση. Στην κα. Αναστασία Δημοπούλου που ήταν καθημερινά συνοδοιπόρος στην πειραματική διαδικασία και δίπλα μου με αμέριστη υπομονή δείχνοντάς μου πώς είναι να σε βοηθούν ανιδιοτελώς. Στα μέλη του εργαστηρίου Βακτηριολογίας του Μπενάκειου Φυτοπαθολογικού Ινστιτούτου που με φιλοξενήσαν όλο αυτό το χρονικό διάστημα και μου προσέφεραν υλικοτεχνική υποστήριξη και συγκεκριμένα την κα. Χολέβα, την κα. Καράφλα, τον κ. Γλυνό, τον κ. Δρακούλη, το Νάσο και φυσικά την Ελευθερία Σιδερέα που ήταν πάντα η χαρούμενη και χιουμοριστική νότα της ημέρας. Τέλος όσους με ανέχτηκαν με υπομονή αυτό το διάστημα καθώς και την εξεταστική επιτροπή για το χρόνο που αφιέρωσαν στη δίορθωση της εργασίας αυτής.

Εξεταστική επιτροπή:

1. Διαλλινάς Γεώργιος, Καθηγητής (Επιβλέπων)
2. Αμαλία Καραγκούνη-Κύρτσου, Καθηγήτρια
3. Χατζηνικολάου Δημήτρης, Αναπληρωτής Καθηγητής
4. Νικόλαος Σκανδάλης, Αναπληρωτής Καθηγητής (Συνεπιβλέπων)

Abstract

The effect of the commercial strain *Bacillus amyloliquefaciens* subsp. *plantarum* MBI600 and its metabolites has been evaluated in iron deficiency conditions, *in vitro* and *in planta*, against the plant pathogens *Pseudomonas syringae* pv *tomato* and *Pseudomonas syringae* pv *tabaci*. *In vitro* assessment was based on formation of inhibition zones, inhibition of growth in broth media and growth kinetic analysis. Inhibition zones formed in agar plates were negatively correlated to iron concentration. Growth of pathogens in the presence of cell free culture filtrate (CFCF) of MBI600 cultures, grown in the presence of different iron concentrations, was observed to be reduced in a manner analogous to iron concentration. *In planta* assessment was held in tomato and *N. benthamiana* plants, following artificial inoculation with the pathogens and treatment with CFCF of MBI600 cultures grown in the presence of different iron concentrations. In the case of low iron concentration treatments, there is a statistically significant reduction in the total population of the pathogens in the leaf compared to the control treatment. Finally, iron starvation and siderophore production by MBI600 led to an antibiotic effect against the non-sensitive, under optimum iron diet conditions, *Pseudomonas* species. Finally, iron starvation upregulated lipopeptide synthase transcription (and thus possibly lipopeptide production) and enhanced competence traits such as swarming and chemotaxis.

Keywords: Siderophores⁽¹⁾, *Bacillus amyloliquefaciens*⁽²⁾, *Pseudomonas*⁽³⁾, plant pathogenic bacteria⁽⁴⁾, iron starvation⁽⁵⁾.

Περίληψη

Η επίδραση του εμπορικού στελέχους *Bacillus amyloliquefaciens* subsp. *plantarum* MBI600 και των μεταβολιτών που παράγει, αξιολογήθηκε *in vitro* και *in planta* σε συνθήκες τροφопενίας σιδήρου, έναντι των φυτοπαθογόνων βακτηρίων *Pseudomonas syringae* pv *tomato* και *Pseudomonas syringae* pv *tabaci*. Η *in vitro* αξιολόγηση βασίστηκε στον σχηματισμό ζώνης αναστολής, στην αναστολή της ανάπτυξης των παθογόνων σε υγρές καλλιέργειες καθώς και στην κινητική τους ανάλυση. Οι ζώνες αναστολής που σχηματίστηκαν παρουσίαζαν αρνητική συσχέτιση με τη συγκέντρωση σιδήρου. Παρουσία απαλλαγμένου από κύτταρα υπερκείμενου καλλιέργειας (CFCF) βακίλλου που είχε αναπτυχθεί σε χαμηλές συγκεντρώσεις σιδήρου εμφανίστηκε μείωση της ανάπτυξης των παθογόνων. Η *in planta* αξιολόγηση της δραστηριότητας του CFCF έναντι φυτοπαθογόνων βακτηρίων πραγματοποιήθηκε σε φυτά τομάτας και *Nicotiana benthamiana* με ταυτόχρονο ψεκάσμο με την ανασταλτική ουσία και τεχνητή μόλυνση. Μία στατιστικώς σημαντική μείωση του εσωτερικού πληθυσμού των παθογόνων στο φύλλο, εμφανίζεται από την πρώτη κιόλας ημέρα μετά τη μόλυνση, στην περίπτωση των χειρισμών CFCF από καλλιέργειες MBI600 που μεγάλωσαν παρουσία χαμηλών συγκεντρώσεων σιδήρου σε σύγκριση με τη δοκιμή ελέγχου. Εν κατακλείδι, σε συνθήκες έλλειψης σιδήρου και παραγωγής σιδηροφορέων το στέλεχος MBI600 παρουσιάζει αντιβιοτική δράση έναντι ειδών του γένους *Pseudomonas* τα οποία δεν είναι ευαίσθητα σε συνθήκες που δεν εξαρτώνται από το σίδηρο, επίσης εμφανίζει αυξημένη έκφραση συνθετασών των λιποπεπτιδίων και κατά συνέπεια πιθανώς και αυξημένη παραγωγή αυτών. Τέλος αυξάνει την έκφραση γονιδίων που σχετίζονται με την ανταγωνιστικότητά του στελέχους στο περιβάλλον του ενδαιτήματος, όπως για παράδειγμα την ομαδική κινητοποίηση (swarming) και τις κινήσεις χημειοτακτισμού.

Λέξεις κλειδιά: Σιδηροφορείς⁽¹⁾, *Bacillus amyloliquefaciens*⁽²⁾, *Pseudomonas*⁽³⁾, φυτοπαθογόνα βακτήρια⁽⁴⁾, συνθήκες έλλειψης σιδήρου⁽⁵⁾.

Table of Contents

Abstract	1
Περίληψη	2
INTRODUCTION.....	6
1.1 Role and properties of iron	6
1.2 Iron acquisition in bacteria.....	6
1.3 Siderophores	7
1.3.1. Bacterial siderophore transport systems	7
1.3.2 <i>Pseudomonas</i> spp. siderophores	9
1.3.3 <i>Bacillus</i> spp. siderophores	11
1.3.4 Plant siderophores	12
1.4 Microbial Biological Control Agents (BCA).....	13
1.5 Mode of action of BCA.....	13
1.6 <i>Bacillus amyloliquefaciens</i> as a BCA	14
1.6.1 <i>B. amyloliquefaciens</i> secondary metabolites with biocontrol function	15
1.6.2 Chemotaxis and swarming motility	16
1.6.3 Biofilm formation and root colonization	17
1.6.4 Induced Systemic Resistance (ISR)	17
1.7 Role of siderophores in biocontrol.....	18
1.8 Purpose of this study.....	19
MATERIALS AND METHODS	20
2.1 Bacterial strains and culture conditions	20
2.2 DNA extraction from <i>B. amyloliquefaciens</i> cells.	22
2.3 Polymerase Chain Reaction – PCR.....	23
2.4 Agarose gel electrophoresis	25
2.5 Gel Extraction	27
2.6 Transformation of DH5α <i>E. coli</i> competent cells.....	27

2.6.1 Preparation of DH5 α <i>E. coli</i> electro-competent cells.	27
2.6.2 Transformation of DH5 α <i>E. coli</i> electrocompetent cells.	28
2.6.3 Selection of transformed colonies.....	28
2.7 Plasmid DNA isolation	28
2.8 Digestions using restriction enzymes.....	29
2.9 Ligation Reaction.....	31
2.10 Plasmid vectors used in this study	32
2.11 Cloning method.....	34
2.12 Transformation of <i>B. amyloliquefaciens</i> cells	37
2.13 Chrome azurol S (CAS) assay	37
2.14 Efficacy evaluation of siderophores <i>in vitro</i>	39
2.14.1 Disc diffusion assays.....	39
2.14.2 Broth microdilution method.....	39
2.15 Efficacy evaluation of siderophores <i>in planta</i>	42
2.15.1 Plant material and growth conditions	42
2.15.2 Design and layout of preliminary experiments	42
2.15.3 Design and lay out of full scale experiments	43
2.16 Total RNA extraction from <i>B. amyloliquefaciens</i> cells	44
2.17 Reverse transcription	45
2.18 Quantitative Real-Time PCR	46
2.19 Data analysis (by Dr. Ioannis Theologidis)	48
RESULTS	50
3.1 Siderophore production of <i>B. amyloliquefaciens</i>	50
3.2 Knock-out of the siderophore synthesis operon.....	51
3.2.1 Cloning of the erythromycin resistance gene into pCR $\text{\textcircled{R}}$ 2.1-TOPO $\text{\textcircled{R}}$	51
3.2.2 Cloning of <i>dhbC</i> and <i>dhbF</i> recombination sites into plasmid pCR $\text{\textcircled{R}}$ 2.1-TOPO $\text{\textcircled{R}}$ - <i>Erm^r</i>	53

3.2.3 Sequencing of <i>dhbC-Erm^r-dhbF</i> construct	60
3.2.4 Transformation of <i>B. amyloliquefaciens</i> in order to achieve homologous recombination in siderophore synthesis operon.....	62
3.3 Efficacy evaluation of siderophores <i>in vitro</i>	64
3.3.1 <i>B. amyloliquefaciens</i> was found to inhibit the growth of <i>Pseudomonas sp.</i> in agar plates under iron-limited conditions	64
3.3.2 CFCF from <i>B. amyloliquefaciens</i> grown under iron-limited conditions was found to affect <i>Pseudomonas sp</i> growth.....	66
3.4 Efficacy evaluation of siderophores <i>in planta</i>	71
3.4.1 Preliminary experiment in <i>Nicotiana benthamiana</i> shows that CFCF from <i>B. amyloliquefaciens</i> grown under iron limited conditions is more effective against wildfire disease	71
3.4.2 Full scale efficacy evaluation of MBI600 siderophores antibacterial activity in <i>Nicotiana benthamiana</i> plants	74
3.4.3 Full scale efficacy evaluation of MBI600 siderophores antibacterial activity in tomato plants.....	76
3.5 Determination of <i>B. amyloliquefaciens</i> gene expression in different iron concentrations	78
DISCUSSION	89
Future prospects.....	93
BIBLIOGRAPHY	95

INTRODUCTION

1.1 Role and properties of iron

Iron is an important micronutrient for all living organisms. It ranks as fourth most abundant element in the earth. Iron is abundant in the environment, but under normal conditions is not readily available to plants and microorganisms (Desai and Archana 2011). Iron is a first-row transition metal. Under physiological conditions, it mainly exists in one of two readily interconvertible redox states: the reduced Fe^{2+} ferrous form and the oxidized Fe^{3+} ferric form. It can also adopt different spin states (high or low) in both the ferric and ferrous form, depending on its ligand environment (Andrews *et al.* 2003). These properties make iron extremely multilateral when it is incorporate into proteins as an electron carrier or as a catalytic center. Microorganisms growing under aerobic conditions need iron for a numerous biological processes which include photosynthesis, respiration, the tricarboxylic acid cycle, oxygen transport, gene regulation, DNA biosynthesis for formation of heme, and for other essential purposes (Das *et al.* 2007, Krewulak and Vogel 2008).

1.2 Iron acquisition in bacteria

Bacteria require 10^{-6} M intracellular iron, indicating that efficient iron acquisition systems are essential. Some microorganisms have transport systems that import Fe (III) by oxidizing Fe (II), such as YwbLMN for *Bacillus subtilis* and Ftr1p/Fet3p for *Saccharomyces cerevisiae*, but many microorganisms cannot uptake Fe (III) without a chelator (Fukushima *et al.* 2014).

Iron is soluble in ferrous form and can be easily assimilated by microbial cell. However, at neutral to alkaline pH and under aerobic conditions, ferrous iron is oxidized to ferric iron, an insoluble hydroxide (Neilands 1995). A sufficient supply of iron is essential for survival. To cope with this low iron bioavailability, bacteria have adapted to aerobic environments by developing several techniques for absorbing iron in almost any condition.

1.3 Siderophores

Under certain conditions, the level of physiologically available concentration of iron in terrestrial as well as in aquatic environments can drop far below 1 mM, thus becoming growth-limiting for bacteria (May *et al.* 2001). To survive, many bacteria elaborate and secrete high-affinity extracellular ferric chelators, called siderophores (a Greek word for iron carriers), to solubilize iron prior to transport. This function also plays a crucial role in successful infection of pathogens in their host (Quadri 2000, May *et al.* 2001). These compounds are small molecules (often >1000 Da, although some are bigger). They are generally synthesized and secreted by bacteria (fungi and monocotyledonous plants also produce siderophores) through short, well-defined metabolic pathways in response to iron restriction (Perez-Miranda *et al.* 2007). Currently, there are almost 500 compounds that have been identified as siderophores.

Siderophores classified according to the functional groups they use as iron ligands. They usually form hexadentate or octahedral complexes with ferric iron and typically employ hydroxamates, α -hydroxycarboxylates and catechols as extremely effective Fe^{3+} ligands and thus can be classified as either hydroxycarboxylate, catecholate, or hydroxamate type siderophores (Andrews *et al.* 2003, Raymond and Dertz 2004, Krewulak and Vogel 2008) (Figure 1.1).

1.3.1. Bacterial siderophore transport systems

Fe-siderophore transport systems in Gram-positive and Gram-negative bacteria differ (Figure 1.2). Gram-negative bacteria use outer-membrane transporters (OMTs), such as *Escherichia coli* FecA (ferric citrate transporter) (Yue *et al.* 2003) and FhuA (ferrichrome transporter) (Eisenhauer *et al.* 2005), to recognize and bind extracellular Fe-siderophores. Binding a Fe-siderophore signals the TonB-ExbBD system to move the substrate across the outer membrane from the OMT to a periplasmic siderophore-

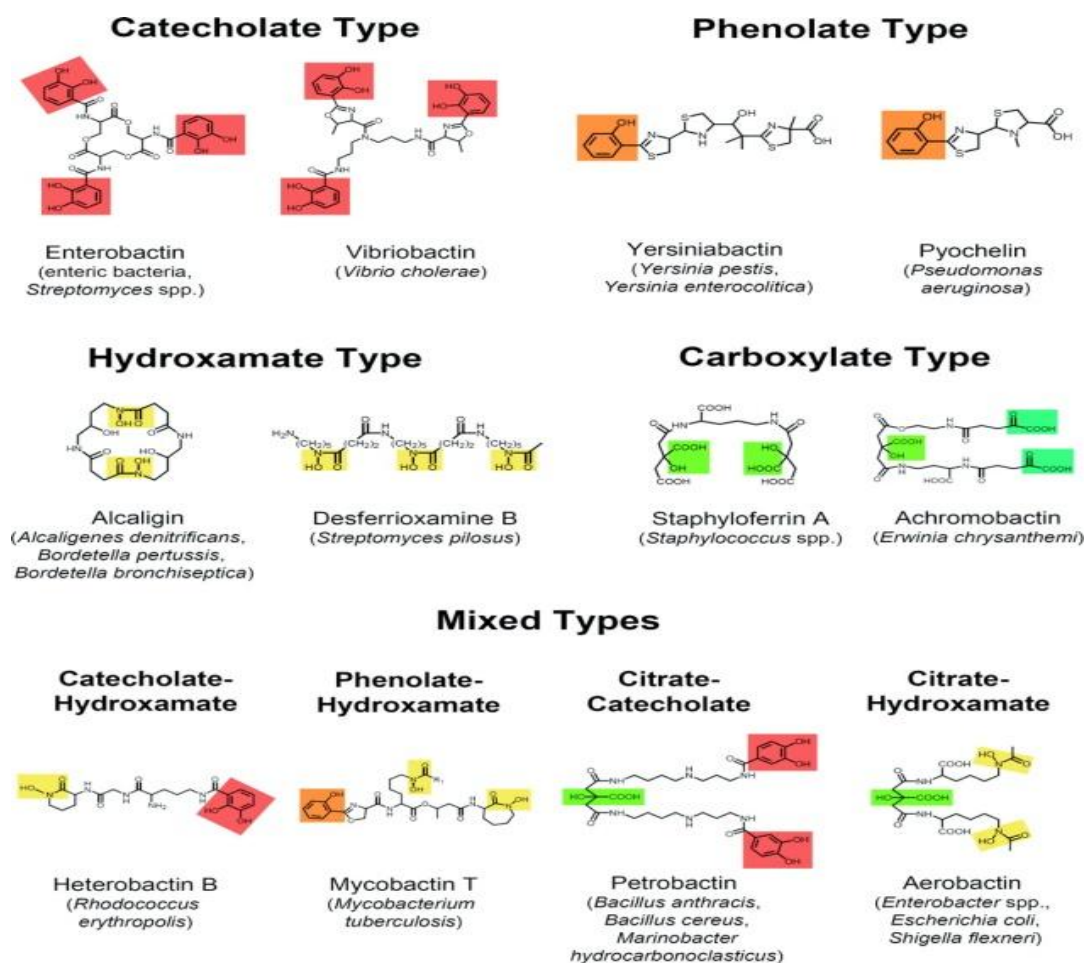


Figure 1.1: Representative examples of different siderophores and their natural producers. Moieties involved in iron coordination are highlighted as follows: catecholates are in red, phenolates are in orange, hydroxamates are in pale yellow, α -hydroxy-carboxylates are in light green, and α -keto-carboxylates are in blue-green. Adopted by (Miethke and Marahiel 2007).

binding protein (periplasmic SBP) (Koebnik 2005). The SBP then delivers the Fe-siderophore to the appropriate siderophore-permease(s)-ATPase system to be transported through the inner membrane to the cytoplasm (Braun and Braun 2002). Gram-positive bacteria do not have siderophore-binding OMTs. Instead, lipoprotein SBPs anchored to the cell membrane bind extracellular Fe-siderophores to be imported by a siderophore-permease(s)-ATPase system (Ollinger *et al.* 2006). The lipoprotein SBP-permease(s)-ATPase system in Gram-positive bacteria is similar to the periplasmic SBP-permease(s)-ATPase system in Gram-negative bacteria.

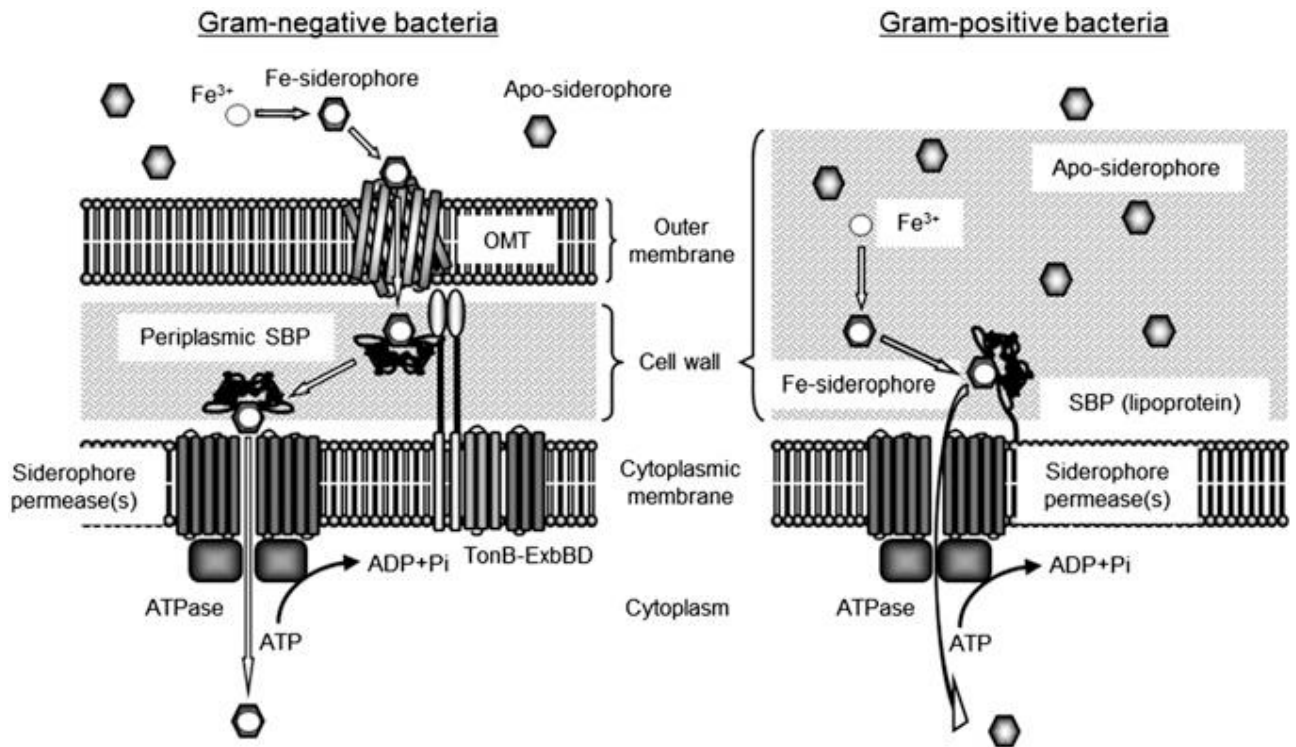


Figure 1.2: Siderophore uptake machineries in Gram-negative bacteria (Left) and Gram-positive bacteria (Right) (Fukushima *et al.* 2013).

1.3.2 *Pseudomonas* spp. siderophores

Pseudomonas spp. include gram-negative bacteria that typically inhabit all kind of environments like terrestrial, air and aquatic. Many of them are known as important human, animal, and plant pathogens, as well as biocontrol agents.

Pseudomonads produce over 50 different siderophores called pyoverdines in addition to a wide variety of other siderophore types. The list of well-characterized siderophores include compounds like pyochelin, pseudobactins and pyoverdines (Raaska *et al.* 1993). *Pseudomonads* were grouped into 28 *taxa* including 15 well-defined species depending on the different siderophore types (Ahmed and Holmstrom 2014). *P. aeruginosa* is the most well-studied species and synthesizes two known siderophores, pyoverdine and pyochelin. Fluorescent *Pseudomonas* also synthesizes pyoverdines. *Pseudomonas* species are known for their ability to utilize a very wide range of iron carriers for iron acquisition, with their genomes encoding a large number of outer membrane siderophore receptors (Llamas *et al.* 2014).

Chapter 1: Introduction

The mammalian pathogen *P. aeruginosa* can utilize a variety of xenosiderophores, siderophores that are used by an organism other than the one that produces them. This specific species is able to use heterologous pyoverdines, but also siderophores of other bacterial genera and fungi. The use of multiple siderophores by *P. aeruginosa* is consistent with the presence of multiple receptor homologues in its genome sequence. Use of xenosiderophores appears, in many cases, to require induction of outer membrane receptors that specifically recognize xenosiderophores. Accordingly, the use of heterologous siderophores is common in *P. aeruginosa* because of the presence of an array of inducible receptors that respond specifically to these heterologous siderophores (Crosa *et al.* 2004).

In specific *P. aeruginosa* strains have generally more than 30 genes encoding TonB-dependent receptors (TBDRs), the majority of them involved in the uptake of ferrisiderophores (Bodilis *et al.* 2009). The different TBDRs can be classified into two categories, the simple TBDR and the TonB-dependent transducers (TBDT) (Hartney *et al.* 2011). The TBDT, of which the ferripyoverdine receptor FpvA is an example, can sense the presence of the cognate ferrisiderophore by interacting with a membrane protein which acts as an anti-sigma factor (Hartney *et al.* 2011). Upon recognition of the ferrisiderophore by the cognate receptor, the anti-sigma factor undergoes a proteolytic degradation liberating the extracytoplasmic sigma factor (ECF σ), which associates with the RNA polymerase to transcribe the receptor gene, causing an auto-induction reaction (Cornelis 2010) (Hartney *et al.* 2011) (Mettrick and Lamont 2009). The majority of *P. aeruginosa* strains (98%) have a second receptor for type I ferripyoverdine, FpvB, which means that almost all strains have the capacity to use this pyoverdine as source of iron (Ghysels *et al.* 2004, Bodilis *et al.* 2009). *P. aeruginosa* is also able to utilize the *E. coli* siderophore enterobactin via two different receptors, PfeA and PirA since only a double *pfeA pirA* mutant is unable to take up ferrienterobactin (Dean and Poole 1993, Ghysels *et al.* 2005, Cornelis and Bodilis 2009). Other characterized receptors are FoxB and FiuA for the uptake of ferrioxamine and ferrichrome (Llamas *et al.* 2006, Hannauer *et al.* 2010), FemA for the utilization of mycobactin and carboxymycobactin (Llamas *et al.* 2008), FecA for Fe-citrate uptake (Marshall *et al.* 2009), ChtA for rhizobactin, aerobactin, and schizokinen (Cuiv *et al.* 2006), and FvbA for the uptake of vibriobactin (Elias *et al.* 2011). However, the importance of these xenosiderophore uptake systems in

infections has not, to the best of our knowledge, been established. They could however be of importance in case of polymicrobial infections where *P. aeruginosa* could be at advantage because of its capacity to steal siderophores produced by other microorganisms (siderophore piracy) (Traxler *et al.* 2012) while depriving the competitors from iron because they would be unable to recognize the complex pyoverdine siderophore.

1.3.3 *Bacillus* spp. siderophores

When confronted with iron limitation, *B. subtilis* produces bacillibactin 2,3-dihydroxybenzoate (DHB)-glycine, an 882-Da trilactone siderophore. The 12-kb *dhbACEBF* operon required for bacillibactin synthesis is located within a single operon. Figure 1.3 illustrates the genetic organization of the *dhb* operon and the biosynthetic steps involved in the production of bacillibactin from chorismate, the breakpoint precursor of carbocyclic aromatic compounds (Raza *et al.* 2008).

Transcription of the *dhb* operon is iron regulated; this regulation is controlled by the activity of the Fur (ferric uptake repressor) protein (Baichoo *et al.* 2002). Transcription of this operon occurs during periods of iron starvation. It is facilitated by a σ^A -dependent promoter and is repressed by the binding of Fur protein to a Fur binding consensus sequence found in the operator region (Rowland and Taber 1996). Fur regulation in *B. subtilis* has been demonstrated for a number of genes and operons, many of which are known or thought to encode iron uptake systems (Baichoo *et al.* 2002). Transcription from the *dhb* operon promoter, which possesses a perfect Fur box, was shown to be extremely sensitive to iron concentrations. Indeed, transcription from this promoter was significantly repressed by iron concentrations as low as 100 nM and completely repressed by 1 μ M of iron (Baichoo *et al.* 2002). In studies of additional Fur-regulated genes, less perfect matches to the Fur consensus, were found indicating that their repression levels were not as sensitive to iron concentrations, were repressed by iron concentrations as low as 5 μ M (Crosa *et al.* 2004, Ollinger *et al.* 2006).

Chapter 1: Introduction

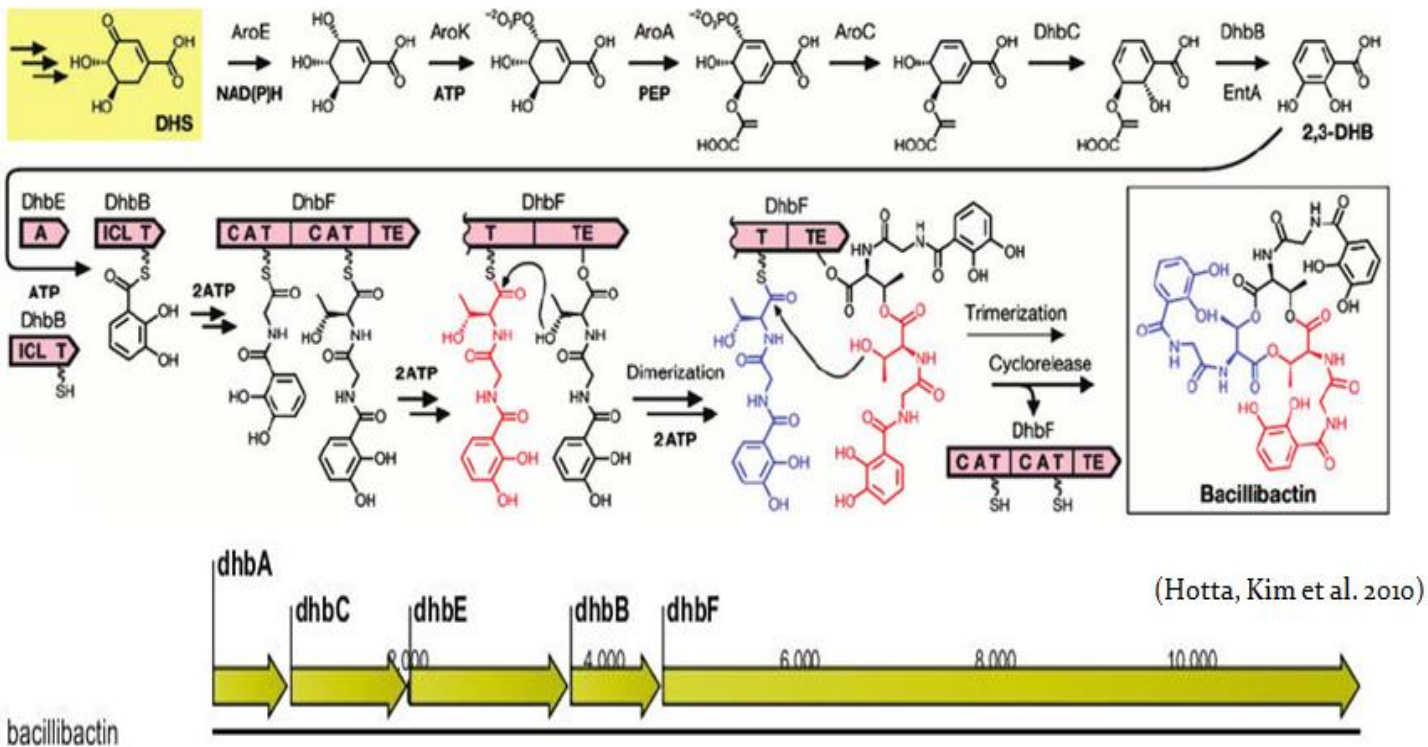


Figure 1.3: The biosynthetic pathway of bacillibactin (top) (adopted from (Hotta *et al.* 2010)) and map of the *dhbACEBF* operon in *B. amyloliquefaciens* (bottom).

In Gram-positive bacteria, the iron-siderophore complexes are regained from the extracellular environment by specific membrane-binding receptors and transport proteins belonging to the ABC type transporters (Miethke *et al.* 2006). *B. subtilis* has at least five substrate-binding lipoproteins anchored to the cell membrane that recognize and bind bacillibactin and xenosiderophores (Ollinger *et al.* 2006). These substrate-binding proteins (SBPs) scavenge iron-loaded siderophores, which upon interaction with the transmembrane permease components of the ABC-transporters are channeled into the cell. Transport is facilitated by cytoplasmic ABC subunits that provide energy for siderophore translocation. These substrate-binding proteins show specificity and high affinity for ferric ligands (Zawadzka *et al.* 2009).

1.3.4 Plant siderophores

Iron is an essential micronutrient for plant growth (Sahoo 2015). Under conditions of Fe deficiency, graminaceous plants secrete Fe(III)-chelating compounds called phytosiderophores. Phytosiderophores are hexadentate ligands that form specific

strong complexes with Fe (III) due to their amino and carboxyl groups (Ma 2005). The phytosiderophore is released to the rhizosphere, it chelates Fe from the soil by forming Fe (III)–phytosiderophore compounds (Hsieh and Waters 2016). These are complexes that are transported across the root plasma membrane. The molecular mass of phytosiderophores ranges between 500 and 1000 Da (Ahmed and Holmstrom 2014).

1.4 Microbial Biological Control Agents (BCA)

Plant pests are the most important biotic factors that cause crop loss with economic impact. Hence, various strategies are currently in place to manage and control plant pests. In addition to good agronomic and cultural practices, growers often rely on the application of chemical pesticides. However, environmental pollution caused by excessive use of agrochemicals as well as the strict regulations on the use of chemical pesticides and public opinion pressure to remove dangerous chemicals from the market has led to significant changes in people's attitudes to pesticide use in agriculture (Baker 1987). Therefore, biological control by beneficial microorganisms, termed as Biological Control Agents (BCA) has been established as an environmentally friendly pesticide alternative (Heydari and Pessarakli 2010).

1.5 Mode of action of BCA

BCA act in many different ways to protect plants from pathogens and to have a continuous and mutually beneficial relationship between them. The various mechanisms employed by BCA are broadly classified into direct or indirect antagonism.

Concerning the former, hyperparasitism is the most sophisticated and most direct form of competition (Pal B and Gardener 2006). In this case, biological control agents act directly to the pathogen by killing it or by not allowing it to multiply. Some other biocontrol agents have the ability to produce and secrete one or more compounds with antibiotic activity (Thomashow *et al.* 1990, Beneduzi *et al.* 2012). Antibiotics produced by microorganisms have been shown to be particularly effective at repressing plant pathogens and the diseases they cause (Shanahan *et al.* 1992, Choudhary and Johri 2009). Various microorganisms used as BCAs secrete other

metabolites, including lytic enzymes that can hydrolyze a wide variety of polymeric compounds, such as DNA, proteins, cellulose, hemicellulose, and chitin that can interfere with pathogen growth and activities (Anderson *et al.* 2004). Expression and secretion of these enzymes by microbes can sometimes result directly in the suppression of plant pathogen activities.

In many cases BCA act, indirectly, by promoting plant growth. BCA can reduce the disease incidence of crops due to disease escape. This is achieved by increasing their growth at least during the early stages of the life cycle. Growth promotion is often the result of increased solubilization and sequestration of nutrients and nutrient uptake through enhanced root growth of nutrients.

Induction of defense responses in plants by BCA has been suggested and shown as another mode of action of indirect antagonists (Ippolito and Nigro 2000). Disease resistance induced in the plants by necrogenic pathogen, nonpathogen microorganisms, antifungal compounds (Yakoby *et al.* 2001) or by certain natural or synthetic chemical compounds (Kessmann *et al.* 1994, Gomez-Vasquez *et al.* 2004) and by accumulation of phytoalexins (Sbaihat *et al.* 2015). Production of antifungal compounds by microbial antagonists in the host cells helps in inducing defense mechanism and hence provide biocontrol (Sharma *et al.* 2009). Systemic acquired resistance (SAR) is also triggered when plants are colonized by plant growth-promoting rhizobacteria (PGPR) (Sticher *et al.* 1997, Beneduzi *et al.* 2012). Many strains of PGPR have been shown to be effective in controlling plant diseases by inducing plant systemic resistance.

1.6 *Bacillus amyloliquefaciens* as a BCA

Bacillus amyloliquefaciens (*B. amyloliquefaciens*) is Gram-positive and aerobic. It is capable to form stable dormant structures called endospores in nutrient void and stressful environmental conditions. Spores are generally viable for a long period even under harsh conditions (Niazi *et al.* 2014). At first, it was categorized as *Bacillus subtilis*, but later it was identified as a separate species divided in two subspecies: *B. amyloliquefaciens* subsp. *amyloliquefaciens* and *B. amyloliquefaciens* subsp. *plantarum*. The two species differ significantly in their metabolic profile due to the

horizontal transfer of operons/genes and to genetic diversity, which reflects different evolution pathways (Priest *et al.* 1987, Logan and Vos 2015).

Members of the *Bacillus* genus have been described as BCAs for controlling phytopathogenic microorganisms and especially phytopathogenic fungi but also nematodes. The most known species hosting biocontrol agents are *B. subtilis* and *B. amyloliquefaciens*, but also *B. firmus* and *B. pumilus* (Kumar *et al.* 2011).

B. amyloliquefaciens is a plant root-colonizing environmental species which has the ability to stimulate plant growth and suppress plant pathogenic organisms. *B. amyloliquefaciens* strains have been shown to efficiently colonize roots and overcome the antibacterial action of some plant root exudates. Many of them are used commercially as biofertilizers and BCA in agriculture because of their dual ability to stimulate plant growth and suppress plant pathogenic organisms. Their action may be direct or indirect. Direct action concerns synthesis and secretion into the rhizosphere of secondary metabolites with antimicrobial activity. The indirect action concerns competition (Zhang *et al.* 2015) and displacement for root colonization, preventing the entry of phytopathogens and secretion of substances that act as promoters to trigger induced systemic resistance (ISR) (Chowdhury *et al.* 2015).

1.6.1 *B. amyloliquefaciens* secondary metabolites with biocontrol function

Analysis of the *B. amyloliquefaciens* genome revealed an impressive ability to produce a diverse range of different secondary metabolites including cyclic lipopeptides (cLPs) and polyketides (PKs) with antimicrobial action aimed to suppress harmful microbes and nematodes living within the plant (Chen *et al.* 2009). Such peptides may facilitate root colonization and interaction with host plant and prime plant defense responses. 11 gene clusters which occupy 9% of the genome are involved in the synthesis of antimicrobial metabolites. Five of these clusters are involved in non-ribosomal synthesis of cyclic lipopeptides such as surfactin, bacillomycin, fengycin and the siderophore bacillibactin (Figure 1.4) (Koumoutsi *et al.* 2004). Surfactins are antibiotic compounds that show hemolytic, antimicrobial and antiviral activities by altering membrane integrity whereas fengycin is specifically

Chapter 1: Introduction

active against filamentous fungi and inhibits phospholipase A₂ (Nishikiori *et al.* 1986).

Metabolite	Genes and gene cluster	Size	Function	Expression <i>in situ</i>	Effect against
Sfp-dependent non-ribosomal synthesis of lipopeptides					
Surfactin	<i>srfABCD</i>	32.0 kb	Biofilm, ISR	Strong, during root colonization	Virus
Bacillomycin D	<i>bmyCBAD</i>	39.7 kb	Direct suppression, ISR	Weak, during root colonization	Vungi
Fengycin	<i>fenABCDE</i>	38.2 kb	Direct suppression, ISR	Weak, during root colonization	Fungi
Bacillibactin	<i>dhbABCDEF</i>	12.8 kb	Siderophore	During iron deficiency in soil	Microbial competitors
Unknown	<i>nrsABCDEF</i>	17.5 kb	Unknown	Unknown	Unknown
Sfp-dependent non-ribosomal synthesis of polyketides					
Macrolactin	<i>mInABCDEFGH</i>	53.9 kb	Direct suppression	Not shown	Bacteria
Bacillaene	<i>baeBCDE,acpK, baeGHIJLMNRS</i>	74.3 kb	Direct suppression	Not shown	Bacteria
Difficidin	<i>dfnAYXBCDEFGHIJKLM</i>	71.1 kb	Direct suppression	Not shown	Bacteria
Sfp-independent non-ribosomal synthesis					
Bacilysin	<i>bacABCDE,ywfG</i>	6.9 kb	Direct suppression	Not shown	Bacteria, cyanobacteria
Ribosomal synthesis of processed and modified peptides (bacteriocins)					
Plantazolicin	<i>pznFKGHIAJC DBEL</i>	9.96 kb	Direct suppression	Unknown	<i>B. anthrax</i> , nematodes
Amylocyclicin	<i>acnBACDEF</i>	4.49 kb	Direct suppression	Unknown	Closely related bacteria
Synthesis of volatiles					
Acetoin/2,3-butandiol	<i>bdh,alsDRS</i>	3.6 kb	ISR	During root colonization	Plant pathogens

Figure 1.4: Genes and gene cluster encoding for biocontrol metabolites in *B. amyloliquefaciens* subsp. *plantarum* strain FZB42. Adopted from (Chowdhury *et al.* 2015).

Bacillomycin D is a member of the iturin family with wide range of antibacterial and antifungal properties and hemolytic activities (Thimon *et al.* 1995, Moynes *et al.* 2004). Bacillibactin is a catecholate siderophore possessing a monomer unit 2,3-dihydroxybenzoyl-Gly-Thr which is a cyclic trimeric lactone. It enables *Bacillus* cells to accumulate and take up iron ions from their natural environment under iron limitation conditions. These bacterial iron chelators are thought to sequester the limited supply of iron available in the rhizosphere making it unavailable to pathogenic fungi and bacteria, thereby restricting their growth (Chen *et al.* 2007).

1.6.2 Chemotaxis and swarming motility

B. amyloliquefaciens exhibits swarming motility. It is able to respond in chemical changes of the environment by modulating the flagellar machinery to move towards the appropriate direction. The response is based on inducing both genes for chemoreceptors and factors that control flagellar rotation. The presence of gene clusters of chemotaxis (*cheD, cheC, cheW, cheY, cheV, cheB, cheR*), flagellar biosynthesis and components assembly (*flg, flh, fli* and *mot* operons) together with the *swrA* gene that up-regulates the expression of genes and increases swarming motility

supports the high rhizosphere competence (Kearns *et al.* 2004, Ghelardi *et al.* 2012). Production of lipopeptide biosurfactants is also an essential feature that lowers the surface tension and facilitates swarming motility (Niazi *et al.* 2014).

1.6.3 Biofilm formation and root colonization

Adhesion to plant roots is a prerequisite for colonization and establishing relationships with host plants. Bacterial agents such as flagellin, exopolysaccharides and adhesions help bacteria to attach to the surface of the plant roots leading to surface colonization (Reva *et al.* 2004). Biofilm formation is essential for efficient surface colonization by bacteria (Romero *et al.* 2011). A variety of extracellular polymeric products are important components of the extracellular matrix making up the biofilm (Branda *et al.* 2006). *B. amyloliquefaciens* has been shown to perform biofilm formation and colonize plant seeds and seedlings (Reva *et al.* 2004). Biofilms have permeable water channels that allow exchange of nutrients, toxins and protection from environmental stresses (Davey and O'Toole 2000). The biofilm produced a hydrophobic layer on the surface that probably also provide protection to the host plant from pathogenic toxins and antimicrobial compounds (Niazi *et al.* 2014).

1.6.4 Induced Systemic Resistance (ISR)

Plants have the ability to induce enhanced level of resistance to pathogens after exposure to biotic stimuli. Induced defense mechanisms occur in two major forms; Systemic Acquired Resistance (SAR) and Induced Systemic Resistance (ISR) (Choudhary and Johri 2009). ISR that is mediated by non-pathogenic rhizobacteria is similar to SAR that is induced by pathogens (Pieterse *et al.* 2001). In SAR, resistance to pathogens is enhanced at the uninfected parts of the plants (Choudhary *et al.* 2007). Different signal pathways induce the mechanisms of ISR and SAR. Induction of ISR is mediated via the phytohormone jasmonic acid (JA) and ethylene (ET) signaling pathway while SAR requires salicylic acid (SA) (Pieterse *et al.* 2001). SA plays a crucial role in plant defense against pathogens. In response to pathogen attack, SA levels were increased in both infected and distal leaves. Exogenous application of SA can also induce a set of pathogenesis-related (PR) genes and establish SAR (Uknes *et al.* 1992). Signal transduction leading to ISR requires a response from both JA and

ET. Methyl jasmonate (MeJA) and the ET precursor are effective in inducing resistance against phytopathogenic microorganisms (Yan *et al.* 2002). Mutation in plant signaling pathways point to an active role by SA or JA and/or ET in activating ISR. JA and ET act in concert in activating defense responses. JA and derivatives induce expression of genes that encode defense-related proteins whereas ET activates several members of the pathogenesis-related (PR) gene family. They also act synergistically in stimulating elicitor-induced PR gene expression and systematically induce defense responses (Choudhary and Johri 2009).

Other compounds, such as volatile organic compounds (VOCs), may also be involved in the stimulation of ISR (Farag *et al.* 2013). Volatile organic compounds (VOCs), like 3-hydroxy-2-butanone(acetoin) and 2,3-butanediol, are active organic compounds with high vapor pressure that play an important role in communication with plants (Farag *et al.* 2013). VOCs emitted by the *B. amyloliquefaciens* and other rhizobacteria can induce plant growth but have also been implicated in a role in the triggering of ISR in plant-bacterial systems (Ryu *et al.* 2004).

1.7 Role of siderophores in biocontrol

Microorganisms that grow in the rhizosphere are ideal as biocontrol agents, since rhizosphere provides the first line of defense. In the soil, plant roots normally coexist with bacteria and fungi that may produce siderophores capable of sequestering the available soluble iron, which could interfere with plant growth and function. However, plant roots are sometimes capable of taking up ferric complexes of siderophores and using these as sources of iron (Aznar and Dellagi 2015). Thus, siderophores may play an important role in the competition between microorganisms and may also act as growth promoters. *Pseudomonas fluorescens* siderophore pyoverdine has been recently found to promote *A. thaliana* growth in iron-deficient conditions (Trapet *et al.* 2016). Moreover, siderophores produced by plant beneficial rhizobacteria were also shown to protect different plant species against pathogens by eliciting induced systemic resistance (ISR). For example, purified pyoverdines from *Pseudomonas putida* WCS358 were shown to trigger ISR in *A. thaliana* against *P. syringae* pv. *tomato* and in bean and tomato plants against *B. cinerea* (Meziane *et al.* 2005). *P. fluorescens* WCS374 can trigger ISR-mediated resistance in rice against the

leaf blast fungal pathogen *Magnaporthe oryzae* (De Vleeschauwer *et al.* 2008) and its siderophore pseudobactin has similar effects to other well-known elicitors, such as cell extracts containing lipopolysaccharides (LPS) (van Loon *et al.* 2008). In conclusion, siderophores have been demonstrated to play a major role in plant disease suppression by some bacterial biocontrol agents which inhibit the growth or the metabolic activity of plant pathogens by sequestering iron (Haggag 1999).

1.8 Purpose of this study.

Siderophores are nonribosomal peptides that produced in iron-limited conditions. They have been mentioned as biocontrol metabolites in specific as microbial competitors. In previous experimental procedures of the research group *Pseudomonas* species were found to be insensitive to *B. amyloliquefaciens*. The ability of both *B. amyloliquefaciens* and *Pseudomonas* to produce and secrete siderophores and to absorb xenosiderophores led to the idea that may *B. amyloliquefaciens* siderophores have antibiotic effect against *Pseudomonas* species. So, it was decided to investigate the ability of *B. amyloliquefaciens* to grow in iron limited conditions in order to produce and secrete siderophores. Then, we wanted to prove whether under the conditions of iron deficiency there is increasing the scope of the biological control agent and whether there is antibiotic activity against selected *Pseudomonas* strains both *in vitro* and *in planta* tests. In order to answer the above scientific questions a plasmid will be designed and constructed that will be used for homologous recombination obtaining a knock-out for siderophore synthesis operon *B. amyloliquefaciens* strain. Finally, the expressions levels of other antibiotic genes and genes that take part in *B. amyloliquefaciens* competition will be studied in iron limited conditions.

MATERIALS AND METHODS

2.1 Bacterial strains and culture conditions

B. amyloliquefaciens strain **MBI600** is a commercial biocontrol agent, used as a fungicide, under the Serifel[®] trademark. BASF SE (Germany) has granted permission to use this strain for the scopes of this project.

Cell Free Culture Filtrate (CFCF) preparation: *B. amyloliquefaciens* cultures were grown on succinate medium (Table 2.1) provided with different iron concentrations (0, 50, 1000, 2000 $\mu\text{g/L}$ FeCl_3) and incubated inside an orbital shaker at 200 rpm for 48 hours at 37 °C. Since the optical density (OD_{600}) at different iron concentrations was significantly different, the cultures were diluted with sterile distilled water so that all cultures had the same OD_{600} . Cultures were then were centrifuged at 4500 rpm for 15 minutes and the supernatant was filtrated in Sartorius[™] Sartolab[™] RF/BT Vacuum Filtration Units with 0.22 μm pore size to obtain CFCF.

Escherichia coli **DH5 α** was user for transformation (§ 2.12). *E. coli* DH5 α cultures were grown on LB medium (Table 2.2) and incubated overnight inside an orbital shaker at 200 rpm and at 37 °C.

Table 2.1: Succinate medium

KH ₂ PO ₄	6 g/L
K ₂ HPO ₄	3 g/L
MgSO ₄	0.2 g/L
(NH ₄) ₂ SO ₄	1 g/L
Sodium succinate	4 g/L
Glucose	10 g/L

Table 2.2: Luria Broth (LB) medium

Tryptone	10 g/L
Sodium chloride	10 g/L
Yeast Extract	3.5 g/L
For agar plates add 1.4% Agar Technical	

Note: LB medium containing the appropriate antibiotic was used for selection and culture of transformed E. coli cells.

SOC medium (Table 2.3) was used in transformation assay for the recovery of *E. coli* DH5 α cells after electroporation.

Pseudomonas syringae pv. *tomato* (*Pto*) and *Pseudomonas syringae* pv. *tabaci* (*Pta*) were used in disc diffusion assays and microtiter experiments. Both strains were grown on succinate agar medium plates (Table 2.4) provided with different iron concentrations (0, 50, 1000 μ g/L FeCl₃) or liquid LB medium. Cultures were incubated at 28 °C for 48 h. *Pto* and *Pta* rifampicin-resistant strains were used in efficacy evaluation of siderophores *in planta*. Both strains were grown on LB (Table 2.2) supplemented with 5 μ g/mL rifampicin and incubated inside an orbital shaker at 200 rpm and 28 °C for 48 h.

Table 2.3: SOC medium

Tryptone	2% (w/v)
Yeast extract	0.5% (w/v)
NaCl	10 mM
KCl	2.5 mM
MgCl ₂	10 mM
Glucose	20 mM

Table 2.4: Succinate agar medium

KH ₂ PO ₄	6 g/L
K ₂ HPO ₄	3 g/L
MgSO ₄	0.2 g/L
(NH ₄) ₂ SO ₄	1 g/L
Sodium succinate	4 g/L
Agar	15 g/L

2.2 DNA extraction from *B. amyloliquefaciens* cells.

Genomic DNA extracted by *B. amyloliquefaciens* cells was used as a template for the PCR amplification of the partial genes *dhbC* and *dhbF*. DNA extraction was performed using NucleoSpin® Plant kit (MACHEREY-NAGEL). 1 mL of bacterial culture was centrifuged for 5 min at 8,000 *g*. The resulting pellet was resuspended in 180 µL Buffer T1 by pipetting. 25 µL Proteinase K were added to the mix solution. The suspension was then incubated at 56 °C for 3 hours. Following incubation, 200 µL of B3 were added to the solution and samples were incubated for 10 minutes at 70 °C. Subsequently, the mixture was loaded onto NucleoSpin® Tissue Column and centrifuged for 1 minute at 11,000 *g*. The silica membrane was then washed with 500

μ L Buffer BW and 600 μ L Buffer B5, followed by centrifugation for one minute at 11,000 g. The silica membrane was then centrifuged for 1 minute at 11,000 g, in order to remove excess of B5 Buffer. The highly pure genomic DNA was finally eluted by pipetting 100 μ L of Elution Buffer BE, pre-heated at 70 °C, onto the membrane after incubation for 5 min at room temperature followed by centrifugation for 1 minute at 11,000 g.

2.3 Polymerase Chain Reaction – PCR.

The polymerase chain reaction (PCR) is a technology that is used to amplify a single or a few copies of a certain piece of DNA across several orders of magnitude, generating thousands to millions of copies of this particular DNA sequence (Bartlett and Stirling 2003). In every PCR a pair of primers (primers used in this study described in table 2.6) are used for the amplification of the DNA sequence wanted. Primers are oligonucleotides, usually 17 – 30 base pairs, complementary with the 3' and 5' ends of the sequence that is amplified. A standard PCR reaction mix is described in Table 2.5 and a typical PCR protocol in Table 2.7.

Table 2.5: Standard PCR reaction mix (KapaTaq DNA Polymerase).

Component	Final Concentration
PCR grade water	
10x buffer with Mg ²⁺	1X
10 mM dNTPs	200 μ M
10 μ M Forward Primer	0.4 μ M
10 μ M Reverse Primer	0.4 μ M
Template DNA	< 250 ng
KapaTaq (5U/ μ L)	1.0 unit/50 μ L PCR

Chapter 2: Materials and Methods

Table 2.6: Primers names and sequences used in this study.

Primers name	Primers sequence	Target-gene
<i>dhbC359_BamHI_fw</i>	CAGGATCCCCAATACATATGACATCCGTCC	<i>dhbC</i> partial sequence
<i>dhbC870_SacII_rv</i>	GCCGCGGAAGTGATGTCGTTGAC	(<i>B. amyloliquefaciens</i> genomic DNA)
<i>dhbF142_MluI_fw</i>	ACGCGTCGCGTGCTGACGGAAG	<i>dhbF</i> partial sequence
<i>dhbF866_ApaI_rv</i>	GAAGGGCCCCGAGAAAGCCGTAAAGGCAGAAG	(<i>B. amyloliquefaciens</i> genomic DNA)
<i>Erm^r_MluI_fw</i>	ACGCGTGTGCCACCTGACGTCTAAG	<i>Erm^r</i> gene
<i>Erm^r_SacII_rv</i>	CCGCGGGAATTATTCCTCCCGTTAAA	(pMUTIN-GFP vector)

Table 2.7: A general PCR protocol

Step1:	Initial denaturation of DNA template at 94 °C for 2 minutes
Step 2: (20-40 cycles)	<ul style="list-style-type: none"> ✓ Denaturation of DNA at 95 °C for 30 seconds. ✓ Hybridization of primers to the complementary DNA sequence for 30 seconds ⁽¹⁾. ✓ Polymerization of PCR product ⁽²⁾
Step 3:	Final extension for 5 – 10 minutes.
Step 4:	Storage of PCR product at 4 °C.

⁽¹⁾The annealing temperature depends on the melting temperature of primers (T_m).

- For *dhbC* gene amplification the T_m was 62 °C.
- For *dhbF* gene amplification the T_m was 63.5 °C.

- For *Erm^r* gene amplification the T_m was 59 °C.

⁽²⁾ The temperature of polymerization depends on the Taq polymerase. Usually 72 °C are used. The extension time of this step depends on the size of the PCR product. Usually, a minute of extension is enough for the amplification of 1,000 base pairs.

- For *dhbC* gene amplification the extension time was 30 sec.
- For *dhbF* gene amplification the extension time was 45 sec.
- For *Erm^r* gene amplification the extension time was 1 min.

2.4 Agarose gel electrophoresis

Agarose gel electrophoresis is a method used to separate and identify DNA on the basis of their size and rate of movement through a gel under the influence of an electric field. Since the nucleic acids are negatively charged due to the negatively charged phosphate group, they will migrate to the positively charged electrode (anode). Distinct bands, based on the molecule size, will form on the gel. Shorter DNA molecules will move faster than longer, since they are able to slip through the matrix more easily. The band can be visualized by staining the DNA with ethidium bromide, which causes the DNA to fluoresce in ultra violet light. Ethidium bromide is a ring-formed structure that intercalates between the base pairs in the DNA double helix.

Preparing the gel

A 1% agarose gel was made by mixing 1 g of agarose with 90 mL distilled water and 10 mL 10X TAE buffer. The mixture was heated in a microwave oven until all agarose had melted and the solution had started to boil. The gel solution was then left to cool (to approximately 65 °C). 10 µL of ethidium bromide were added after the mixture had cooled, and gently mixed into the agar. The gel was poured slowly into a gel rack, the comb being set at one side of the gel. Bubbles in the solution were removed. The gel was allowed to set for 20 to 30 minutes. After that, when the gel had solidified, the comb was removed and the gel, together with the rack, was soaked into a chamber with 1X TAE gel running buffer (Table 2.8). The gel was placed with the wells facing the electrode that provide the negative current (cathode). The comb was then gently removed.

Loading and running the gel

Loading buffers were added to the DNA samples to assist visualization and sedimentation into the gel wells. A DNA ladder, a mixture of DNA fragments of known size, was loaded into the first well. This was used to determine the absolute size of the separated DNA strand by comparing their migration with that of the ladder (examples depicted in Figure 2.1). Samples were loaded into the wells, the lid of the electrophoresis chamber was closed and the current was applied. Voltage was adjusted to 90 volts and gel was allowed to run for approximately 30 minutes to 1 hour. The ethidium bromide stained gel was visualized under UV light and photographed using E-box gel documentation imaging (Vilber, France)

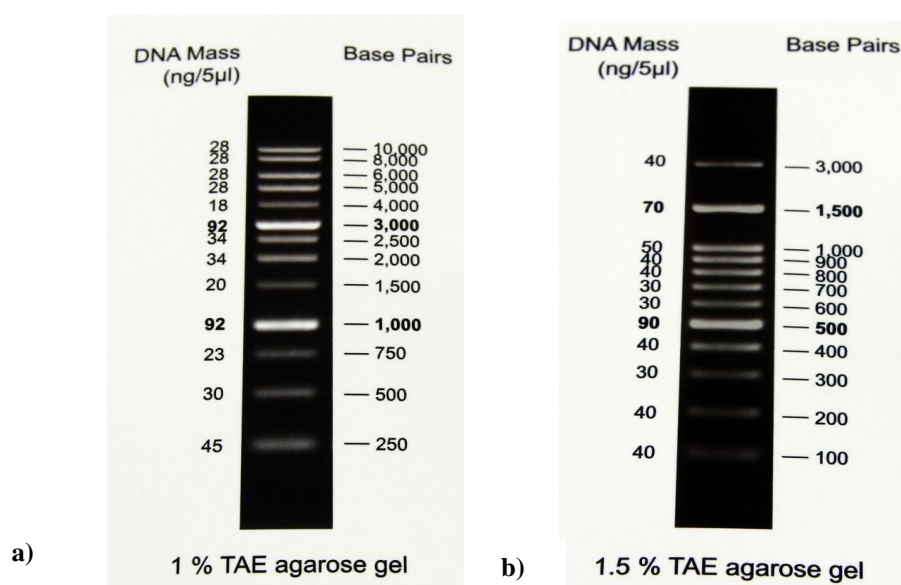


Figure 2.1: Sketch of **a)** the 1 Kb DNA Ladder and **b)** the 100 bp DNA Ladder (Nippongenetics)

Table 2.8: 50X TAE electrophoresis buffer (Stock Solution)

Tris-base	242 g/L
Glacial Acetic Acid	57.1 mL
EDTA (0.5 M, pH 8)	100 mL
dH ₂ O	up to 1 L

Note: For 1X TAE electrophoresis buffer (working solution), dilute 50:1 (dH₂O:50X TAE)

2.5 Gel Extraction

DNA bands were purified from the gel matrix using QIAquick Gel Extraction Kit. In detail, the required DNA fragment was excised from the agarose gel using a scalpel and transferred to a microcentrifuge tube. The size of the gel slice was determined by weight and 3 volumes of Buffer QG were added to 1 volume of gel (100 mg \approx 100 μ L). The tube was incubated at 50 °C until the gel slice had dissolved completely. To help dissolve the gel, the tube was mixed by vortexing several times during the incubation period. After the gel slice had dissolved, an equal volume of isopropanol was added to the sample and mixed. To bind DNA, the sample was applied to a QIAquick column, and centrifuged at 13000 rpm for 1 minute. The flow-through was discarded. The column was washed by adding 0.75 mL Buffer PE and centrifuged for 1 minute. The flow-through was discarded again and the column was centrifuged for an additional minute. The QIAprep spin column was placed in a clean 1.5 mL microcentrifuge tube and the DNA was eluted by adding 30 μ L Buffer EB (pre-heated at 70 °C) to the center of the membrane, incubating at room temperature for 5 minutes and centrifuging for 1 minute at 11,000 g.

2.6 Transformation of DH5 α *E. coli* competent cells.

2.6.1 Preparation of DH5 α *E. coli* electro-competent cells.

E. coli strain DH5 α was streaked on LB agar plate and were incubated at 37 °C overnight. A single colony was inoculated to 5 mL LB medium and incubated overnight at 37 °C in a rotating shaker at 200 rpm. 1 mL of overnight culture was added in to 450 mL LB medium and incubated at 37 °C in a rotating shaker until OD₆₀₀ reaches 0.5-0.6. The culture was chilled in ice water for 20 minutes and the cells were harvested in a pre-chilled centrifuge and centrifuged for 10 minutes at 4500 rpm at 4 °C. The supernatant was removed and the cell pellet was gently resuspended in 450 mL ice cold 10% glycerol. The supernatant was removed and the cell pellet was resuspended in 225 mL of ice cold 10% glycerol. The samples were also centrifuged for 15 minutes at 4500 rpm at 4 °C. The supernatant was removed and the cell pellet was resuspended in 18 mL of ice cold 10% glycerol. The samples were centrifuged for 15 minutes at 4500 rpm at 4 °C. The supernatant was removed and the cell pellet was resuspended in 0.9 mL of ice cold 10% glycerol. Aliquots of 50 μ L

were made in 1.5 mL pre-chilled eppendorfs. The cells were freezeed in liquid nitrogen and store at -80 °C.

2.6.2 Transformation of DH5α *E. coli* electrocompetent cells.

The electroporator was turned on and set to 1.7-2.5 kv (optimize for strain), 200 ohms and 25 μF. The cells were thawed on ice and for each sample, a 0.2 cm electroporation cuvette was placed on ice. 50 μL of the cell suspension was mixed with 2 μL plasmid DNA and incubated on ice for 60 seconds. The appropriate settings were set to the micropulser. The mixture of cells and DNA was transferred to a cold electroporation cuvette. The electroporation cuvette was placed in the electroporation module and the pulse was pressed. 1 mL of SOC medium was immediately added to the cuvette, mixed by pipetting up and down once and then the mixture was transferred to a 15 mL-falcon tube and was incubated at 37 °C for 1 hour at 225 rpm. The mixture was plated on LB agar plates with the appropriate antibiotic.

2.6.3 Selection of transformed colonies

To screen for colonies carrying plasmids with the correct insert, a selection of colonies from the transformation procedure was picked, by stabbing a sterile tip into the soft agar. The inoculums were transferred into tubes of LB medium containing the appropriate antibiotic before the tubes were incubated overnight into an orbital shaker at 200 rpm and 37 °C.

2.7 Plasmid DNA isolation

Isolation of plasmid DNA was performed using the QIAprep Spin Miniprep Kit. In detail, 5 mL of an overnight culture of *E. coli* in LB medium was centrifuged at 8000 rpm for 3 minutes, at room temperature. The supernatant was discarded and pelleted bacterial cells were resuspended in 250 μL Buffer P1 and transferred in a microcentrifuge tube. 250 μL of Buffer P2 (lysis buffer) was added and mixed carefully. The solution became viscous and slightly clear. The solution was incubated for 5 minutes at room temperature. 350 μL of Buffer N3 (neutralization buffer) was added and mixed immediately, but thoroughly by inverting the tube. The solution was

centrifuged for 20 minutes at 14000 rpm. A compact white pellet formed. The supernatants were applied to a QIAprep spin column by pipetting and were centrifuged for 60 seconds. The flow-through was discarded. The QIAprep spin column was washed by adding 0.75 mL Buffer PE and centrifuging for 60 seconds. The flow-through was again discarded, and columns were centrifuged for an additional minute to remove residual wash buffer. The QIAprep spin column was then placed in a clean 1.5 mL microcentrifuge tube and the DNA was eluted from the QIAprep column by adding 50 μ L of buffer EB (pre-heated at 70 $^{\circ}$ C) to the center of the membrane. The column was left for 5 minutes at 70 $^{\circ}$ C and then centrifuged for 1 minute. The DNA yield of the eluate was then determined using a spectrophotometer to measure absorbance at a wavelength of 260 nm.

2.8 Digestions using restriction enzymes.

Restriction endonucleases are enzymes that have the ability to recognize specific sequences of DNA (usually 6-8 nucleotides), known as restriction sites, and cleave those creating specific sticky or blunt ends. Restriction endonucleases are usually isolated from bacteria and archaea. In this study, restrictive digestions were used primary to ligation, in order to obtain compatible ends between the insert and the vector or between inserts. Digestions used in this study described at tables 2.9-2.14.

Table 2.9: *Erm^r* direction digestion at PCR[®]2.1-TOPO[®]-*Erm^r*

<i>Sac</i> I	10 - 20 units / 1 μ g DNA
<i>Sac</i> II	10 - 20 units / 1 μ g DNA
10X Buffer T (Takara)	1X
0.1% BSA	1X
PCR [®] 2.1-TOPO [®] - <i>Erm^r</i>	\leq 1 μ g
ddH ₂ O	As required

Chapter 2: Materials and Methods

Table 2.10: Diagnostic digestion for *Erm^r* at PCR[®]2.1-TOPO[®]-*Erm^r*

<i>EcoRI</i>	10 - 20 units / 1µg DNA
10X Buffer <i>EcoRI</i> (Minotech)	1X
PCR [®] 2.1-TOPO [®] - <i>Erm^r</i>	≤ 1 µg
ddH ₂ O	As required

Table 2.11: Digestion for *Erm^r* at PCR[®]2.1-TOPO[®] - *Erm^r*

<i>MluI</i>	10 - 20 units / 1µg DNA
<i>SacII</i>	10 - 20 units / 1µg DNA
10X Buffer T (Takara)	1X
0.1% BSA	1X
PCR [®] 2.1-TOPO [®] - <i>Erm^r</i>	≤ 1 µg
ddH ₂ O	As required

Table 2.12: Digestion for *dhbC* at PCR[®]2.1-TOPO[®] -*dhbC-Erm^r* and at pGem[®]-T Easy

<i>BamHI</i>	10 - 20 units / 1µg DNA
<i>SacII</i>	10 - 20 units / 1µg DNA
10X Buffer C (Promega)	1X
PCR [®] 2.1-TOPO [®] - <i>dhbC-Erm^r</i>	≤ 1 µg
ddH ₂ O	As required

Table 2.13: Digestion for *dhbF* at PCR[®]2.1-TOPO[®] -*dhbC-Erm^r - dhbF* and at pGem[®]-T Easy

<i>ApaI</i>	10 - 20 units / 1µg DNA
<i>MluI</i>	10 - 20 units / 1µg DNA
10X Buffer L (Takara)	1X

PCR [®] 2.1-TOPO [®] - <i>dhbC-Erm^r- dhbF</i>	≤ 1 μg
ddH ₂ O	As required

Table 2.14: Digestion for *dhbC-Erm^r- dhbF* at PCR[®] 2.1-TOPO[®] - *dhbC-Erm^r- dhbF*

<i>KpnI</i>	10 - 20 units / 1μg DNA
<i>ApaI</i>	10 - 20 units / 1μg DNA
10X Buffer L (Takara)	1X
PCR [®] 2.1-TOPO [®] - <i>dhbC-Erm^r- dhbF</i>	≤ 1 μg
ddH ₂ O	As required

2.9 Ligation Reaction.

The ligation of two DNA molecules, usually a plasmid and a PCR product, is performed due to the ability of T4 DNA ligase to conjugate DNA molecules with complementary “sticky” or “blunt” ends. This procedure results to circular molecules of plasmid with the desirable insert. The mixture of a ligation reaction is used for the transformation of *E.coli* competent cells, in order to multiply the modified plasmid containing the desired transgene.

The appropriate amount of digested plasmid DNA and PCR product is added to a final reaction volume of 10 μL along with ddH₂O ⁽¹⁾.25 units of T4 DNA ligase and T4 DNA ligase Buffer are added and the mixture is incubated at 16 °C for 12 hours.

⁽¹⁾ The molar ratio between plasmid vector and insert is calculated with the formula below:

$$\frac{\text{ng of vector} \times \text{kb size of insert}}{\text{kb size of vector}} \times \text{molar ratio of } \frac{\text{insert}}{\text{vector}} = \text{ng of insert}$$

2.10 Plasmid vectors used in this study

Three different plasmids were used in this study. PCR[®]2.1-TOPO[®] was used to insert the construct. pGem[®]-T Easy vector was used to clone partial sequences of *dhbC* and *dhbF* before subcloned in PCR[®]2.1-TOPO[®] - *Erm^r* to enhance restriction enzymes activity and pMUTIN-GFP to amplify erythromycin resistance gene (*Erm^r*) (Figure 2.2).

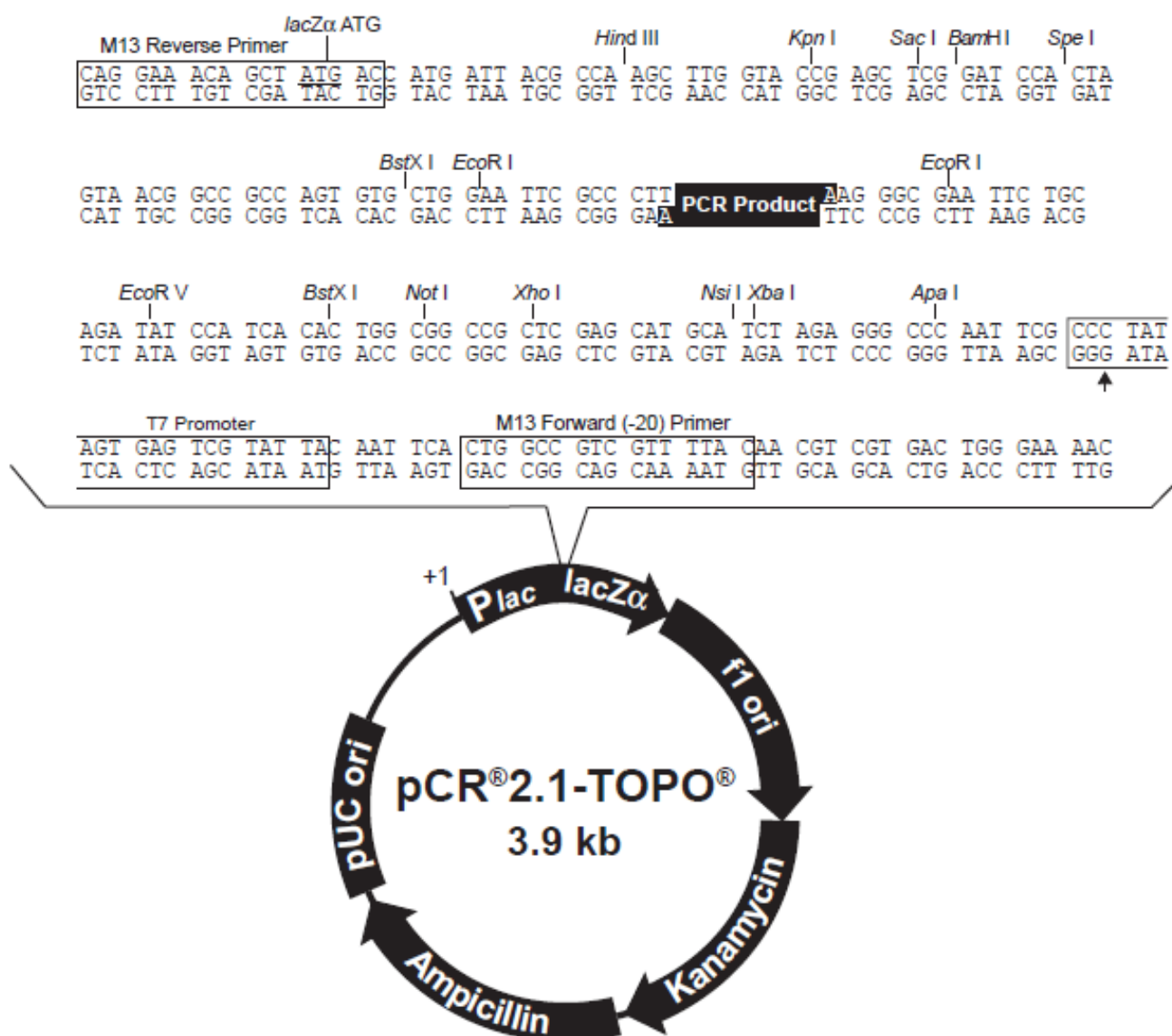


Figure 2.2 a: The sequence map of plasmid PCR[®]2.1-TOPO[®].

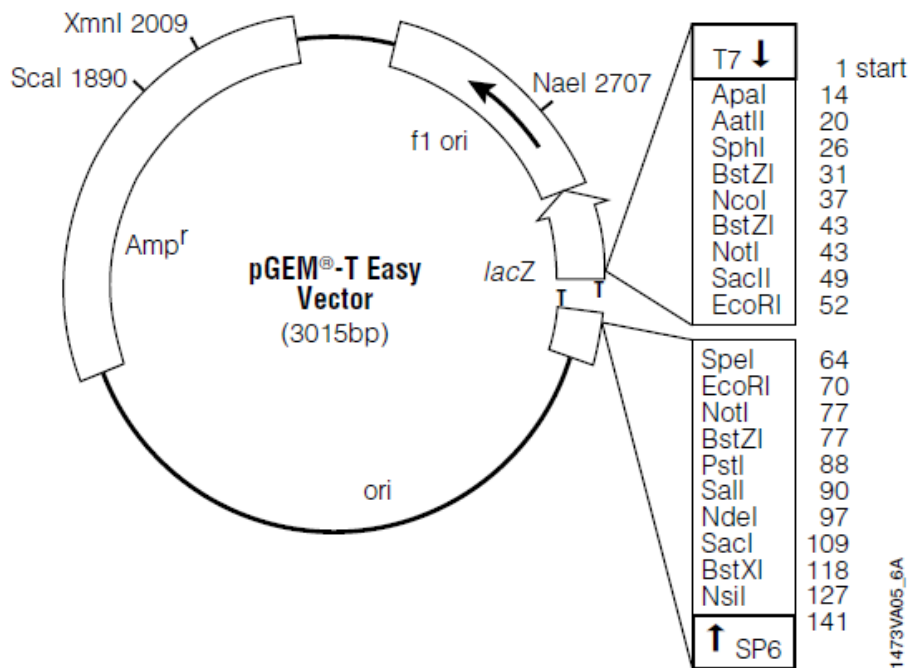


Figure 2.2 b: The sequence map of plasmid pGem[®]-T Easy.

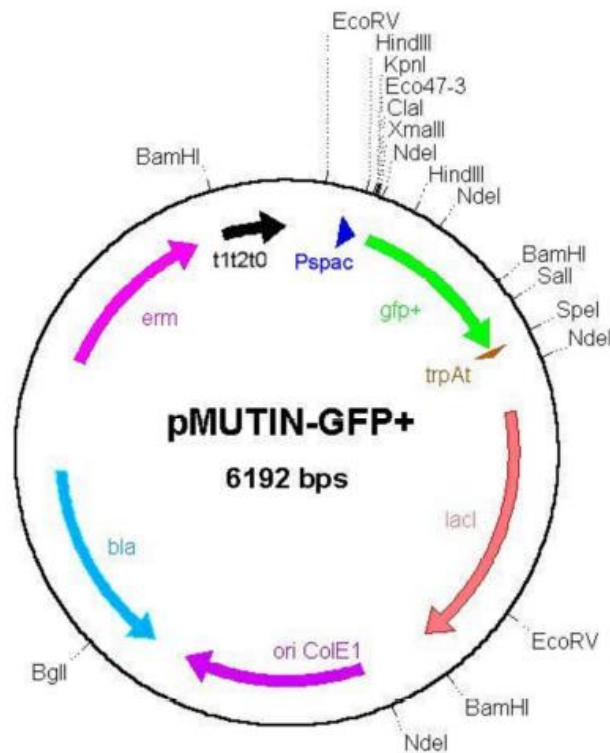


Figure 2.2 c: The sequence map of plasmid pMUTIN-GFP.

2.11 Cloning method

The procedure of making a construct consists of three major steps:

1. PCR amplification of the desirable sequence.
2. Digestion of PCR product and plasmid DNA with the appropriate restriction enzymes, DNA purification using gel extraction methods (§2.5) and directional cloning to the appropriate plasmid using ligation reaction (§2.9).
3. Transformation to *E. coli* DH5 α competent cells.

To obtain a knock-out of siderophore (bacillibactin) operon strain of *B. amyloliquefaciens* a construct was made that contains **a)** partial sequence of *dhbC* gene **b)** erythromycin resistance gene **c)** partial sequence of *dhbF* gene (Figure 2.3)

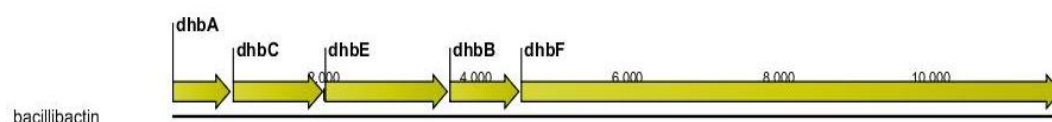


Figure 2.3: Map of the *dhbACEBF* (siderophore synthases) operon in *B. amyloliquefaciens*.

The erythromycin resistance gene was amplified from plasmid pMUTIN-GFP (Figure 2.2c) using polymerase chain reaction (PCR) and ligated into plasmid vector pCR[®]2.1-TOPO[®] (Invitrogen[™]) (Figure 2.2a) with A-tailing to develop plasmid pCR[®]2.1-TOPO[®]-*Erm*^r. With the ligation mixture, *E. coli* competent cells were transformed (§2.6) and the clones containing the transgene were checked with specific digestions. Direction of the erythromycin resistance gene (*Erm*^r) in pCR[®]2.1-TOPO[®] was also assessed by restriction digestion with *Mlu*I or *Sac*II enzymes (Table 2.11) that recognize the *Erm*^r restriction sites, in combination with *Sac*I that only cuts into the plasmid multicloning site (Table 2.10). Directional cloning of *Erm*^r was evaluated base on DNA fragment size.

Primer pairs *dhbC*359_*Bam*HI_fw/*dhbC*870_*Sac*II_rv or *dhbF*121_*Mlu*I_fw/*dhbF*866_*Kpn*I_rv (Table 2.6) have been used to amplify, using PCR (§2.3), partial sequence of *dhbC* or *dhbF* genes from total genomic DNA of *B. amyloliquefaciens* (§2.2).

Cloning the partial *dhbC* sequence in pGem[®]-T Easy vector preceded the cloning in PCR[®]2.1-TOPO[®]-*Erm*^r by restriction digestion with *Bam*HI or *Sac*II enzymes that recognize the *dhbC* restriction sites (Table 2.12).

Amplified DNA fragments were extracted from the agarose gel (§ 2.5), cloned into the plasmid vector pGem[®]-T Easy (Figure 2.2b) to develop plasmid pGem[®]-T Easy-*dhbC*. *E. coli* strain DH5 α competent cells were transformed and the clones containing the partial gene sequence were checked with specific digestions.

The *dhbC* DNA fragment was extracted from the gel and then ligated (§2.9) into the PCR[®]2.1-TOPO[®]-*Erm*^r to develop plasmid PCR[®]2.1-TOPO[®]-*dhbC-Erm*^r. The ligation product was transformed into competent *E. coli* DH5 α cells and clones containing the partial gene sequence were selected based on *Bam*HI and *Sac*II digestion (Table 2.12) that yields the partial *dhbC* sequence.

Cloning the partial *dhbF* sequence in pGem[®]-T Easy vector preceded the cloning in PCR[®]2.1-TOPO[®]-*dhbC-Erm*^r by restriction digestion with *Mlu*I or *Apa*I enzymes that recognize the *dhbF* restriction sites (Table 2.13).

Amplified DNA fragments were extracted from the agarose gel, cloned into the plasmid vector pGem[®]-T Easy (Figure 2.2b) to develop plasmid pGem[®]-T Easy-*dhbF*. *E. coli* strain DH5 α competent cells were transformed and clones containing the partial gene sequence were selected by digestion with *Mlu*I and *Apa*I restriction enzymes, yielding the partial *dhbF* sequence (Table 2.13).

The *dhbF* DNA fragment was extracted from the gel and then ligated into the PCR[®]2.1-TOPO[®]-*dhbC-Erm*^r. The ligation product was transformed into competent *E. coli* DH5 α cells and the clones containing the partial *dhbF* sequence were checked by digestion with *Mlu*I and *Apa*I digestion that yields the partial *dhbF* sequence (Table 2.13) digested with *Mlu*I and *Apa*I or *Kpn*I and *Apa*I that yields the *dhbC-Erm*^r-*dhbF* complex (Table 2.14).

Sequential cloning resulted in the plasmid pCR[®]2.1-TOPO[®]-*dhbC-Erm*^r-*dhbF* (Figure 2.4). The partial sequences of and genes will help the homologous recombination. The sequences of the *dhbC* and *dhbF* genes help to effect homologous recombination in *B. amyloliquefaciens* genomic DNA in order to eliminate the siderophore synthesis operon and replace it with the erythromycin resistance gene.

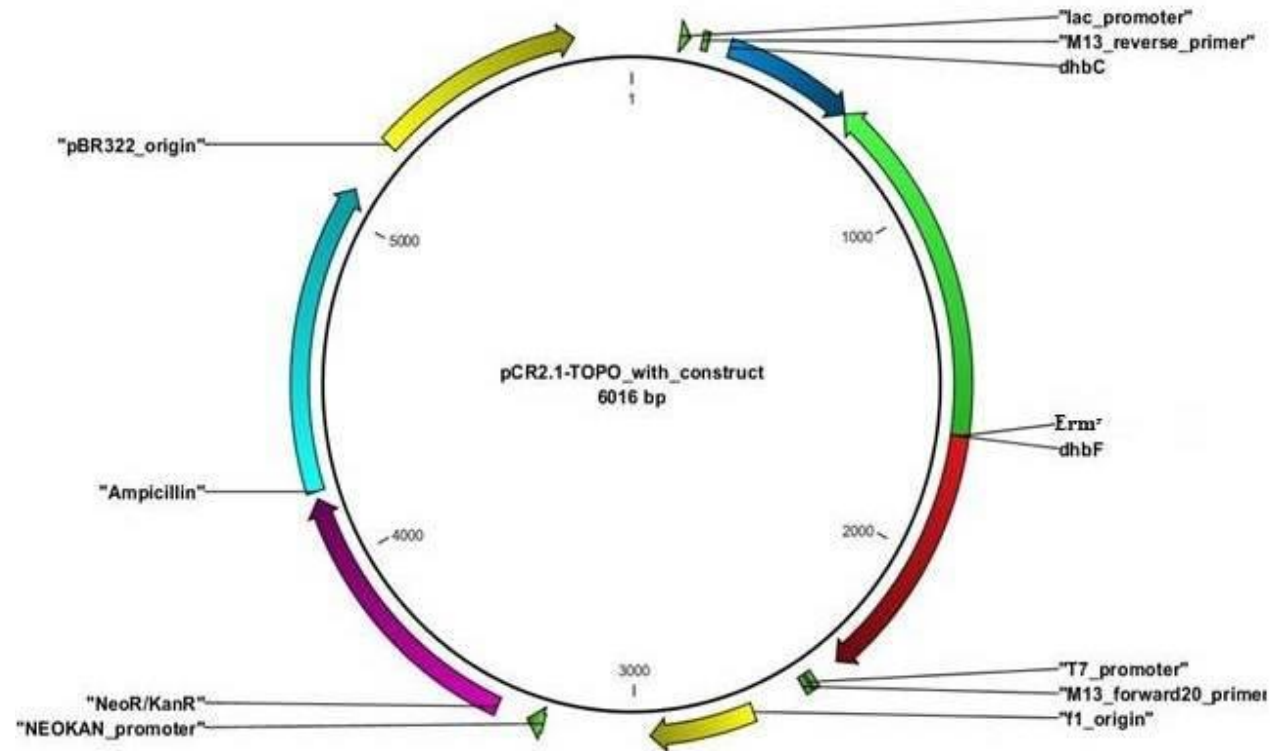


Figure 2.4: Schematic representation of **a)** pCR[®]2.1-TOPO[®]-*dhbC-Erm^r-dhbF* plasmid and **b)** homologous recombination in siderophore biosynthesis operon.

2.12 Transformation of *B. amyloliquefaciens* cells

The three different protocols that were used for *B. amyloliquefaciens* transformation are depicted in Figure 2.5.

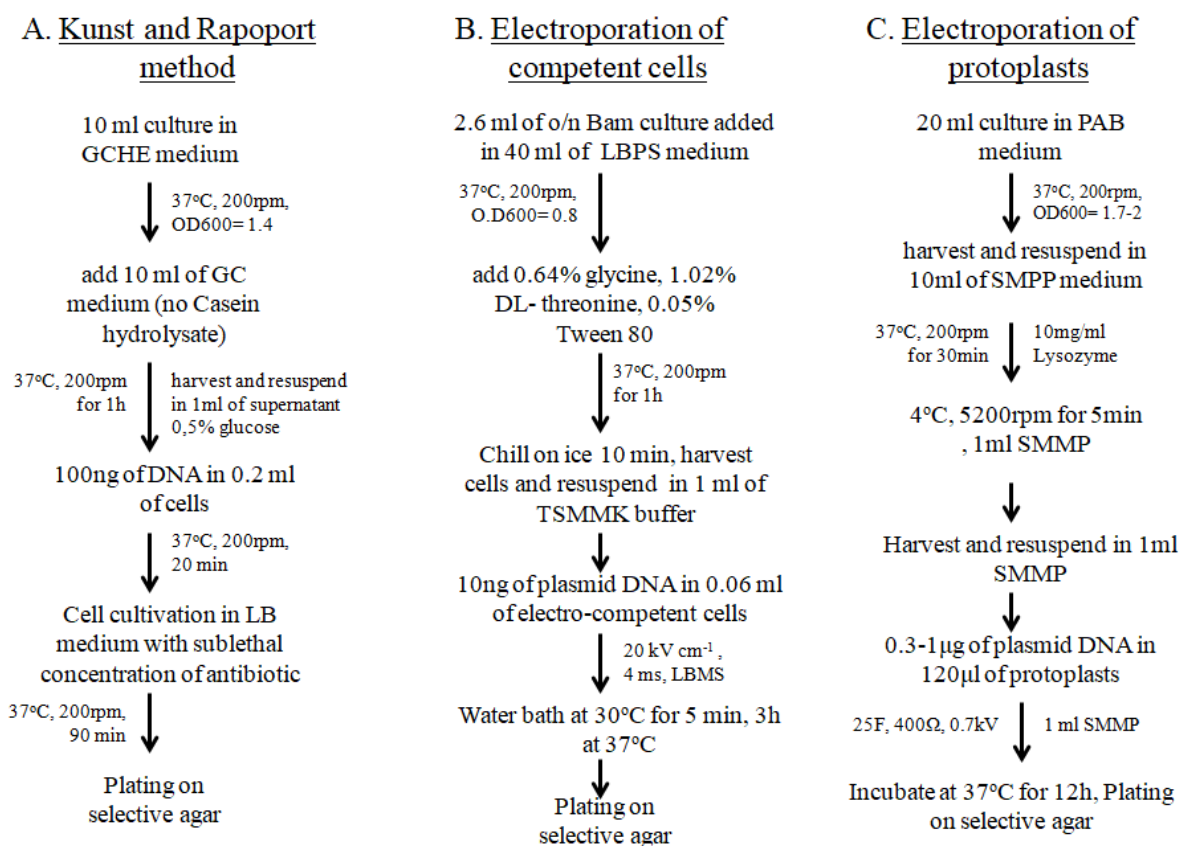


Figure 2.5: Protocols used for *B. amyloliquefaciens* transformation A) (Koumoutsis *et al.* 2004) B) (Zhang *et al.* 2015) C) (Romero *et al.* 2006)

2.13 Chrome azurol S (CAS) assay

(Schwyn and Neilands 1987) developed a universal siderophore assay using chrome azurol S (CAS) and hexadecyltrimethylammonium bromide (HDTMA) as indicators. HDTMA complexes bind tightly with ferric iron to produce a blue color. When a strong iron chelator such as a siderophore removes iron from the dye complex, the color changes from blue to orange. The procedure followed for the preparation of the CAS plates is described in the Figure 2.6.

A. Blue Dye:

a. Solution 1:

Dissolve 0.06 g of CAS in 50 mL of ddH₂O.

b. Solution 2:

Dissolve 0.0027 g of FeCl₃·6 H₂O in 10 mL of 10 mM HCl.

c. Solution 3:

Dissolve 0.073 g of HDTMA in 40 mL of ddH₂O.

d. Mix Solution:

1 with 9 mL of Solution 2.

Then mix with Solution 3.

Solution should now be a blue color.

Autoclave and store in a plastic container/bottle

B. Mixture solution:

a. Minimal Media 9 (MM9) Salt Solution Stock

Dissolve 15 g KH₂PO₄, 25 g NaCl and 50 g NH₄Cl in 500 mL of ddH₂O.

b. 20% Glucose Stock

Dissolve 20 g glucose in 100 mL of ddH₂O.

c. NaOH Stock

Dissolve 25 g of NaOH in 150 mL ddH₂O;

pH should be ~12.

d. Casamino Acid Solution

i. Dissolve 3 g of Casamino acid in 27 mL of ddH₂O.

ii. Extract with 3% 8-hydroxyquinoline in chloroform to remove any trace iron.

iii. Filter sterilize.

C. CAS agar Preparation:

a. Add 100 mL of MM9 salt solution to 750 mL of ddH₂O.

b. Dissolve 32.24 g piperazine-N,N'-bis(2-ethanesulfonic acid) PIPES. PIPES will not dissolve below pH of 5. Bring pH up to 6 and slowly add PIPES while stirring. The pH will drop as PIPES dissolves. While stirring, slowly bring the pH up to 6.8.

c. Add 15 g Bacto agar.

d. Autoclave and cool to 50 °C.

e. Add 30 mL of sterile Casamino acid solution and 10 mL of sterile 20% glucose solution to MM9/ PIPES mixture.

f. Slowly add 100 mL of Blue Dye solution along the glass wall with enough agitation to mix thoroughly.

g. Aseptically pour plates.

Figure 2.6: CAS agar plates preparation protocol.

2.14 Efficacy evaluation of siderophores *in vitro*

2.14.1 Disc diffusion assays

Antimicrobial activity of diffused products of *B. amyloliquefaciens* cells grown at different iron concentrations was assessed using 9 mm antibiotic filter disks (Whatman, Grade AA DISCS, 9 mm, GE Healthcare Life Sciences), based on formation of inhibition zones. In detail, *P. syringae* pv. *tomato* (*Pto*) and *P. syringae* pv. *tabaci* (*Pta*) were grown in 50 mL LB medium and incubated overnight inside a rotating shaker at 200 rpm and 28 °C, until naive stationary phase growth. Liquid cultures were then centrifuged at 4500 rpm for 15 minutes and bacterial pellet was resuspended in equal volume of sterile dH₂O. 195 mL of succinate agar medium with an increasing concentration of iron were inoculated with 5 mL of the diluted bacterial cells to adjust a final concentration of 5×10^6 cfu mL⁻¹. The mixture was poured into 120 x 120 mm square Petri dishes. Plates were pre-incubated at 28 °C for 24 hours before adding *B. amyloliquefaciens* suspension.

B. amyloliquefaciens was grown in 5 mL LB medium cultures that were incubated overnight inside an orbital shaker rotating shaker at 200 rpm and 37 °C. Liquid cultures were centrifuged for 15 minutes at 4500 rpm and bacterial pellet was resuspended in 2.5 mL of sterile dH₂O. Following one day of incubation at 28°C, an aliquot of 70 µL of *B. amyloliquefaciens* culture suspension was pipetted on a 9 mm Whatman disc that were placed on succinate plates containing each pathogen suspension. As a control, sterile distilled water was used in place of *B. amyloliquefaciens* suspension. Plates were incubated at 28 °C for 7 days before the diameter of the clear halo surrounding the disk was measured in three different axes. Radial growth of *B. amyloliquefaciens* strains outside the disk, if any, was also recorded.

2.14.2 Broth microdilution method

Overnight grown naive stationary phase cultures of each bacterial pathogen were streaked on LB plates to check their purity. Cultures were then adjusted to a concentration of 5×10^6 cfu mL⁻¹. The adjusted bacterial *inocula* (10 µL) were added to each well of sterile U based microtitre plates (COSTAR 3595, CORNING INCORPORATED) containing appropriate concentration of LB or succinate medium

and CFCF to reach 1x and test concentrations respectively in the total volume, which was 100 μL on each well. Consequently, a final *inoculum* concentration of 10^5 cfu mL^{-1} was obtained in each well. Plates were incubated at 28 °C for 48 hours.

One target bacterium was assayed on each plate, representing one experiment, in five replicates (wells) for each of the 50%, 25% and 10% CFCF concentrations. The experiments were carried out on *B. amyloliquefaciens* CFCF with increasing iron concentration (0, 50, 400, 1000 $\mu\text{g/L}$) as inhibitory agent. Blank wells (CFCF and medium only) containing each test concentration were also included. Two independent biological experiments (*inocula*, CFCF extracts, tested plates) were performed for each target bacterium. Absorbance measurements were recorded at 0, 24 and 48 hours at 28 °C using triplicate readings of a multi-detection microplate reader (Fluostar galaxy, BMG Lab technologies) at 595 nm. Blanks were subtracted from these readings. The plate design is depicted in Figure 2.7.

Broth tests were elaborate using a kinetic study for *Pto* and based on the same design in a single biological experiment. Optical densities were measured for 48 hours at 28 °C using a multi-detection microplate reader (Bio-Tek-Synergy HT Microplate Reader, Bio-Tek Instruments, Winooski, Vt, USA) at 600 nm and automatically recorded for each well every 30 minutes.

Note: CFCF was obtained as described in session 2.1. Three different concentrations of CFCF were prepared:

- 50% CFCF concentration (2.775 mL CFCF in 2.220 mL 2XLB)
- 25% CFCF concentration (1.385 mL CFCF in 3.610 mL 2XLB)
- 10% CFCF concentration (0.555 mL CFCF in 4.440 mL 2XLB)

	1	2	3	4	5	6	7	8	9	10	11	12
A	0µg/L 10%	0µg/L 25%	0µg/L 50%	50µg/L 10%	50µg/L 25%	50µg/L 50%	400µg/L 10%	400µg/L 25%	400µg/L 50%	1000µg/L 10%	1000µg/L 25%	1000µg/L 50%
B	0µg/L 10%	0µg/L 25%	0µg/L 50%	50µg/L 10%	50µg/L 25%	50µg/L 50%	400µg/L 10%	400µg/L 25%	400µg/L 50%	1000µg/L 10%	1000µg/L 25%	1000µg/L 50%
C	0µg/L 10%	0µg/L 25%	0µg/L 50%	50µg/L 10%	50µg/L 25%	50µg/L 50%	400µg/L 10%	400µg/L 25%	400µg/L 50%	1000µg/L 10%	1000µg/L 25%	1000µg/L 50%
D	0µg/L 10%	0µg/L 25%	0µg/L 50%	50µg/L 10%	50µg/L 25%	50µg/L 50%	400µg/L 10%	400µg/L 25%	400µg/L 50%	1000µg/L 10%	1000µg/L 25%	1000µg/L 50%
E	0µg/L 10%	0µg/L 25%	0µg/L 50%	50µg/L 10%	50µg/L 25%	50µg/L 50%	400µg/L 10%	400µg/L 25%	400µg/L 50%	1000µg/L 10%	1000µg/L 25%	1000µg/L 50%
F	0µg/L 10%	0µg/L 25%	0µg/L 50%	50µg/L 10%	50µg/L 25%	50µg/L 50%	400µg/L 10%	400µg/L 25%	400µg/L 50%	1000µg/L 10%	1000µg/L 25%	1000µg/L 50%
G	0µg/L 10%	0µg/L 25%	0µg/L 50%	50µg/L 10%	50µg/L 25%	50µg/L 50%	400µg/L 10%	400µg/L 25%	400µg/L 50%	1000µg/L 10%	1000µg/L 25%	1000µg/L 50%
H	MOCK	MOCK	MOCK	MOCK	MOCK	MOCK	MOCK	MOCK	MOCK	MOCK	MOCK	MOCK

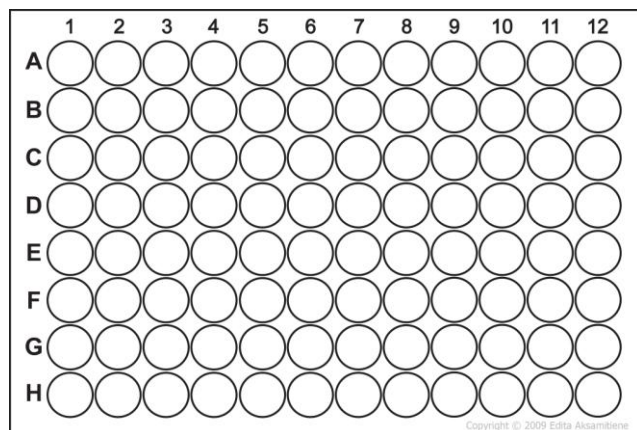


Figure 2.7: Virtual representation of the 96 wells culture plate used for sensitivity tests. Gray cells are blanks. In each plate wells from H1-H12 are used as MOCK to estimate the pathogens' growth in LB medium without any inhibition factor. 0, 50, 400 and 1000 µg/L Fe are the concentration of iron used in succinate medium for *B. amyloliquefaciens* growth.

2.15 Efficacy evaluation of siderophores *in planta*

2.15.1 Plant material and growth conditions

Tomato plants (*Solanum lycopersicum*) cv. ‘Belladonna F1’ and tobacco plants (*Nicotiana benthamiana*) were used throughout this study.

All experiments were carried out under environmentally controlled conditions. In detail, plants were grown at 25 and 18 °C (day and night, respectively) in an insect-proof greenhouse with 16 hours photoperiod. Additional daylight illumination was provided by standard mercury vapor reflector lamps (Sylvania HSR-400/4500K). Plants were potted in a mixture containing Klasmann Potgrond P blocking substrate and perlite (approximately 4:1). The first 10 days from potting, supplementary fertilizer (Comp 12-4-6 + micro; Aglukon) was used. Humidity was adjusted (approximately 90% using a Faran Cesio humidifier (Faran Industrial Ltd.).

2.15.2 Design and layout of preliminary experiments

Inoculum was prepared by suspending 48 hours liquid cultures of *Pta* rifampicin-resistant strain in *B. amyloliquefaciens* CFCF and adjusting cell densities to approximately 1×10^9 cfu/mL. The experimental process contained 3 blocks of plants of 12 plants each. Treatments differed at iron concentration of *B. amyloliquefaciens* LB cultures that were used to harvest CFCF. CFCF grown on Fe concentrations of 0 and 1000 µg / L were used in addition to a water suspension that was used as control treatment. Individual plants were inoculated by spraying (20 mL per plant) a hand-pump sprayer. Leaves were allowed to dry before collecting samples.

The total population of *Pta* was monitored on four upper leaves of *N. benthamiana* plants at the six true leaf stage. Pathogen population growth was determined by cell counts in leaf disc samples taken 11 and 15 days post inoculation (dpi). Four pooled samples, each containing three leaf discs (one disc per plant) were assembled in a total number of 12 plants per treatment. Samples were extracted as 8-mm-diameter leaf. Leaf discs were homogenized for 60 seconds with a hand tissue homogenizer in 0.8 mL of sterile distilled water. 0.2 mL of glycerol sterile was added and samples were stored at -20 °C. Aliquots of 0.1 mL from a 10-fold dilution series were plated on NA medium supplemented with 5 µg/mL rifampicin at 28 °C for 48 hours.

2.15.3 Design and lay out of full scale experiments

Two independent experiments were performed to evaluate *in planta* efficacy of *B. amyloliquefaciens* siderophores, one for each pathogen tested. The experimental design contained 5 plots of 12 plants each. Treatments differ in Fe concentration of succinate broth cultures used to harvest CFCF. In specific, treatment of Fe concentration of 0, 50, 1000, 2000 µg/L were used, while succinate medium (0 µg/L) served as a control. *Inoculum* was prepared by suspending stationary phase liquid cultures (grown for 48 h) of *Pta* or *Pto* rifampicin-resistant strain in *B. amyloliquefaciens* CFCF and adjusting cell densities to approximately 1×10^9 cfu/mL. Individual plants were sprayed to run off using a hand-pump sprayer and allowed to dry before sampling.

Colonization of *Pta* on *Nicotiana benthamiana* plants was monitored on four upper leaves of plants at the six true leaf stage. Pathogen population growth was determined by cell counts in leaf samples taken after 1, 7 and 14 days post inoculation (dpi). Four pooled samples, each containing six leaves from three different plants (two leaves per plant), were collected, summing up a total number of 12 plants per treatment. Leaves were homogenized for 60 seconds with a tissue homogenizer (HCT Shaping system SA) in BIOREBA extraction bags containing 10 mL of sterile distilled water. In 1 mL of the homogenized sample 0.2 mL of sterile glycerol was added to each sample to allow storage at -20 °C. Aliquots of 0.1 mL from a 10-fold dilution series were plated on NA medium supplemented with the 5 µg/mL rifampicin.

Colonization of *Pto* on tomato plants was monitored on four upper leaves of plants at the six true leaf stage. Pathogen population growth was determined by cell counts in leaf samples taken after 1, 4, 8 and 16 days post inoculation (dpi). Four pooled samples, each containing six leaves from three different plants (two leaves per plant), were collected, summing up a total number of 12 plants per treatment. Leaves were homogenized for 60 s with a tissue homogenizer (HCT Shaping system SA) in BIOREBA extraction bags containing 10 mL of sterile distilled water. In 1 mL of the homogenized sample 0.2 mL of sterile glycerol was added to each sample to allow storage at -20 °C. Aliquots of 0.1 mL from a 10-fold dilution series were plated on NA medium supplemented with the 5 µg/mL rifampicin.

2.16 Total RNA extraction from *B. amyloliquefaciens* cells

Total RNA was used as a template during the first strand cDNA synthesis. For the total RNA isolation from *B. amyloliquefaciens* cells, a TRIzol™ modified protocol was used.

Step 1: Isolation of nucleic acids (RNA-DNA).

Sample preparation

B. amyloliquefaciens cultures were incubated on succinate medium with different iron concentrations (0, 50, 1000, 2000 µg/L FeCl₃) at 37 °C in a rotating shaker at 200 rpm for 48 hours. 5 mL of each culture was centrifuged for 15 minutes at 4500 rpm and 4 °C. The supernatant was discarded and bacterial cell pellet was instantly frozen into liquid nitrogen and stored at -80 °C until use.

Homogenization of samples

The bacterial cell pellet was resuspended in 100 µL TE buffer (10 mM Tris-HCl, 1 mM EDTA, pH 8), containing 1 mg/mL lysozyme, by vigorous vortexing. It was then incubated for 20 minutes at 37 °C. Following incubation, 1 mL of TRIzol™ reagent (Thermo Fisher Scientific, USA) was added. Samples were vortexed vigorously and the homogenate was incubated for 10 minutes at room temperature. Samples were then centrifuged at 12000 g for 5 minutes at 4 °C and the supernatant was collected in a fresh tube.

Phase separation

0.2 mL of chloroform was added per 1 mL of TRIzol™ reagent (Thermo Fisher Scientific, USA). Samples were vortexed vigorously for 15 seconds and incubated for 10 minutes at room temperature. They were then centrifuged at 12,000 g for 15 minutes at 4 °C. Following centrifugation, the mixture separated into a lower red, phenol-chloroform phase, an interphase, and a colorless upper aqueous phase. RNA remains exclusively in the aqueous phase. The upper aqueous phase was carefully transferred without disturbing the interphase into fresh tube.

RNA precipitation

RNA was precipitated from the aqueous phase by mixing with 0.25 mL isopropanol and 0.25 mL of high salt solution (NaCl 1.2M and C₆H₅Na₃O₇ 0.8M). Samples were then vortexed vigorously for 15 seconds, incubated at room temperature for 10 minutes and centrifuged at 12,000 g for 30 minutes at 4 °C.

RNA wash

The supernatant was removed completely. The RNA pellet washed once with 0.5 mL 70% ethanol. The samples mixed by vortexing and centrifugated at 12,000 *g* for 10 minutes at 4 °C. The pellet was left to air dry for no more than 10 minutes in order to remove all leftover ethanol.

Redissolving RNA

RNA was dissolved in 30 µL ddH₂O by aspirating solution a few times through a pipette tip.

Step 2: Degradation of genomic DNA

In order to take highly pure total RNA, it is recommended to treat the samples with DNase I to avoid contamination with genomic DNA. Approximately 5 µg of total RNA are resuspended in 1x DNase I Buffer to a final volume of 100 µL. 2 units of DNase I (Biolabs) enzyme solution are added. The mixture was incubated at 37 °C for 10 minutes. Subsequently, 1µL of 0.5 M EDTA was added, to a final concentration of 5 mM. The DNase I enzyme was heat inactivated for 10 minutes at 75 °C. 10 µL of CH₃COONa 3M and 250 µL ice-cold ethanol (100%) were then added in order to precipitate the total RNA molecules. Precipitation took place at -20 °C, overnight. The samples were then centrifuged samples at 4 °C for 30 minutes at full speed and the formed pellet, that contained the RNA molecules, was then washed with 75% ethanol and air dried 10 minutes. The pellet was resuspended into 15 µL sterile double-distilled water (ddH₂O)

2.17 Reverse transcription

Reverse transcription is a procedure of first strand cDNA synthesis, using as template total mRNA. The responsible enzyme for this process is reverse transcriptase. Reverse transcriptase is an RNA-dependent DNA polymerase that uses RNA as a template to synthesize single strand DNA molecules. Reverse transcription provides a useful tool for studying of RNA transcripts through more stable DNA molecules. Reverse transcription takes place in two steps: (i) firstly the total isolated RNA is denaturated and primers are hybridized, (ii) then the reverse transcriptase polymerizes the RNA-primer molecules and synthesizes first strand cDNA. A typical reverse transcription protocol is demonstrated below (Table 2.15).

Table 2.15: A typical reverse transcription protocol.

Step 1: RNA denaturation and primer hybridization	Add to a PCR tube: <ul style="list-style-type: none"> • 0.1-0.5 µg of total RNA template, • primer Oligo dT₁₇ (50 pmoles) • dNTPs⁽²⁾ (10mM). 	Mix well and heat at 65 °C for 5 minutes.
Step 2: RNA dependent DNA polymerization	Add: <ul style="list-style-type: none"> • 20 units of RNase inhibitor, • Reverse transcriptase Buffer • 200 units Reverse transcriptase⁽⁴⁾ 	Mix well and incubate at 42 °C for 1 hour.
Step 3: Enzyme deactivation		Incubate the tube at 75 °C for 15 minutes.
Step 4: Store		Store the mixture at 4 °C.

⁽¹⁾Oligo dT₁₇ primer consists of 17 thymines and hybridizes to the polyA end of mRNA. For non polyadenylated RNA's (for example rRNA's), primers that hybridize randomly to RNA can be used.

⁽²⁾dNTP's mixture consists of dATP, dCTP, dGTP and dTTP and are used as "buildingblocks" for DNA polymerization.

⁽³⁾In this study Primescript Reverse Transcriptase (Takara) was used.

2.18 Quantitative Real-Time PCR

Primer Design

Primer pairs for all qRT-PCR assays were designed with Primer Express™ Software (Thermo Fisher Scientific, USA). The amplicons generated by these primers were 90 long. Primer pairs used for expression studies were designed based on *B. amyloliquefaciens* corresponding to gene sequences. The complete list of primer sequences is provided in table 2.16.

Chapter 2: Materials and Methods

Table 2.16: Primers names and primers sequences used for qPCR

Primers name	Primers sequence
<i>gyrA_fw</i>	ACCGTAACGGAATGAGAATCGT
<i>gyrA_rv</i>	GCAGGGCCGTTTGTGGTAC
<i>dhbC_fw</i>	TGACCGCTGAAAAGGATATCG
<i>dhbC_rv</i>	TCACATCCGCAGCGAATGTA
<i>bmyC_fw</i>	ACGGCTGCTGCAGATGCT
<i>bmyC_rv</i>	ACGGTCATAGACTTGTTTATTAAACA
<i>yczE_fw</i>	TCTTTCTGTTCGGCCAATGGT
<i>yczE_rv</i>	TCGGGAGTGTCTCGTGAAC
<i>fenC_fw</i>	TACACAGCTCCCCGCAATG
<i>fenC_rv</i>	TGAGTCCTCAATCCCGACTTG
<i>srfAC_fw</i>	GCATGAATGTGATTATGGACCG
<i>srfAC_rv</i>	TGTCGGTTACATGTGTCAGATCG
<i>comK_fw</i>	GCCGATTCACATCATCGACA
<i>comK_rv</i>	ATGTGATTTGAAGGGTCCACCA
<i>cheC_fw</i>	GAATGGAAGGCGACATGACC
<i>cheC_rv</i>	AATATCAAATCCGGATTCCCG
<i>deqU_fw</i>	GGTAGCAGAAGGTGACGATGG
<i>deqU_rv</i>	CCTCTACACCATTTACATTCGGC
<i>yusV_fw</i>	GAGAGCTCGCTATTTTGCCG
<i>yusV_rv</i>	GCCACTGCGTCTTCGTCCT
<i>swrA_fw</i>	ACGGATATTAAACGGTCCATGC
<i>swrA_rv</i>	TCTCTCCGTCATCCACAACG

qRT-PCR amplification

StepOnePlus™ Real-Time PCR System (Thermo Fisher Scientific, USA) was used for qPCR and the samples were treated according to the manufacturer's instructions. 0.2 mM forward and reverse primers and SYBR™ Green PCR Master Mix (Thermo Fisher Scientific, USA) was used in each PCR reaction. Samples and standards were run in triplicates on 96 well PCR plates (Thermo Fisher Scientific, USA) according to the manufacturer's instructions. An optimized volume of cDNA was used for the amplification of each gene. The reaction components were exactly as above and for every single test sample a qPCR for both the target (*dhbC*, *bmyC*, *fenC*, *sfpAC*, *yczE*, *comK*, *cheC*, *swrA*, *deqU*, *yusV*) and the housekeeping gene (*gyrA*) was performed. The following PCR program was used to amplify all genes (Table 2.17).

95 °C	10 minutes	} 40 cycles
95 °C	15 seconds	
60 °C	1 minute	

2.19 Data analysis (by Dr. Ioannis Theologidis)

In vitro tests

Measurements for each species were collected in triplicate 96-well plates, which were considered as different experimental blocks. OD measurements were modeled using Linear Mixed Effects Models (LMMs) in statistical language R in two steps.

First, in order to test for the existence of background effects, control samples (wells where pathogens were absent) were modeled using a LMM in which the dependent variable was the logOD. The second step comprised the actual analysis, in which only samples containing pathogens were included. Each species was analyzed separately. Ordinary least square estimates of OD and their corresponding standard errors were extracted and plotted.

For the analysis of disk diffusion susceptibility tests, radial growth was modelled by the use of LMMs, as above.

In planta tests

Total pathogen growth was modeled using LMM to log₁₀-transformed data (number of bacterial CFU) for each time point. Time after inoculation and treatment as well as their interaction were modeled as fixed factors, while plant individuals nested within block were the random independent variables. The *z*-ratio tests were used for testing the significance of responses and Tukey tests for post hoc comparisons.

qPCR

The quantitative output of the qRT-PCR consists of an amplification curve, which is composed of a set of cycle numbers and associated fluorescence intensities that are ulteriorly summarized in a single value called the cycles to threshold (Ct). Ct is a unitless value defined as the fractional cycle number at which the sample fluorescence signal passes a fixed threshold above the baseline.

For quantification of gene expression the cycle of threshold (Ct) for each gene transcript was determined. The baseline signal and threshold signal of fluorescence were determined automatically by the PCR machine.

Delta Ct method

Calculation was conducted in Microsoft Excel 2007. Relative mRNA levels of the genes of interest were calculated via $2^{-\Delta Ct}$ method, where ΔCt represents the difference in threshold cycle values between the gene of interest and the housekeeping reference gene.

$$Ct_{\text{target gene}} - Ct_{\text{housekeeping gene}} = \Delta Ct$$

$$\text{Relative quantity} = 2^{-\Delta Ct}$$

Linear Mixed Models analysis

Log Fold Changes (logFC) between each treatment and the reference concentration of 2000 $\mu\text{g} / \text{L}$ Fe were calculated by the implementation of Linear Mixed Models analysis in R using the housekeeping gene *gyrA* as control for normalization (Steibel *et al.* 2009)

RESULTS

3.1 Siderophore production of *B. amyloliquefaciens*

The ability of *B. amyloliquefaciens* to produce siderophores was measured by CAS agar assay (§2.13). Siderophore production is detected by color change from blue to orange/yellow (Figure 3.1). To get the iron out of the dye, bacteria express high affinity uptake system chelators called siderophores but only to a level that satisfies their requirements for the metal. This results in relatively small halos around the colonies. Probably due to polymerization of the blue dye, diffusion seems to be minimal and the zones are well focused.

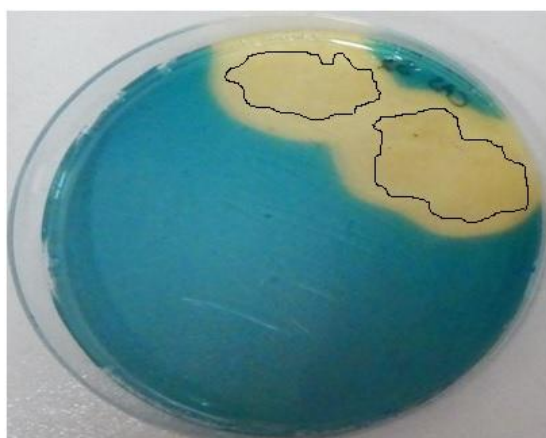


Figure 3.1: Siderophore production is detected by CAS agar assay. Color change from blue to orange/yellow indicates siderophore production.

3.2 Knock-out of the siderophore synthesis operon

3.2.1 Cloning of the erythromycin resistance gene into pCR®2.1-TOPO®

Primers *Erm^r_MluI_F* and *Erm^r_SacII_R* (Table 2.6) have been used to amplify the erythromycin resistance gene from plasmid pMUTIN-GFP using polymerase chain reaction (PCR) (§ 2.3). PCR products were electrophoresed on agarose gel 1% (w/v) and successful DNA fragment amplification was determined on the basis of the expected molecular weight (Figure 3.2).

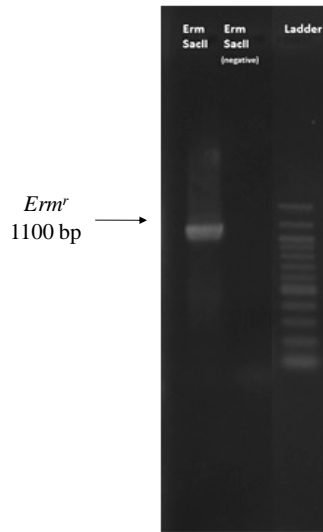


Figure 3.2: Electrophoresis of PCR products with *Erm^r_MluI_F* and *Erm^r_SacII_R* primers. The *Erm^r* gene amplicon is depicted in lane 1, in the lane 2 the negative control and in lane 3 the 100 bp DNA Ladder (Figure 2.1 b).

Amplified DNA fragments were extracted from the agarose gel (§ 2.4) and ligated into plasmid vector pCR®2.1-TOPO® (Invitrogen™) (Figure 2.2a) with A-tailing to develop plasmid pCR®2.1-TOPO®-*Erm^r*. *E. coli* strain DH5α was transformed (§ 2.6) using plasmid pCR®2.1-TOPO®-*Erm^r*. Clones carrying this plasmid were selected after growth of the cells in nutrient agar (NA) plates supplemented with kanamycin (50 µg/mL) as selective factor. The colonies that showed kanamycin resistance were considered to have received the plasmid. Plasmid DNA was extracted by selected colonies and isolated plasmids were digested with *EcoRI* (Table 2.9) and digestion products were electrophoresed on 1% (w/v) agarose gel. Successful cloning was determined based on the expected molecular weight (Figure 3.3).

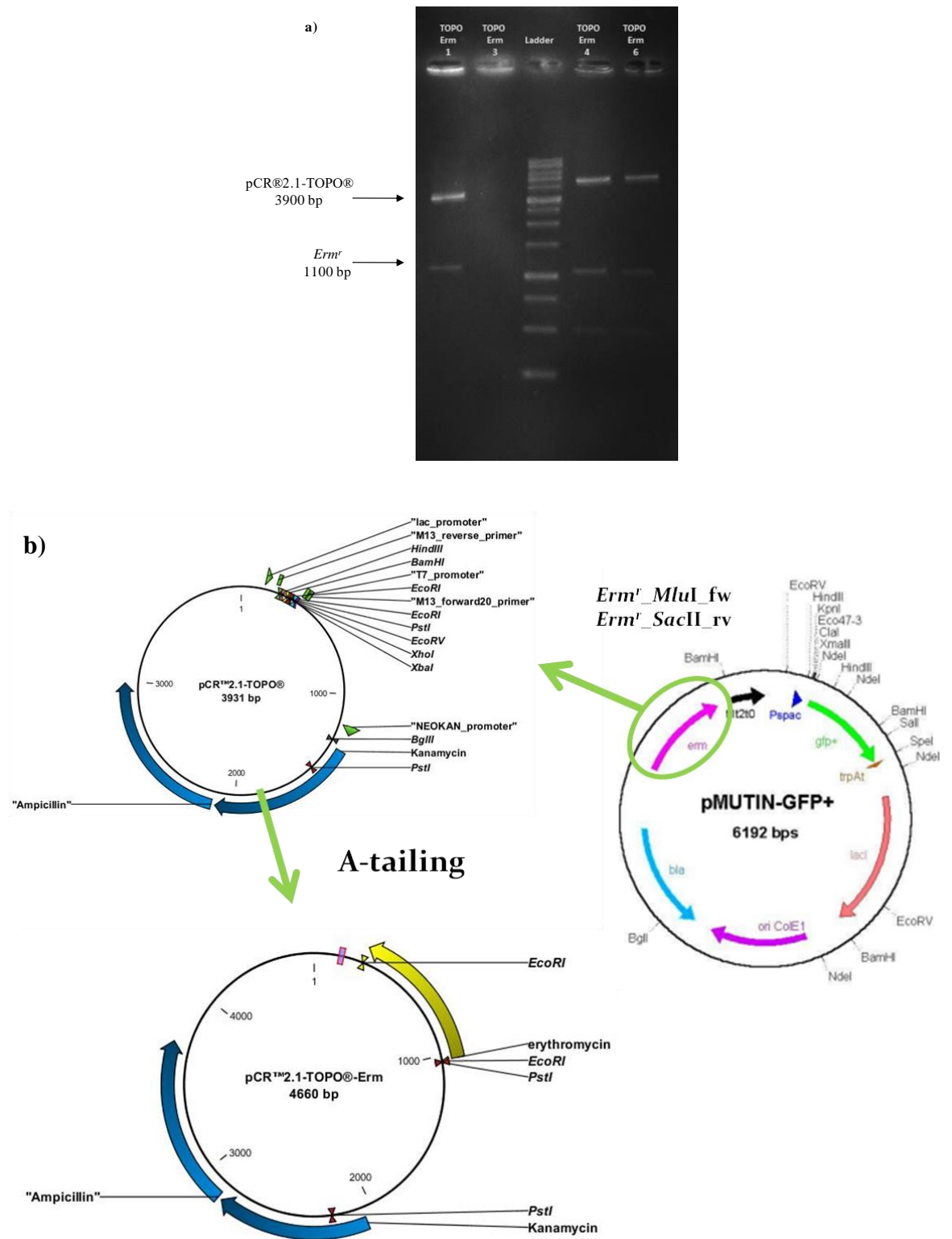


Figure 3.3: a) The *Erm^r* cut out from pCR®2.1-TOPO® vector. The *Erm^r* in lane 1, 4 and 6 is cut out from the vector pCR®2.1-TOPO® with *EcoRI*. Two bands are formed, the upper band indicates the rest of the pCR®2.1-TOPO® vector on about 3900 bp while the lower band on 1100 bp indicate the *Erm^r* insert. The 1 Kb DNA Ladder is depicted in lane 3. b) Schematic representation of *Erm^r* cloning.

Direction of the erythromycin resistance gene (*Erm^r*) in pCR®2.1-TOPO® was also assessed by restriction digestion with *Mlu*I or *Sac*II enzymes that recognize the *Erm^r* restriction sites, in combination with *Sac*I that only cuts into the plasmid multicloning site (Table 2.10-11). Digestion products were electrophoresed on 1% (w/v) agarose gel (Figure 3.4) and directional cloning of *Erm^r* was evaluated based on DNA fragment size.

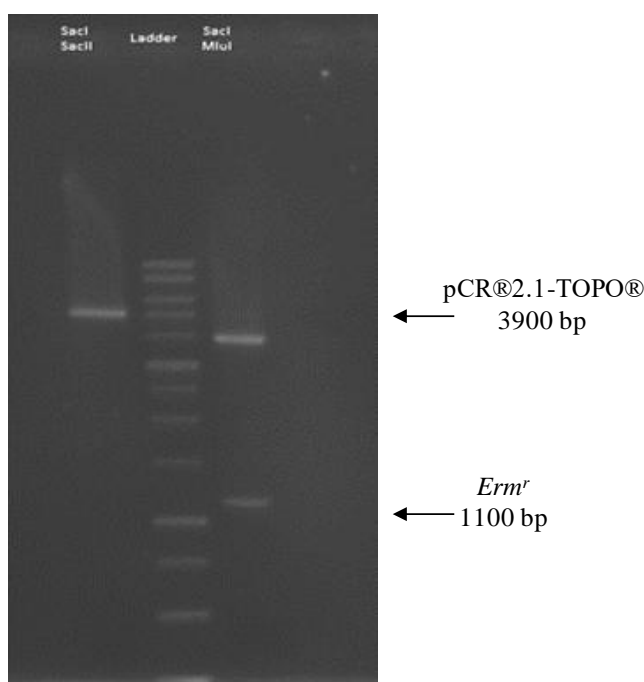


Figure 3.4: Direction of *Erm^r* in pCR®2.1-TOPO®. The *Erm^r* at 1100 bp depicted in lane 3 is cut out from the pCR®2.1-TOPO® vector at 3900 bp with *Mlu*I/*Sac*I otherwise the band formed in lane 1 on almost 5000 bp, indicates pCR®2.1-TOPO®-*Erm^r* vector cut with *Sac*I/*Sac*II. In lane 2 is the 1 Kb DNA Ladder (Figure 2.1a). It is concluded that the direction of *Erm^r* in pCR®2.1-TOPO® is 3' →5'.

3.2.2 Cloning of *dhbC* and *dhbF* recombination sites into plasmid pCR®2.1-TOPO®-*Erm^r*

Primer pairs *dhbC*359_*Bam*HI_fw/*dhbC*870_*Sac*II_rv or *dhbF*121_*Mlu*I_fw/*dhbF*866_*Kpn*I_rv (Table 2.6) have been used to amplify, using PCR, partial sequence of *dhbC* or *dhbF* genes from total genomic DNA of *B. amyloliquefaciens*. In specific, PCR products were electrophoresed on agarose gel 1% (w/v) and successful DNA fragment amplification was evaluated on the basis of expected molecular weight that corresponds to 511 bp in the case of *dhbC* or 745 bp in the case of *dhbF* (Figure 3.5).

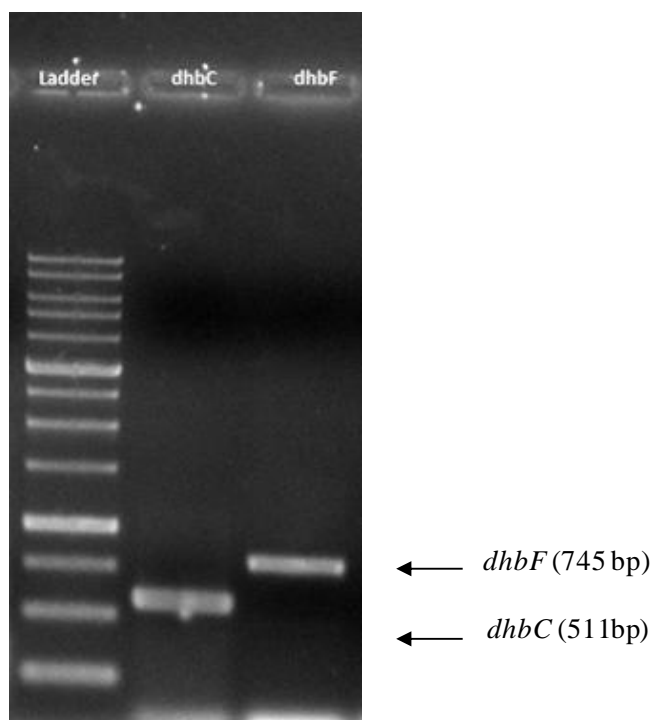


Figure 3.5: Electrophoresis of PCR products. The PCR product amplified using primer pair *dhbC359_BamHI_fw / dhbC870_SacII_rv* is depicted in lane 2. Similarly, the PCR product amplified using primer pair *dhbF121_MluI_fw / dhbF866_KpnI_rv* is depicted in lane 3. The 1 Kb DNA Ladder is depicted in lane 1.

The partial *dhbC* sequence was cloned in pGem[®]-T Easy vector before subcloned in PCR[®]2.1-TOPO[®] -*Erm^r* 1, in order to enhance *Bam*HI and *Sac*II digestion yield. In detail, amplified DNA fragments were extracted from the agarose gel, cloned into the plasmid vector pGem[®]-T Easy (Figure 2.2b) to develop plasmid pGem[®]-T Easy-*dhbC*. *E. coli* strain DH5 α competent cells were transformed (§2.12) and clones carrying the plasmids were selected on nutrient agar (NA) plates containing 100 μ g/mL ampicillin. Colonies that exhibited resistance to ampicillin were considered to have received the plasmid. Plasmid DNA (§2.7) was extracted by such colonies and screened for cloning success by digestion with *Bam*HI and *Sac*II (Table 2.12) and evaluation of the size of digestion products after electrophoresis on 1% (w/v) agarose gel (Table 2.4) (Figure 3.6).

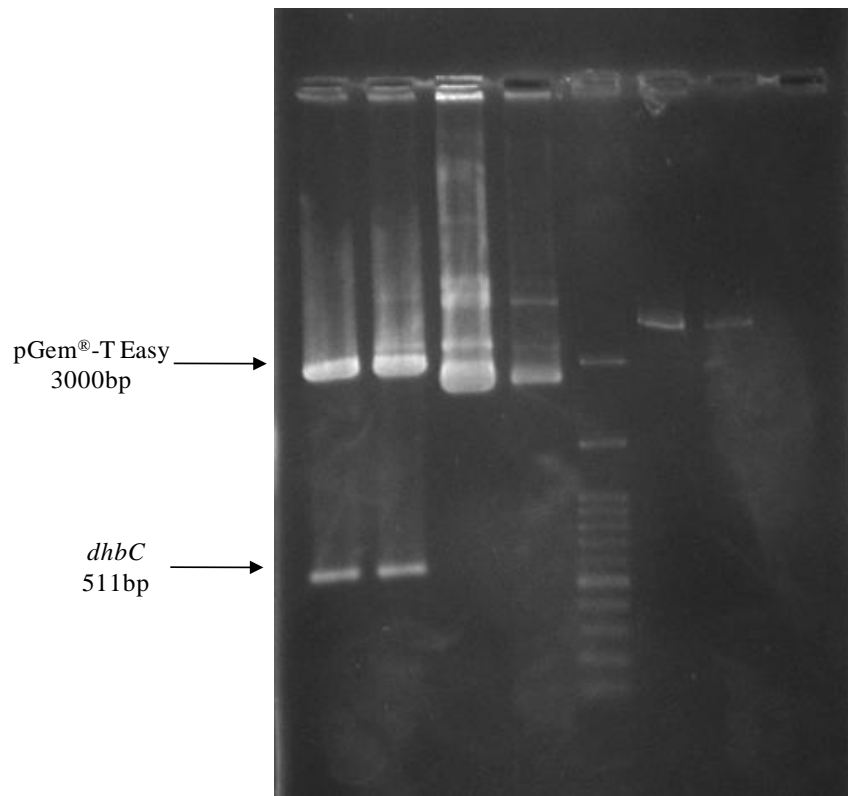


Figure 3.6: The *dhbC* cut out from pGem[®]-T Easy vector. The *dhbC* in lane 1 and 2 is cut out from the vector pGem[®]-T Easy with *Bam*HI and *Sac*II. Two bands are formed, the upper band indicates the pGem[®]-T Easy vector backbone on about 3000 bp while the lower band on 511 bp indicates the *dhbC* insert. In the other lanes no insert appears at 511 bp. The 1 Kb DNA Ladder (Figure 2.1 a) is depicted in lane 3.

The *dhbC* DNA fragment was extracted from the gel and then ligated into the PCR[®]2.1-TOPO[®]-*Erm*^r plasmid (§2.9). The ligation product was transformed into competent *E. coli* DH5 α cells and plated onto media under kanamycin selection (50 μ g/mL). Single colonies were picked from the plates and were grown overnight. Plasmid DNA was extracted and digested with *Bam*HI and *Sac*II (Table 2.12) that yields the partial *dhbC* sequence (Figure 3.7a) or *Bam*HI and *Mlu*I that yields the *dhbC-Erm*^r complex (Figure 3.7b). The resulting DNA fragments were separated on a 1% agarose gel to confirm successful directional cloning of the partial *dhbC* gene into PCR[®]2.1-TOPO[®]-*Erm*^r. Successful cloning would yield two bands following *Bam*HI and *Sac*II digestion; one at about 511 bp and one at about 5000 bp (Figure 3.7a). In addition, two bands were expected following *Bam*HI and *Mlu*I digestion; one band at about 1611 bp and one band at about 3900 bp (Figure 3.7 b). Results suggest that two out of four selected clones (lanes 1 and 4) carry plasmids with the appropriate inserts.

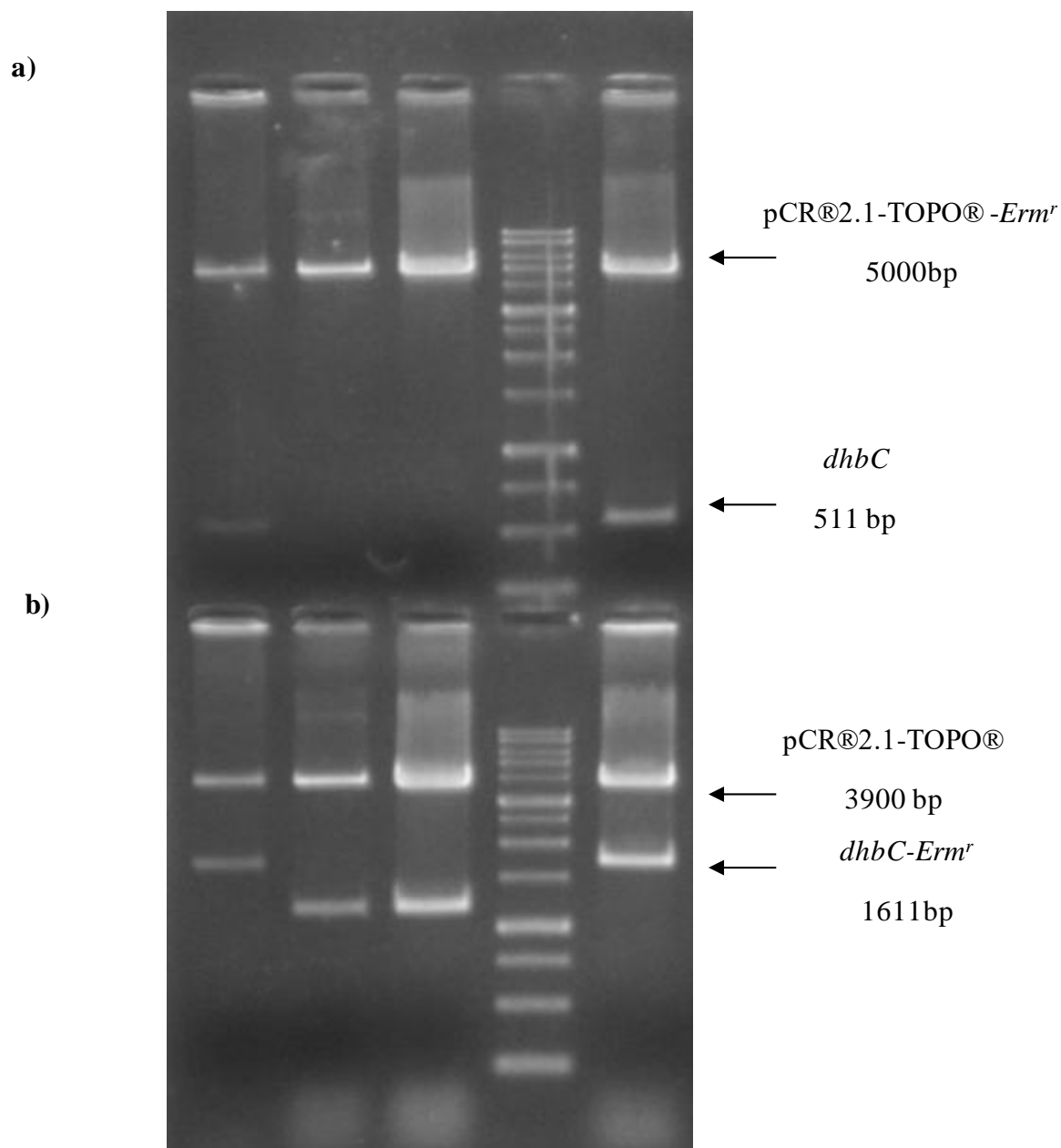


Figure 3.7: The *dhbC-Erm^r* cut out from pCR®2.1-TOPO® vector. a) The *dhbC* in lane 1 and 5 is cut out from vector PCR®2.1-TOPO®-Erm^r using *Bam*HI and *Sac*II. Two bands are formed, the upper band indicates PCR®2.1-TOPO® -Erm^r vector at about 5000 bp while the lower band, at 511 bp indicates the *dhbC* insert b) The *dhbC-Erm^r* in lane 1 and 5 is cut out from the vector PCR®2.1-TOPO® with *Bam*HI and *Mlu*I. Two bands are formed; the upper indicates the PCR®2.1-TOPO® vector backbone at about 3900 bp while the lower band, at 1611 bp, indicates the *dhbC-Erm^r* insert. The 1 Kb DNA Ladder is depicted in lane 4.

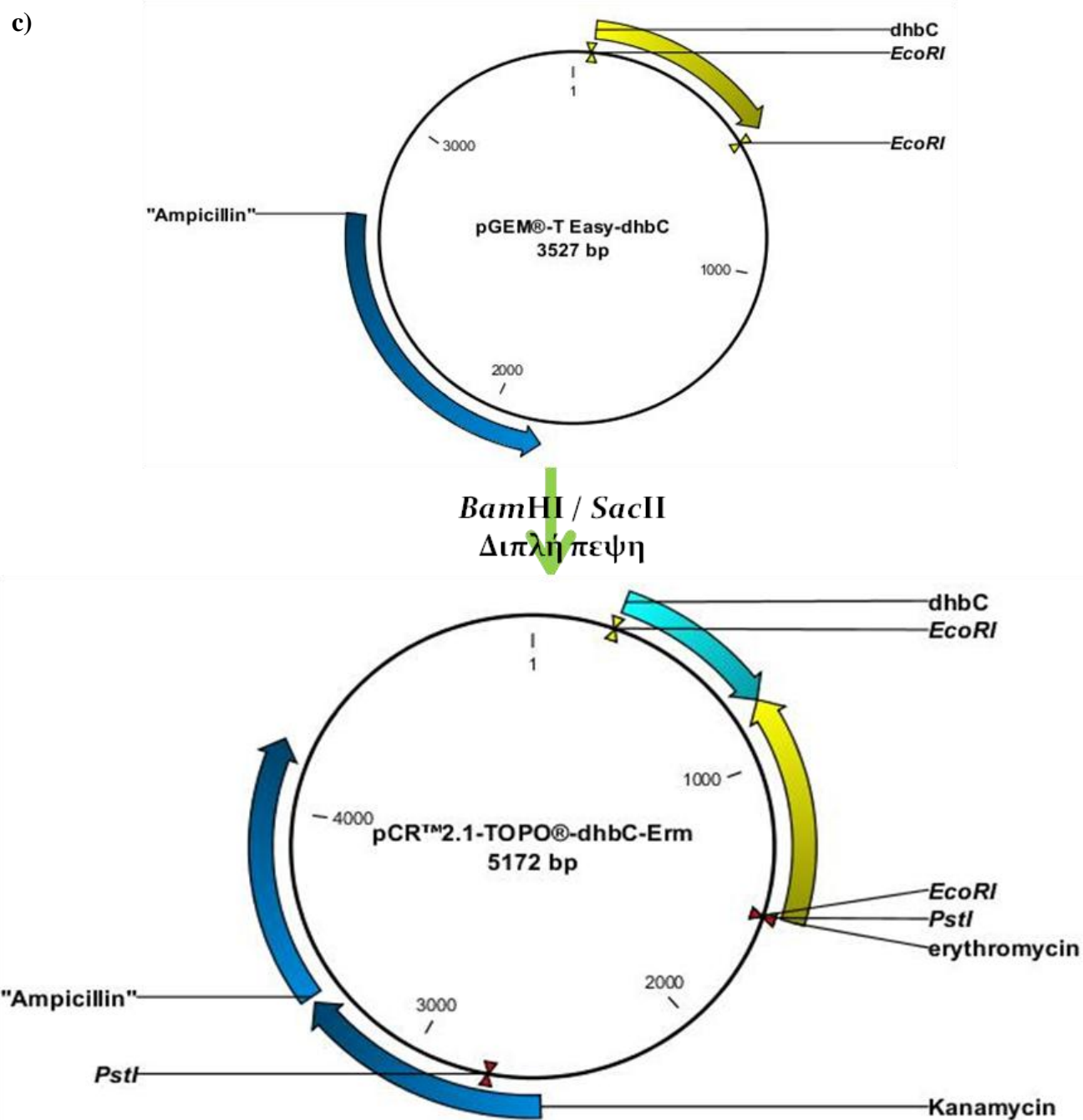


Figure 3.7 c): Schematic representation of *dhbC* cloning in pCR®2.1-TOPO® - *Erm^r*.

The partial *dhbF* sequence was cloned in pGem®-T Easy vector before subcloned in PCR®2.1-TOPO®-*dhbC-Erm^r*, in order to enhance *MluI* and *ApaI* restriction enzymes' yield. In detail, amplified DNA fragments were extracted from the agarose gel and cloned into the plasmid vector pGem®-T Easy to develop plasmid pGem®-T Easy-*dhbF*. *E. coli* strain DH5α competent cells were transformed and clones carrying

plasmids were selected on nutrient agar (NA) plates containing 100 µg/mL ampicillin. Colonies that showed ampicillin resistance were considered to have received the plasmid. Plasmid DNA was extracted by selected colonies and screened for cloning success by digestion with *Mlu*I and *Apa*I and evaluation of the size of digestion products after electrophoresis on 1% (w/v) agarose gel (Figure 3.8).

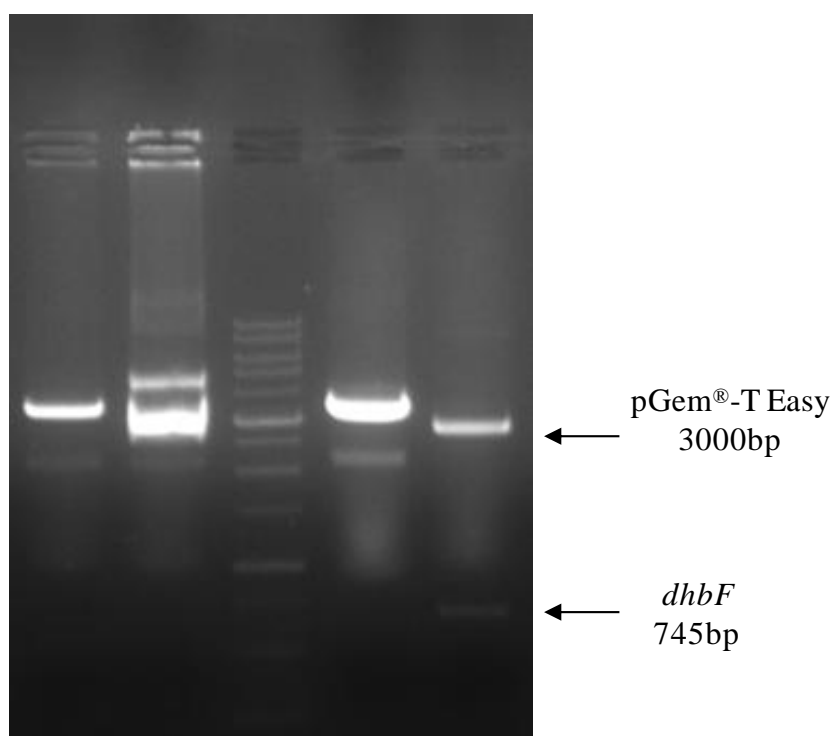


Figure 3.8: Screening for the partial *dhbF* gene cloning into pGem[®]-T Easy vector. The *dhbF* partial sequence band in lane 5 is cut out from the vector pGem[®]-T Easy. In clones carrying the *dhbF* sequence, two bands are formed following *Mlu*I and *Apa*I digestion: the upper band corresponds to the pGem[®]-T Easy vector backbone at about 3000 bp while the lower band, at 745 bp, corresponds to the *dhbF* insert. In the other lanes no insert appears at 745 bp. The 1 Kb DNA Ladder is depicted in lane 3.

The *dhbF* DNA fragment was extracted from the gel and then ligated into the PCR[®]2.1-TOPO[®]-*dhbC*-*Erm*^r. The ligation product was transformed into competent *E. coli* DH5 α cells and plated onto media under kanamycin selection. Single colonies were selected and grown overnight. Plasmid DNA was extracted and digested with *Mlu*I and *Apa*I, yielding the partial *dhbF* sequence; alternatively, plasmid DNA was digested with *Kpn*I and *Apa*I, yielding the *dhbC*-*Erm*^r-*dhbF* complex (Figure 3.9).

Chapter 3: Results

The resulting DNA fragments were separated on a 1% agarose gel to confirm successful directional cloning of the partial *dhbF* gene into PCR®2.1-TOPO®-*dhbC-Erm^r*. Two bands were expected to appear following *Mlu*I and *Apa*I digestion; one band at about 745 bp and one band at about 5511 bp (Figure 3.9). In addition, two bands were expected to appear following *Kpn*I and *Apa*I digestion; one band at about 2356 bp and one band at about 3900 bp (Figure 3.7b).

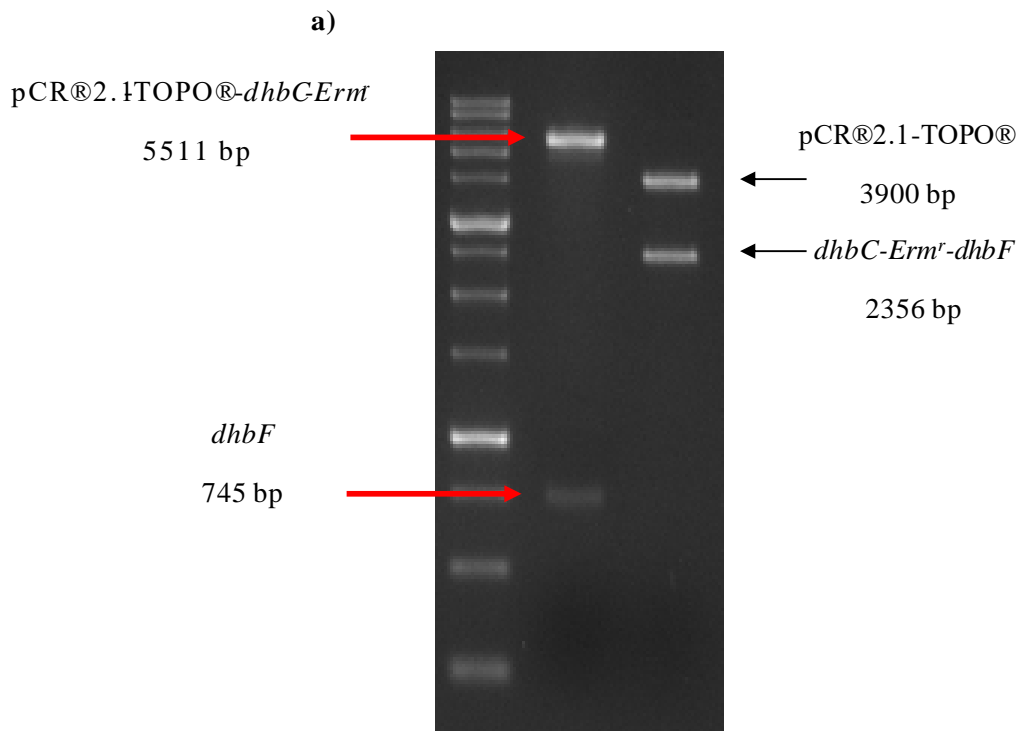


Figure 3.9 a): The *dhbC-Erm^r-dhbF* cut out from PCR®2.1-TOPO® vector.

a) The *dhbF* in lane 2 is cut out from vector PCR®2.1-TOPO®-*dhbC-Erm^r* using *Mlu*I and *Apa*I. Two bands are formed, the upper band indicates PCR®2.1-TOPO®-*dhbC-Erm^r* vector on about 5511 bp while the lower band on 745 bp indicate the *dhbF* insert. The *dhbC-Erm^r-dhbF* in lane 3 is cut out from the vector PCR®2.1-TOPO® using *Kpn*I and *Apa*I restriction enzymes. Two bands are formed; the upper indicates the PCR®2.1-TOPO® vector backbone at about 3900 bp while the lower band, at 2356 bp, indicates the *dhbC-Erm^r-dhbF* insert. The 1 Kb DNA Ladder is depicted in lane 1.

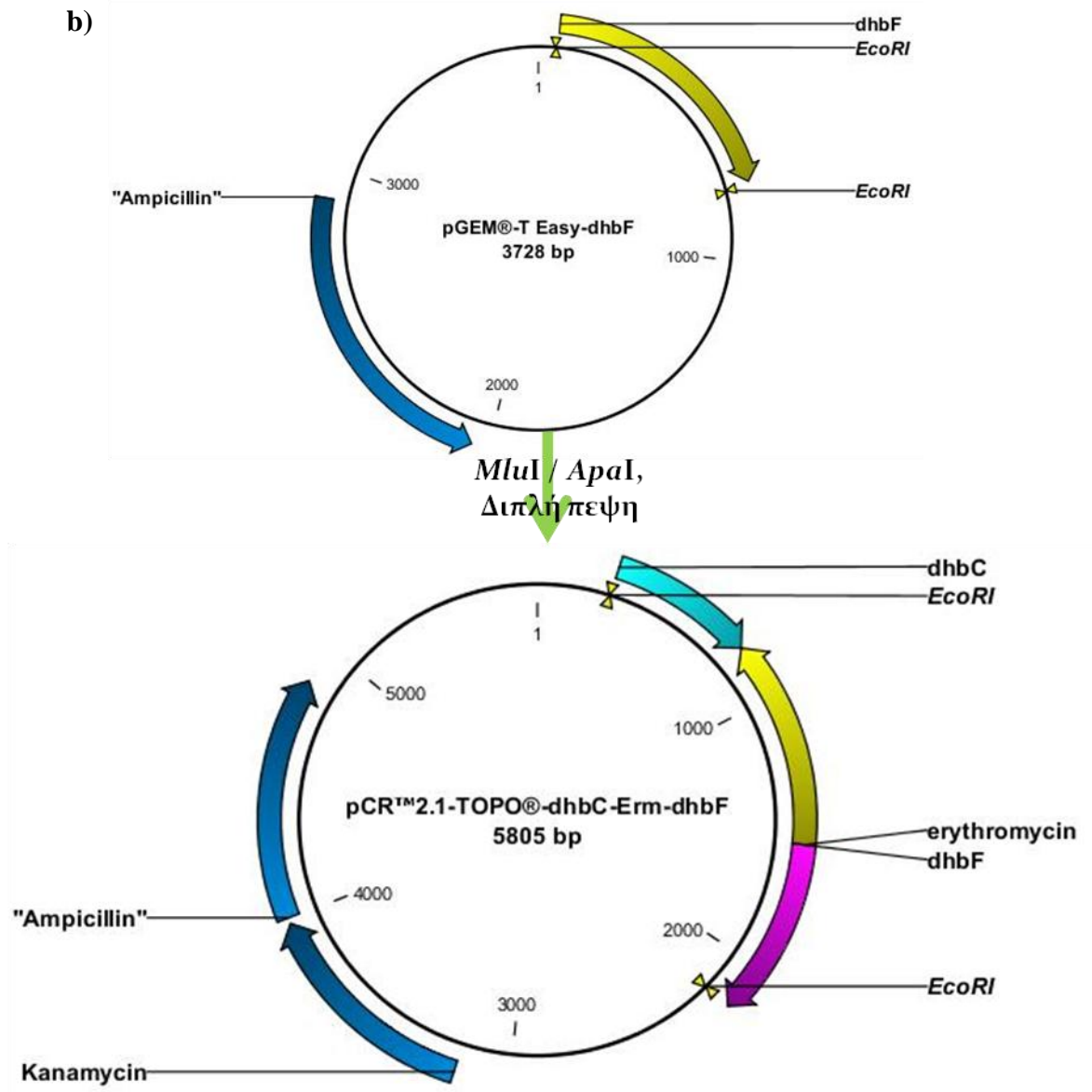


Figure 3.9 b): Schematic representation of *dhbF* cloning in pCR[®]2.1-TOPO[®] - *dhbC*-*Erm*^r.

3.2.3 Sequencing of *dhbC*-*Erm*^r-*dhbF* construct

Following PCR amplification of construct *dhbC*-*Erm*^r-*dhbF* using plasmid PCR[®]2.1-TOPO[®]-*dhbC*-*Erm*^r-*dhbF* as a template were dispatched to VBC Inc. (Austria), that returned bidirectional sequences (Figure 3.10 a). The sequencing revealed the successful cloning of the construct *dhbC*-*Erm*^r-*dhbF* in PCR[®]2.1-TOPO[®]. Alignment of sequences was carried out with the basic sequence alignment BLAST program run against the database from National Center for Biotechnology Information Blast (www.ncbi.nlm.nih.gov/BLAST) (Figure 3.10 b-c). The BLAST search revealed high identity of *dhbC* and *dhbF* with other *Bacillus* sequences. The

Chapter 3:Results

fully annotated *B. amyloliquefaciens* MBI600 genome sequence is confidential and thus has not been submitted to NCBI. *DhbC* and *dhbF* genes are annotated as isochorismate synthase and diguanylate cyclase respectively in other *Bacillus* strains but not in *B. amyloliquefaciens* MBI600.

a)

dhbC

Erm^r
(reverse)

dhbF

```
G/GATCCCCGTTCCGGAGCCTGAGGGCTTTATGAGCGGTGTGGAACAAGGCGTATTCAACATTACGGAC
GGTCCGCTCAGCAAAATCGTGCTGTCAAGGACGCTTCATCTGACCGCTGAAAAGGATATCGACATTCTC
AGGCCGTCAAGCATTGGCGCAGCACAAACCCGCGCGGCTATACATTGCTGCGGATGTGACGGGAACGT
CAGAAACAAGAAAACGCTTTTCGGCGCAAGTCCTGAACTGCTGCTGTCCAAAATGGAACATCGATTG
TGCCAATCCGCTGGCAGGTTCCAGACCTCGCAGCACAGATCCCGCCGAGGATCAGAGAAGAGCGGAA
GAACTGCTGCAATCAGCAAAAGATCTGCATGAACATGCCGTAGTTGTGGCCGCCGTGGCCGCCGCCCTTA
AACCGTTCTGCCGTGTGCTTGATGTGCCGAAAAACCGTCACTCATTAAACTGAGGCGATGTGGCACCT
GTCCACCGAGGTAAAGGGAGAGCTTCGTGATCCGCCGC/GGTACTTGTTTTATATTTATAAGAGTTTT
GAAAATTGCTCACTTTTTCATGAGTTGGTTTATTATTTTGTAACTTAAATTTCTTTGGCTATGGCAAAT
GCTTAACTTGTCCATTTCCCGTAAATTGCTGCTTTGACCGATTTTATTCATTTGTCCATTGCAGATAACTT
AATCTGTCAGTAGATAAGTTGAATAGCAGTCTTTTAAATTTGACTTATGAGCACAGTGAAATTAAGTG
TTCTATAAGATGTCAAAGTTAAGGGATTGTTTGTCTCCATATTTAACAACCCTCATAAGGAATGGTAAA
TTCGTGTGTTTAATAATTTTTTACCAAAAACCTTCGGTACGCAGACTGTAGATAGACTAACAACCTTCTC
CTAAGATGTTTCGCATGGAACCTATAAGTGGCTTGTGATCCCAACGAGAACGTGTGAGTTCAGAGCTAAG
TCGTTAACGAATTCGACGGTGCCTTACGAAAGTAGGATTTGGTTTTCATTTGTACAGAATTATTTGAA
TGGGCGGTATGGTGTCTACAAGGTCTATTTATAACCTTCGATATATGCATGAAACAAAGTTTTACCCAGT
TAGCTCTTATAGCAGTTGACAAATGATTTTATGCAAGTAGTTCGTTACTTTGTGCGGTTTCATTTGTTA
AATTCATGGCAATGAATACTCGTTCATAACAGATAAAAATTATCAATAGATAATAAATTGCCCTCCTTTAT
TA/CGCGTCGCGTGCTGACGGAAGCCGCGTCATTACACGCCCGCTTCGAGGAGGGAGCAGACGGGCCGA
AGCAGATCATCAATCTCCATTTGAGGCTGCGATCGATGTCATAGATGTGAGTTCAGAAGCTGATCCGCA
GCAGGCCGCACTCAGACTCATGCAGACAGATTTGGCTGAGCCCGTTGATATGGCGGCCGGCCTTTGTTC
CGCGACATTTTATTTACAGGCGGGACCGGAACGCTTTTTCTGGTATCAGCGCATTACCACATTGCGATAG
ACGGCTACGGTTTTTCACTGCTGGCACGGCGTACGGCGCAAATGTACACCGCAATACGGGAAGGACGTC
CGGATAACGGGCGCTCCTTCGGCTCTTTGGAGGAGCTGGTAAAAGAAGAACAAGAATACCGCGCGTCTG
ATCAATTCCTGAAAGATCGGGAATTTGGATGGAGAAATTTGCGGATGAACCTGATGTCGTGAGTTTGG
CGGAAAGAGCGCCGCGAACGTCAACAAGTTTTCGGAGAAGTACGGCTTATCTTTCTGAAACGGCTTTAC
AGCATGTAAGCGATTCCGAACTGGCATGAAGCCGTTACTGCCGCAGCGGCGGTATATGTCCACCGGA
TGACAAACGCAGGGGATATCGTGCTCGTTTACCGATGATGGGACGGATCGGCTCGATTCACTGAATA
TTCCGAGTATGGTCATGAATCTTCTGCCGGGCC/C
```

Figure 3.10 a): Sequence of *dhbC-Erm^r-dhbF*.

b)

Description	Max score	Total score	Query cover	E value	Ident	Accession
<input type="checkbox"/> Bacillus methylotrophicus strain CBMB205 complete genome	1317	1317	100%	0.0	100%	CP011937.1
<input type="checkbox"/> Bacillus vallismortis strain NBIF-001 complete genome	1317	1317	100%	0.0	100%	CP020893.1
<input type="checkbox"/> Bacillus velezensis strain JTYP2 complete genome	1317	1317	100%	0.0	100%	CP020375.1
<input type="checkbox"/> Bacillus velezensis strain sx01604 complete genome	1317	1317	100%	0.0	100%	CP018007.1
<input type="checkbox"/> Bacillus amyloliquefaciens strain WS-6 complete genome	1317	1317	100%	0.0	100%	CP018200.1
<input type="checkbox"/> Bacillus velezensis strain LS69 complete genome	1317	1317	100%	0.0	100%	CP015911.1
<input type="checkbox"/> Bacillus velezensis strain S3-1 complete genome	1317	1317	100%	0.0	100%	CP016371.1
<input type="checkbox"/> Bacillus velezensis strain CBMB205 complete genome	1317	1317	100%	0.0	100%	CP014838.1
<input type="checkbox"/> Bacillus velezensis strain YJ11-1-4 complete genome	1256	1256	100%	0.0	98%	CP011347.1
<input type="checkbox"/> Bacillus subtilis strain ATCC 19217 complete genome	1256	1256	100%	0.0	98%	CP009749.1
<input type="checkbox"/> Bacillus velezensis SQR9 complete genome	1256	1256	100%	0.0	98%	CP006890.1
<input type="checkbox"/> Bacillus velezensis strain SYBC H47 complete genome	1251	1251	100%	0.0	98%	CP017747.1
<input type="checkbox"/> Bacillus velezensis strain GH1-13 complete genome	1245	1245	100%	0.0	98%	CP019040.1
<input type="checkbox"/> Bacillus velezensis strain SB1216 complete genome	1245	1245	100%	0.0	98%	CP015417.1
<input type="checkbox"/> Bacillus velezensis AS43.3 complete genome	1245	1245	100%	0.0	98%	CP003838.1
<input type="checkbox"/> Bacillus subtilis strain J-5 complete genome	1240	1240	100%	0.0	98%	CP018295.1

c)

Description	Max score	Total score	Query cover	E value	Ident	Accession
<input type="checkbox"/> Bacillus methylotrophicus strain CBMB205 complete genome	946	946	100%	0.0	100%	CP011937.1
<input type="checkbox"/> Bacillus vallismortis strain NBIF-001 complete genome	946	946	100%	0.0	100%	CP020893.1
<input type="checkbox"/> Bacillus velezensis strain JTYP2 complete genome	946	946	100%	0.0	100%	CP020375.1
<input type="checkbox"/> Bacillus velezensis strain sx01604 complete genome	946	946	100%	0.0	100%	CP018007.1
<input type="checkbox"/> Bacillus amyloliquefaciens strain WS-8 complete genome	946	946	100%	0.0	100%	CP018200.1
<input type="checkbox"/> Bacillus velezensis strain LS69 complete genome	946	946	100%	0.0	100%	CP015911.1
<input type="checkbox"/> Bacillus velezensis strain S3-1 complete genome	946	946	100%	0.0	100%	CP016371.1
<input type="checkbox"/> Bacillus velezensis strain CBMB205 complete genome	946	946	100%	0.0	100%	CP014838.1
<input type="checkbox"/> Bacillus subtilis strain ATCC 19217 complete genome	935	935	100%	0.0	99%	CP009749.1
<input type="checkbox"/> Bacillus velezensis SQR9 complete genome	935	935	100%	0.0	99%	CP006890.1
<input type="checkbox"/> Bacillus amyloliquefaciens UMAF6614 complete genome	929	929	100%	0.0	99%	CP006960.1
<input type="checkbox"/> Bacillus velezensis strain YJ11-1-4 complete genome	928	928	100%	0.0	99%	CP011347.1
<input type="checkbox"/> Bacillus licheniformis strain SRCM100141 complete genome	924	924	100%	0.0	99%	CP021669.1
<input type="checkbox"/> Bacillus velezensis strain 9912D complete genome	924	924	100%	0.0	99%	CP017775.1
<input type="checkbox"/> Bacillus amyloliquefaciens strain S499 complete genome	924	924	100%	0.0	99%	CP014700.1
<input type="checkbox"/> Bacillus velezensis NJN-6 complete genome	924	924	100%	0.0	99%	CP007165.1

Figure 3.10: b) Blast results on the partial *dhbC* sequence c) Blast results on the partial *dhbF* sequence

3.2.4 Transformation of *B. amyloliquefaciens* in order to achieve homologous recombination in siderophore synthesis operon

Sequential cloning resulted in the plasmid pCR®2.1-TOPO®-*dhbC*-*Erm^r*-*dhbF* (Figure 3.11). The partial sequences of the *dhbC* and *dhbF* genes would allow for homologous recombination in *B. amyloliquefaciens* genomic DNA in order to delete the siderophore synthesis operon and replace it with the erythromycin resistance gene. Transformation was based on protocols described in detail in §2.12. Following three unsuccessful attempts, it was decided to halt transformation attempts for a subsequent study and focus instead on other experimental procedures, thus allowing maximum data yield in the defined experimental period.

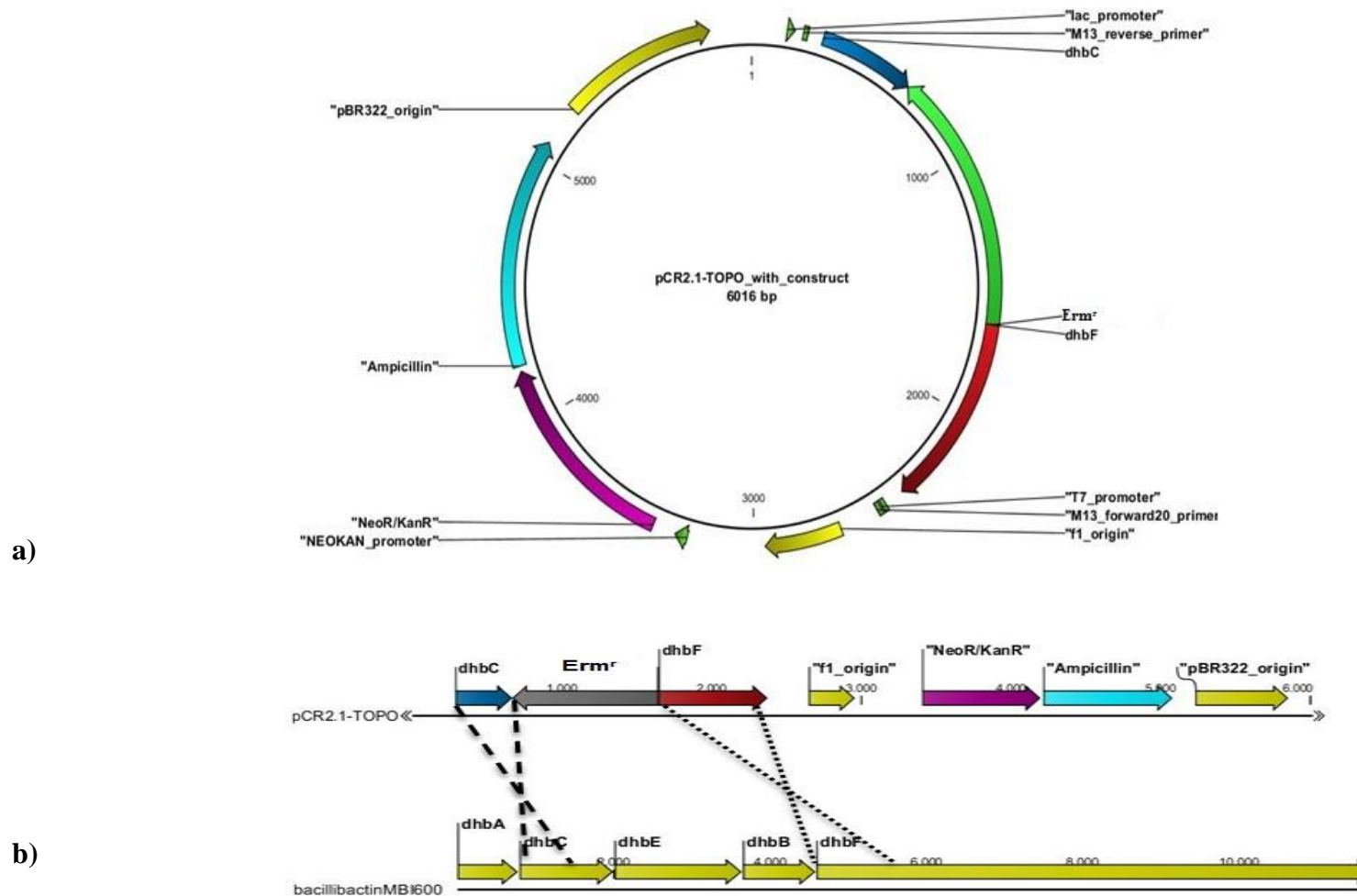


Figure 3.11: Schematic representation of a) pCR®2.1-TOPO®-*dhbC*-*Erm^r*-*dhbF* plasmid and b) The homologous recombination event in *B. amyloliquefaciens* siderophore biosynthetic operon.

3.3 Efficacy evaluation of siderophores *in vitro*

In previous experimental procedures, the antibiotic capacity of *B. amyloliquefaciens* against phytopathogens such as *Xanthomonas campestris* pv. *campestris*, *Xanthomonas campestris* pv. *vesicatoria*, *Agrobacterium tumefaciens*, *Erwinia amylovora*, *Erwinia chrysanthemi*, *Pseudomonas syringae* pv. *tomato* (*Pto*) and *Pseudomonas syringae* pv. *tabaci* (*Pta*). *Pto* and *Pta* were found to be insensitive to *B. amyloliquefaciens*. Since both *B. amyloliquefaciens* and *P. syringae* pathovars are able to produce siderophores and possibly assimilate xenosiderophores it was decided to evaluate Pseudomonads sensitivity to *B. amyloliquefaciens* under iron starvation and upon production of siderophores that was not tested before.

3.3.1 *B. amyloliquefaciens* was found to inhibit the growth of *Pseudomonas* sp. in agar plates under iron-limited conditions

All afore mentioned phytopathogenic bacteria were grown in succinate agar media supplemented with an increasing concentration of iron. Following one day of incubation at 28°C, the *B. amyloliquefaciens* culture suspension was added to paper discs. After 7 days, inhibition zones developed and were measured (§2.14.1). Inhibition zones formed in *Xanthomonas campestris* pv. *campestris*, *Xanthomonas campestris* pv. *vesicatoria*, *Agrobacterium tumefaciens*, *Erwinia amylovora* and *Erwinia chrysanthemi* agar cultures and in the presence of *B. amyloliquefaciens* did not show any differentiation related to the concentration of iron in the medium (data not shown).

Surprisingly, inhibition zones formed in agar plates in the presence of vegetative growth cultures of MBI600 against *Pseudomonas syringae* pv. *tomato* (*Pto*) and *Pseudomonas syringae* pv. *tabaci* (*Pta*) cultures. Radial zones were negatively correlated to iron concentration (Figures 3.12-13). In detail, in the case of *Pto*, radius at 0 µg/L Fe was about 1 cm compared to radius at 400 µg/L Fe that was about 0.5 cm. The difference between these concentrations is statistically significant while the radius at 50 µg/L Fe which was around 0.75 cm did not show a statistically significant difference compared to the other two iron concentrations (Figure 3.12 A1-2). In the case of *Pta* inhibition zone radius around *B. amyloliquefaciens* colonies grown at 0 µg/L Fe was 2.5 cm and showed statistically significant difference compare to radius

Chapter 3: Results

at 50 and 1000 $\mu\text{g/L}$ Fe that were about 2 cm respectively. Radius at 400 $\mu\text{g/L}$ Fe was more than 2 cm and showed no statistically significant difference compared to all other iron concentrations (Figure 3.12 B1).

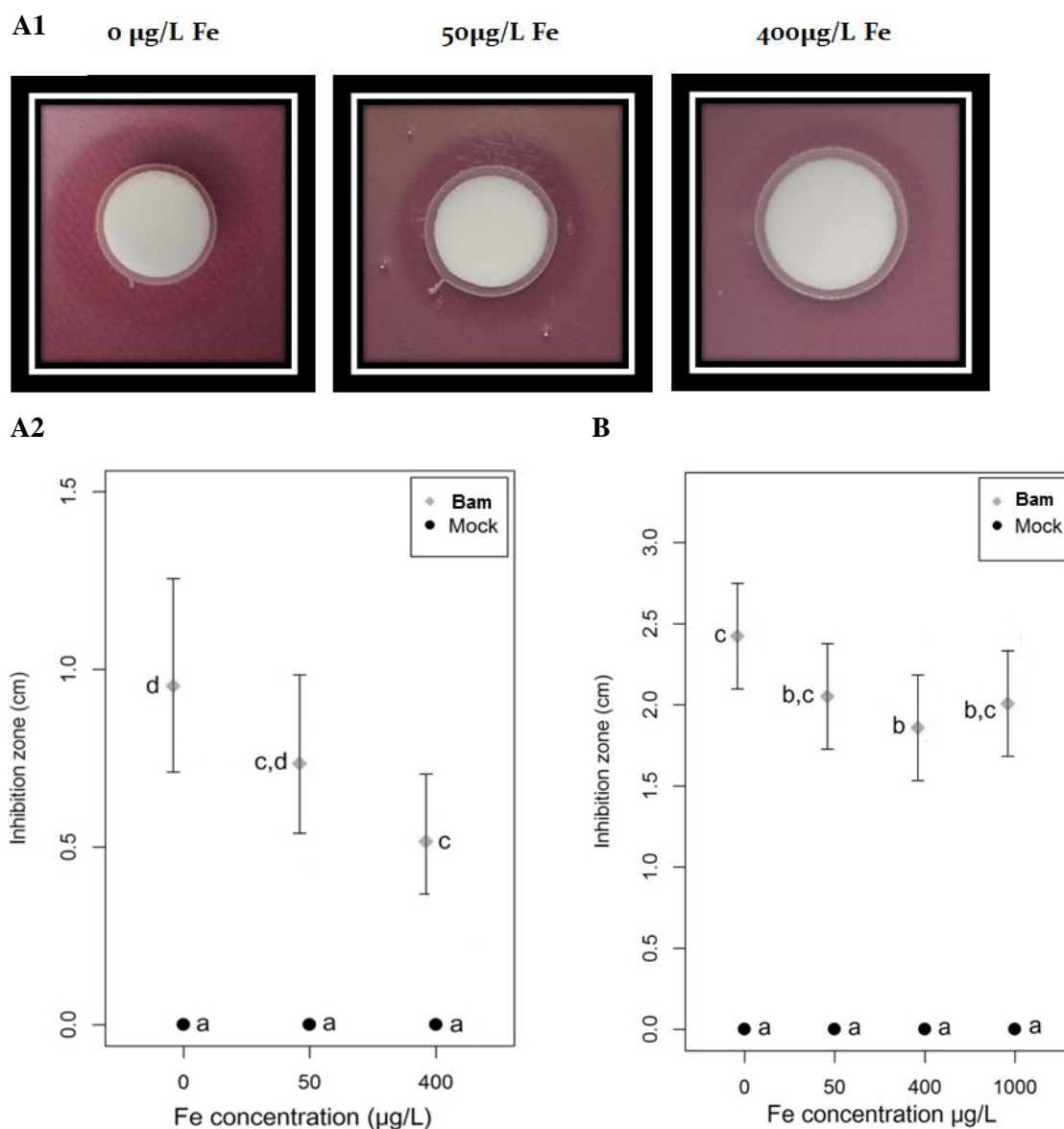


Figure 3.12: Inhibition zones formed in *Pseudomonas syringae* pv. *tomato* (*Pto*) (A1-2) and (B) *Pseudomonas syringae* pv. *tabaci* (*Pta*) agar cultures in the presence of *B. amyloliquefaciens*. *Pta* or *Pto* inoculum suspension was adjusted to 10^9 cfu/mL and allowed to grow in agar medium containing increasing iron concentrations (0, 50, 400 $\mu\text{g/L}$). After 48 h of incubation, 70 μL of a *B. amyloliquefaciens* suspension, adjusted to 10^9 cfu/mL, was added to paper discs. Inhibition zones that developed were measured following incubation for 6 days at 28°C . Values are representing the average of 24 inhibition zone measurements for each iron concentration. Different letters represent statistically different data points at $P \leq 0.05$ according to Tukey post hoc comparisons.

3.3.2 CFCF from *B. amyloliquefaciens* grown under iron-limited conditions was found to affect *Pseudomonas sp* growth

To supplement previous findings, the effect of Cell Free Culture Filtrate (CFCF) of *B. amyloliquefaciens* cultures, grown on different Fe concentrations (§2.14.2), was evaluated against pathogens *Pto* and *Pta*. These pathogens were insensitive against *Ban* CFCF that was extracted from cultures supplemented with iron (data not shown).

In the case of *Pta*, cultures grown in LB medium in the presence of 10% *B. amyloliquefaciens* CFCF (used as an inhibition agent) show growth similar to that of the control (no CFCF) both at 24 hour and 48 hours post inoculation (hpi) of the medium. *Pta* growth in the presence of 25% CFCF did not show a specific trend for increasing Fe concentrations and was similar to that of the control (no CFCF). However, when *Pta* was grown in presence of 50% CFCF, an effect negatively correlated to Fe concentration, occurred on the bacterium growth of treatments compared to mock 48 hpi. In detail, a statistically significant decrease in growth of *Pta* in presence of 50% 0 µg/L Fe CFCF compared to mock is observed while in presence of 50% 2000 µg/L Fe CFCF it seems that the growth of *Pta* was increased with statistically significant difference contrary to mock (Figure 3.13).

In the case of *Pto*, cultures grown in LB medium in presence of 10% *B. amyloliquefaciens* CFCF showed a decrease in growth that was negatively correlated to iron concentration. OD₆₀₀ estimates at 400 and 1000 µg/L Fe have a statistically significant difference compared to the 0 µg/L Fe treatment in the presence of 50 % CFCF (Figure 3.14). This growth delay in the case low Fe concentration is confirmed by the reverse estimated values 48 hpi, since *Pto* growth curve reached the death phase in the case of the control treatment, contrary to *Pto* growth in the presence of CFCF from *B. amyloliquefaciens* cultures grown in increasing Fe concentrations. A similar trend appears in *Pto* growth in the presence of 25% CFCF concentration. In support, addition of 50% CFCF from MBI600 culture grown in 0 µg/L Fe concentration, led to a statistically significant reduction of growth for at least 24 hpi compared to control and other treatments of higher Fe concentration (Figure 3.14). The increased growth of *Pto* or *Pta*, in the presence of CFCF grown in high Fe concentration, compared to the control is in accordance with findings presented in

figures 3.13 and 3.14, suggesting that in the absence of siderophore production *Pto* and *Pta* probably utilizes aminoacids and other nutrient that are readily available in MBI600 CFCF.

Measurements of optical densities at 600 nm, recorded automatically every 30 min over a 48 hour incubation period at 28°C, using a multi-detection microplate reader (Bio-Tek-Synergy HT Microplate Reader), are depicted in figure 3.16. As it turns out in the diagrams, during the exponential phase (up to 16 hours), there is no differentiation among control treatment and MBI600 CFCF extracted from various Fe concentrations. Surprisingly, after 16 hours of incubation or when cell population enters the static phase, during which pathogens secrete and absorb siderophores, there is a vertical drop of optical densities at 600 nm in the case of low Fe concentration treatment compared to higher or the control Fe concentration treatment. The reduction of OD₆₀₀ is steeper as the concentration of CFCF in nutrient increased. It should be noted that in previous experimental procedures of the research group *Pseudomonas* species/pathovars were found to be resistant against MBI600 antibiosis as in corresponding iron-independent experiments there is no differentiation between mock and treatments (Figure 3.15).

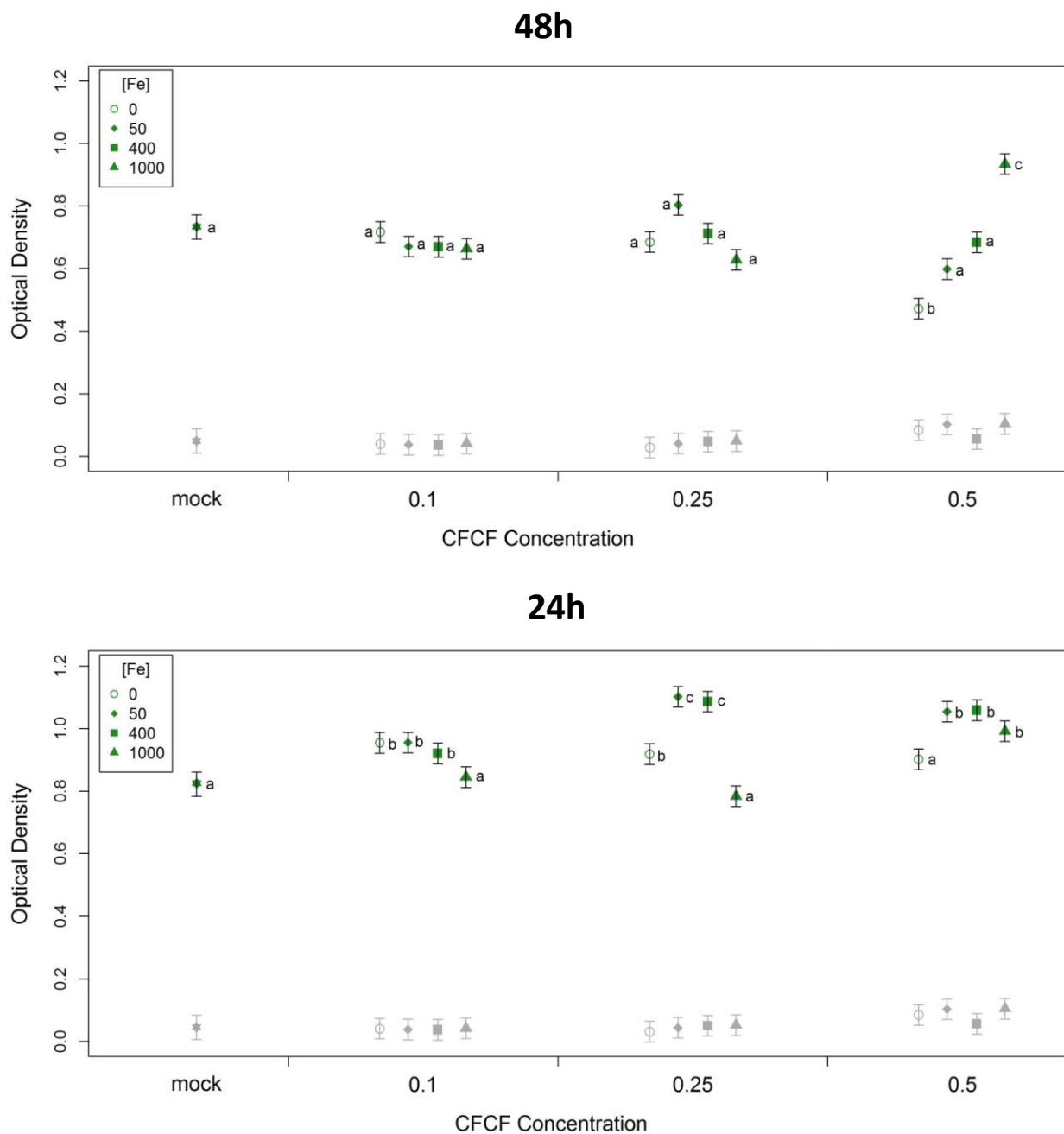


Figure 3.13: Effect on growth of *Pseudomonas syringae* pv. *tabaci* (*Pta*) in LB medium supplemented with a) 10% b) 25% c) 50% *B. amyloliquefaciens* CFCF (cell free culture filtrate) supplemented with different iron concentrations (0, 50, 400, 1000 $\mu\text{g/L}$). The values were taken after 24 and 48 hours culture at 28°C in a microplate spectrophotometer (Fluostar galaxy). CFCF is the filtrated supernatant of *B. amyloliquefaciens*'s 48 hours culture grown in succinate medium.

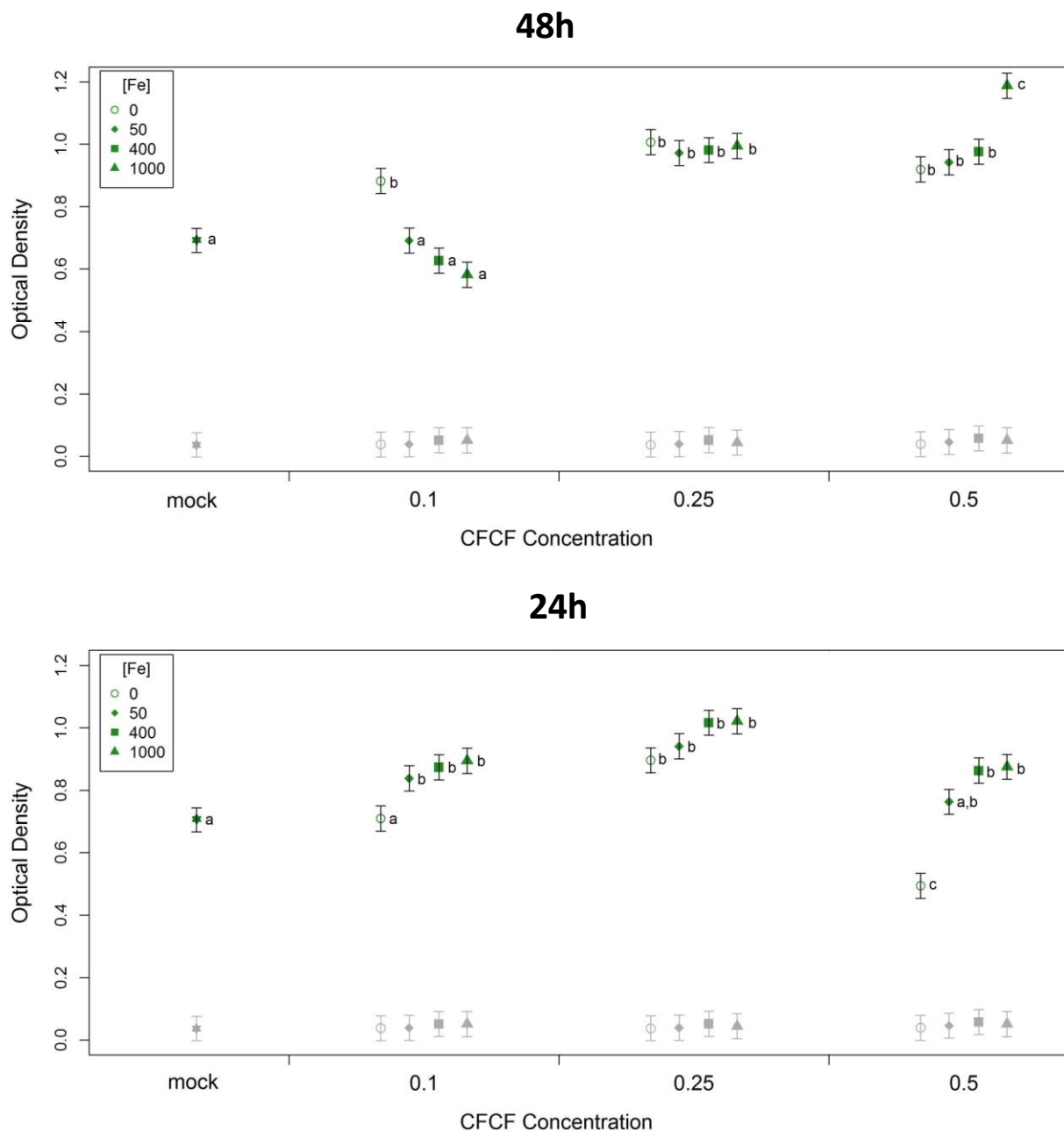


Figure 3.14: Effect on growth of *Pseudomonas syringae* pv. *tomato* (*Pto*) in LB medium supplemented with a) 10% b) 25% c) 50% *B. amyloliquefaciens* CFCF (cell free culture filtrate) supplemented with different iron concentrations (0, 50, 400, 1000 μg/L). Values were taken after 24 and 48 hours culture at 28 °C in a microplate spectrophotometer (Fluostar galaxy). CFCF is the filtrated supernatant of *B. amyloliquefaciens*'s 48 hours culture grown in succinate medium.

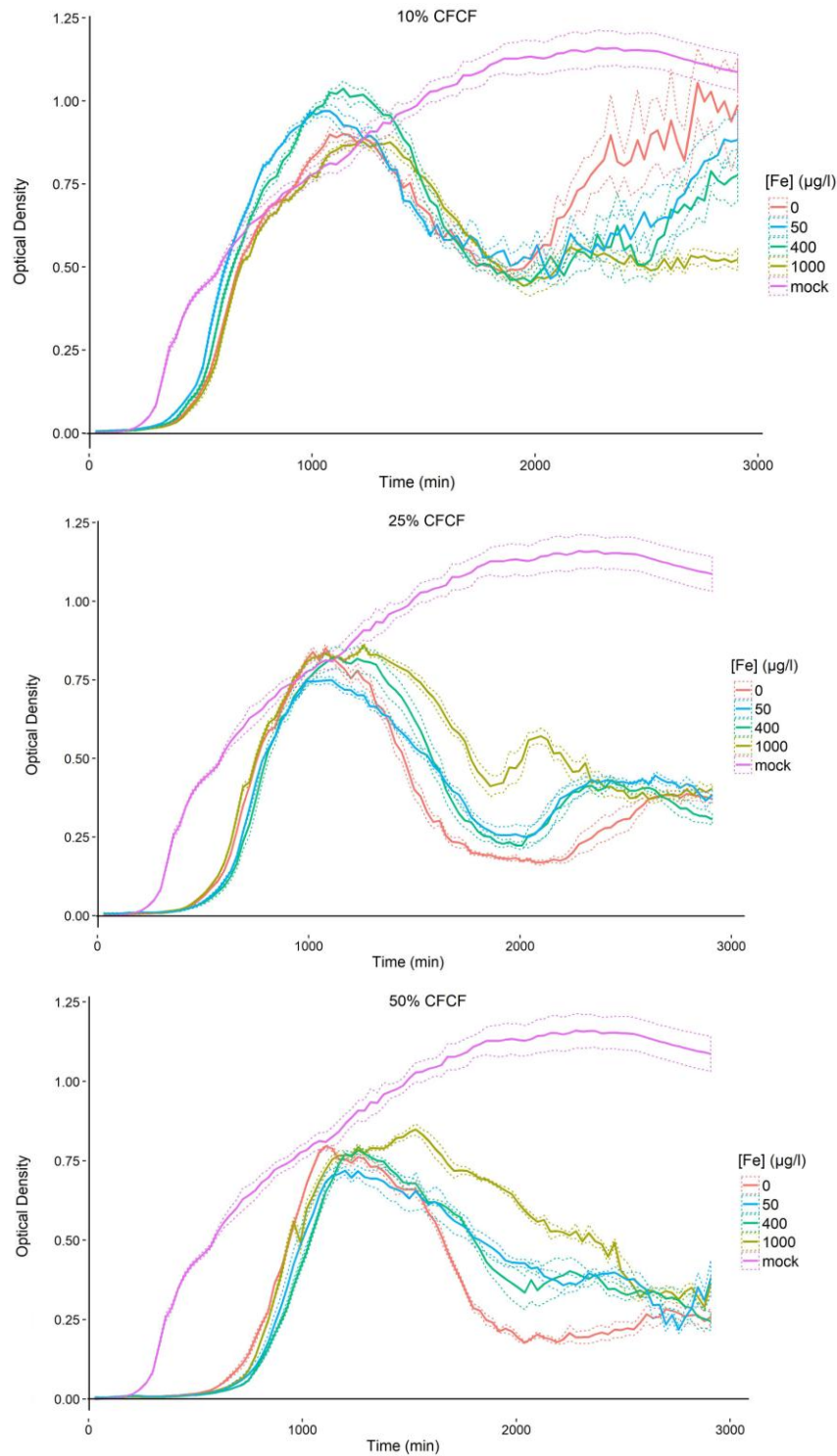


Figure 3.15: Effect on growth of *Pseudomonas syringae* pv. *tomato* (*Pto*) in LB medium supplemented with **a)** 10% **b)** 25% **c)** 50% *B. amyloliquefaciens* MBI600 CFCF (Cell Free Culture Filtrate) supplemented with different iron concentrations (0, 50, 400, 1000 $\mu\text{g/L}$). Values were recorded every 30 minutes over a 48 hour period on a continuous kinetic procedure spectrophotometer (Bio-Tek-Synergy HT Microplate Reader). CFCF is filtrated supernatant of MBI600 48 hours culture in succinate medium.

3.4 Efficacy evaluation of siderophores *in planta*

In vitro findings suggest that *B. amyloliquifaciens* develops antibiotic ability against *Pseudomonas syringae* pv. *tomato* (*Pto*) and *Pseudomonas syringae* pv. *tabaci* (*Pta*) under low concentrations of iron. To evaluate the physiological importance of these findings, we investigated the efficacy of MBI600 under low concentration of iron *in planta*. CFCF was obtained as described in session 2.1 and treatment of plants was performed according to paragraph 2.15. Artificial inoculation of plant was carried out by spraying with a phytopathogen suspension.

3.4.1 Preliminary experiment in *Nicotiana benthamiana* shows that CFCF from *B. amyloliquifaciens* grown under iron limited conditions is more effective against wildfire disease

A preliminary experiment was designed in *Nicotiana benthamiana* using pathogen *Pta*, causing agent of wildfire disease. Wildfire disease symptoms are depicted in figure 3.16. The experimental design was based on 3 plots, each consisting of 12 plants. Treatments included CFCF from MBI600 culture grown in the presence of 0 and 1000 $\mu\text{g} / \text{L}$ Fe, using water instead of MBI600 as control (§2.15). Samples consisted of pools of 3 leaf discs (1 disc per plant) in a total number of 12 plants per treatment. Assessment of efficacy was performed by monitoring symptoms (Figure 3.17) and *Pta* total leaf population (Figure 3.18).

Wildfire disease development (*Pta*) was calculated as severity score (ranked leaf coverage) (Figure 3.17). Plants infected with *Pta* under controlled conditions developed small chlorotic spots which developed into necrotic lesion, 5 to 7 days after spray inoculation. Wildfire disease symptoms are depicted at figure 3.16. Application of CFCF containing 0 $\mu\text{g}/\text{L}$ Fe reduced disease development compared with both the control treatment and the 1000 $\mu\text{g}/\text{L}$ Fe treatment at both 8 and 15 dpi (Fig. 3.17). Differences were found to be statistically significant. On the contrary, differences were not significant between CFCF treatment from MBI600 culture grown in the presence of 1000 $\mu\text{g}/\text{L}$ Fe and the control treatments. In the 8-15 dpi interval, an increase in severity score was observed, which was statistically significant in the case of control compared with CFCF of MBI600 culture grown in 0 $\mu\text{g}/\text{L}$ Fe but not in case of control compared with CFCF MBI600 1000 $\mu\text{g}/\text{L}$ Fe.



Figure 3.16: Wildfire disease symptoms.

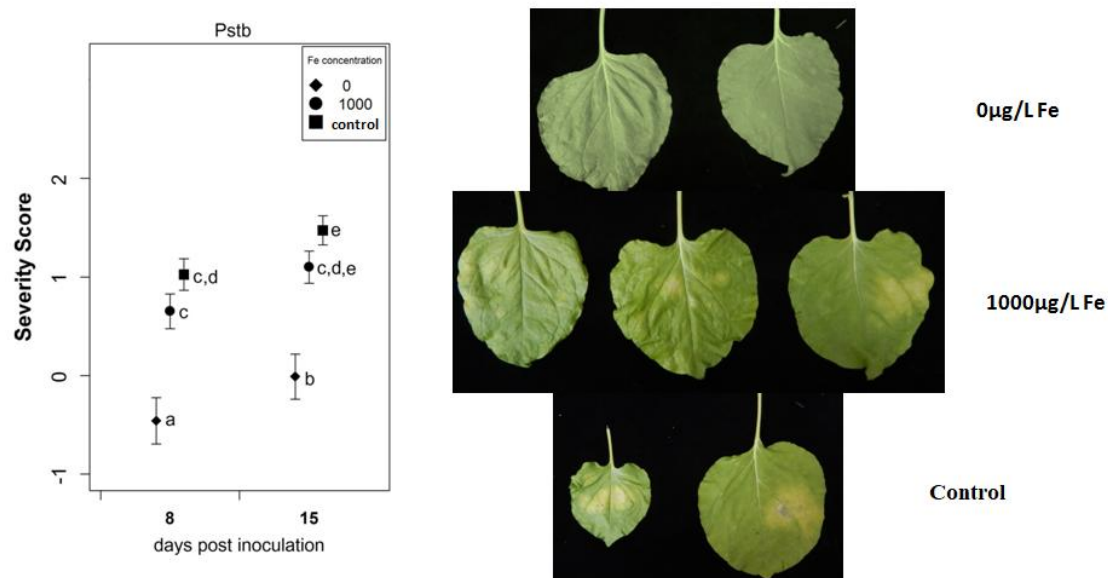


Figure 3.17: Wildfire disease development (*Pta*) calculated as severity score (ranked leaf coverage). Plants were treated with water (control), CFCF from MBI600 cultures grown in 0 and 1000 $\mu\text{g/L}$ Fe. Leaves were inoculated with a 10^6 bacterial suspension and treated with CFCF simultaneously by spraying. Different letters represent statistically different data points at $P \leq 0.05$ according to Tukey post hoc comparisons.

The total *P. syringae* pv. *tabaci* population was examined in leaf discs over a period of 15 dpi (figure 3.18). Application of CFCF from MBI600 cultures grown in 0 $\mu\text{g/L}$

Fe reduced *Pta* total population compared with control treatment and CFCF MB600 1000 $\mu\text{g/L}$ Fe treatment at both 11 and 15 dpi, differences were statistically significant (Fig. 3.18). Differences among the CFCF MBI600 1000 $\mu\text{g/L}$ Fe treatment, control and CFCF MBI600 0 $\mu\text{g/L}$ Fe treatment were not statistically significant at both 11 and 15 dpi. Finally, the total phyllosphere total population at 20 dpi was found to be lower in the case of CFCF MBI600 0 $\mu\text{g/L}$ Fe treatment compared to the respective 1000 $\mu\text{g/L}$ Fe treatment and control treatment but differences were not statistically significant (Figure 3.18). This suggests that, as expected, the pathogen recovered several days after CFCF treatment.

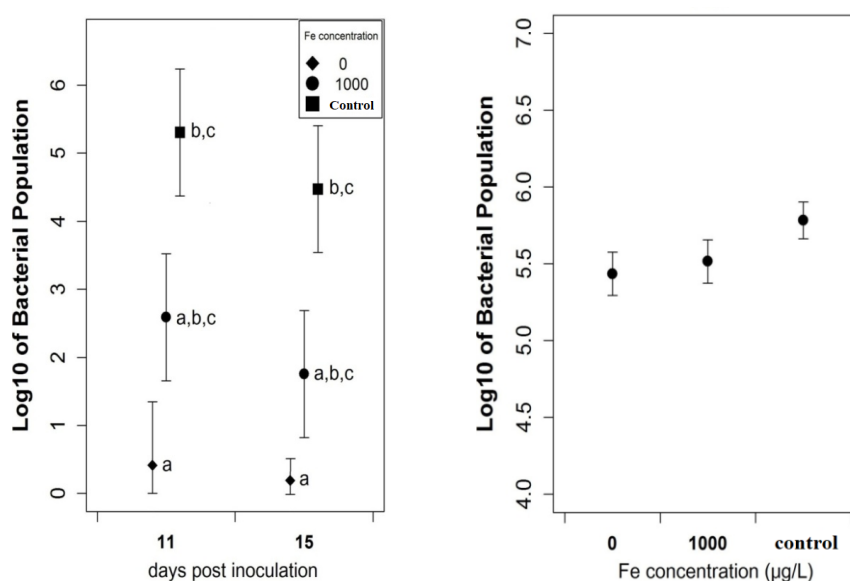


Figure 3.18: *Pta* total population growth, calculated over a period of 20 days post inoculation (dpi). Results are the estimated means of the logarithm of the bacterial population from four samples with standard errors. **a)** Pooled leaf discs samples at 11 and 15 dpi. For each sample 3 discs were used (1 disc per plant) in a total number of 12 plants per treatment. **b)** Homogenized leaf samples from the sum of infected leafs at 20 dpi. Each pool sample represents 3 plants in a total number of 12 plants per treatment. Plants were treated with water (control), CFCF MBI600 0 or 1000 $\mu\text{g/L}$ Fe treatment. Plants were spray-inoculated with a 10^6 bacterial suspension simultaneously to CFCF (or water) treatment. The pooled samples were homogenized in a 10% glycerol solution in sterile distilled water. Serial dilutions were plated on nutrient agar containing 5 $\mu\text{g/mL}$ rifampicin. Different letters represent statistically different data points at $P \leq 0.05$ according to Tukey post hoc comparisons.

3.4.2 Full scale efficacy evaluation of MBI600 siderophores antibacterial activity in *Nicotiana benthamiana* plants

Full scale experiments were evaluated in *Nicotiana benthamiana*/*Pta* pathosystem. The experimental design was based on 5 plots, each consisting of 12 plants. Treatments included CFCF from MBI600 culture grown in succinate medium in the presence of 0, 50, 1000 or 2000 $\mu\text{g/L}$ Fe, using succinate medium instead of MBI600 as control (§2.15). 2000 $\mu\text{g/L}$ Fe was the reference treatment for no siderophore production. Samples consisted of pools of 6 leafs (2 leafs per plant) in a total number of 12 plants per treatment. Assessment of efficacy was performed by monitoring *Pta* total population of the leaf (Figure 3.19)

The total *P. syringae* pv. *tabaci* population was examined in leafs over a period of 14 days (Figure 3.19). The pooled leafs were homogenized in sterile distilled water supplemented with 10% glycerol. A total of 120 samples (8 samples per treatment at 3 time points) were plated in nutrient agar plates with 5 $\mu\text{g/mL}$ rifampicin as the selective agent.

The first day post inoculation (1 dpi) all treatments reduced *Pta* total population compared with control treatment and differences were statistically significant. In detail, application of CFCF from MBI600 cultures grown in 0 $\mu\text{g/L}$ Fe reduced *Pta* total population compared with control treatment and CFCF MBI600 2000 $\mu\text{g/L}$ Fe treatment, differences were statistically significant. Application of CFCF from MBI600 cultures grown in 50 and 1000 $\mu\text{g/L}$ Fe reduced *Pta* total population compared with the other two treatments, but differences were not statistically significant (Figure 3.19).

Seven days post inoculation, application of CFCF from MBI600 cultures grown in with 0 or 1000 $\mu\text{g/L}$ Fe reduced *Pta* total population compared with control treatment and the reference treatment and differences were statistically significant only in the first case. Application of CFCF from MBI600 cultures grown in 50 $\mu\text{g/L}$ Fe did not reduced *Pta* total population compared with control or reference treatment (Figure 3.19).

Finally 14 dpi treatments of 0, 50 or 1000 $\mu\text{g/L}$ Fe reduced *Pta* total population compared with control or reference. Differences were significant only compared to the reference treatment. No significant differences were found among the three treatments (Figure 3.19).

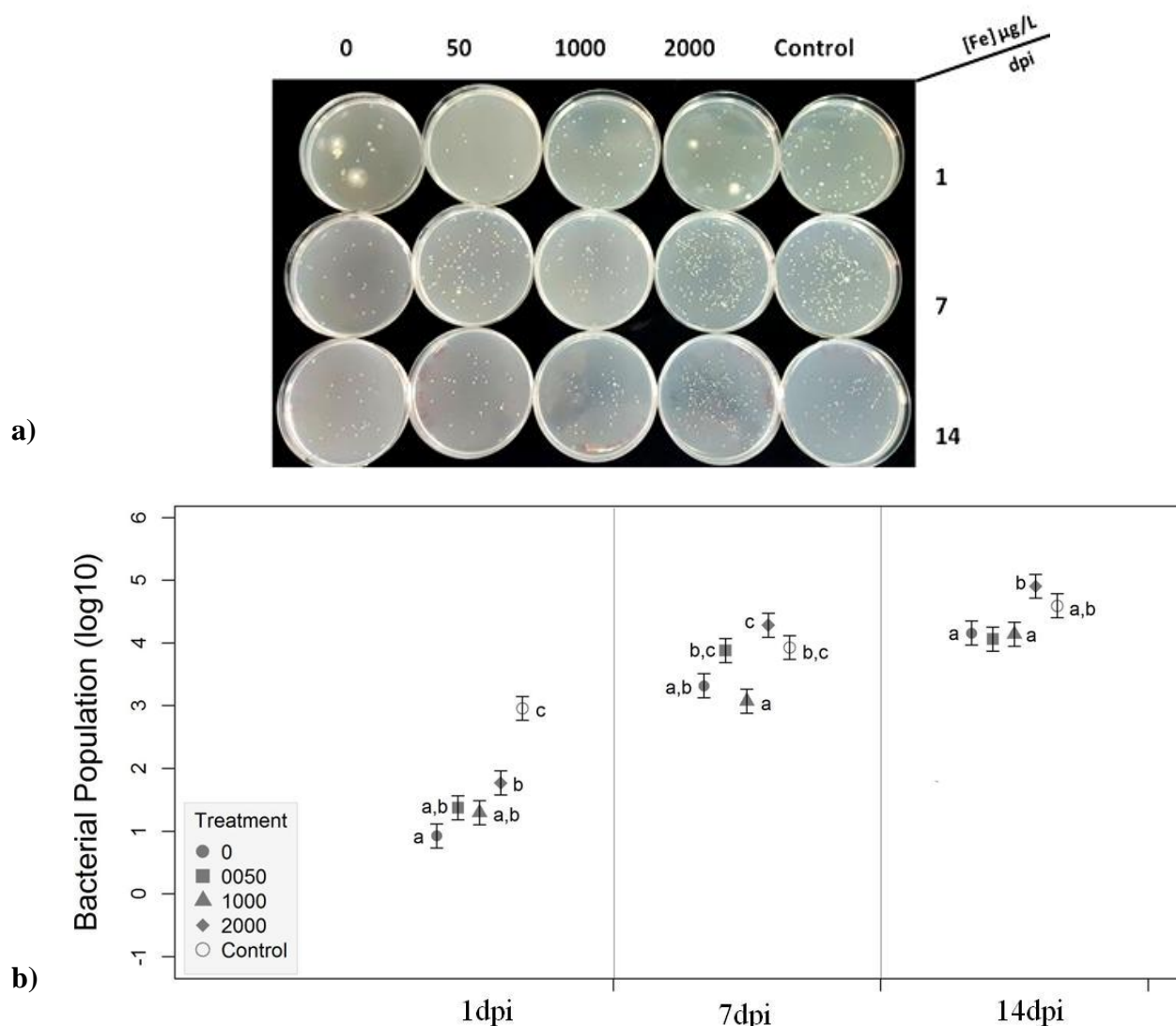


Figure 3.19: *Pta* total population growth, calculated in leaves over a period of 14 days post inoculation (dpi). a) Cfu count in agar plates b) Results are the estimated means of the logarithm of the bacterial population from four samples with standard errors. Four pooled samples (2 leaves per plant) in a total number of 12 plants per treatment. Plants were treated with succinate medium (control), CFCF MBI600 0, 50, 1000 or reference treatment. Plants were spray-inoculated with a 10^6 cfu/mL bacterial suspension simultaneously to CFCF (or succinate medium) treatment. The pooled leaf samples were homogenized in a 10% glycerol solution in sterile distilled H_2O . Serial dilutions were plated on nutrient agar containing $5\mu\text{g/mL}$ rifampicin. Different letters represent statistically different data points at $P \leq 0.05$ according to Tukey post hoc comparisons.

3.4.3 Full scale efficacy evaluation of MBI600 siderophores antibacterial activity in tomato plants

Full scale experiments were designed in tomato using the pathogens *Pto*, cause of bacterial speck disease. Disease symptoms are depicted in Figure 3.20. The experimental design was based on 5 plots, each consisting of 12 plants. Treatments included CFCF from MBI600 culture grown in the presence of 0, 50, 1000 or 2000 µg/L Fe, using succinate medium (instead of MBI600 CFCF) as control treatment (§2.15). Samples consisted of pools of 6 leaflets (2 leaflets per plant) in a total number of 12 plants per treatment. Assessment of efficacy was performed by monitoring *Pto* total population of the leaf (Figure 3.21).

The total *Pto* population was examined in leaflets over a period of 14 dpi (Figure 3.20). Pooled leaflet samples were homogenized in sterile distilled H₂O with 10% glycerol. A total of 160 samples (8 samples per treatment at 4 time points) were plated in nutrient agar plates with 5 µg/mL rifampicin as selective agent.

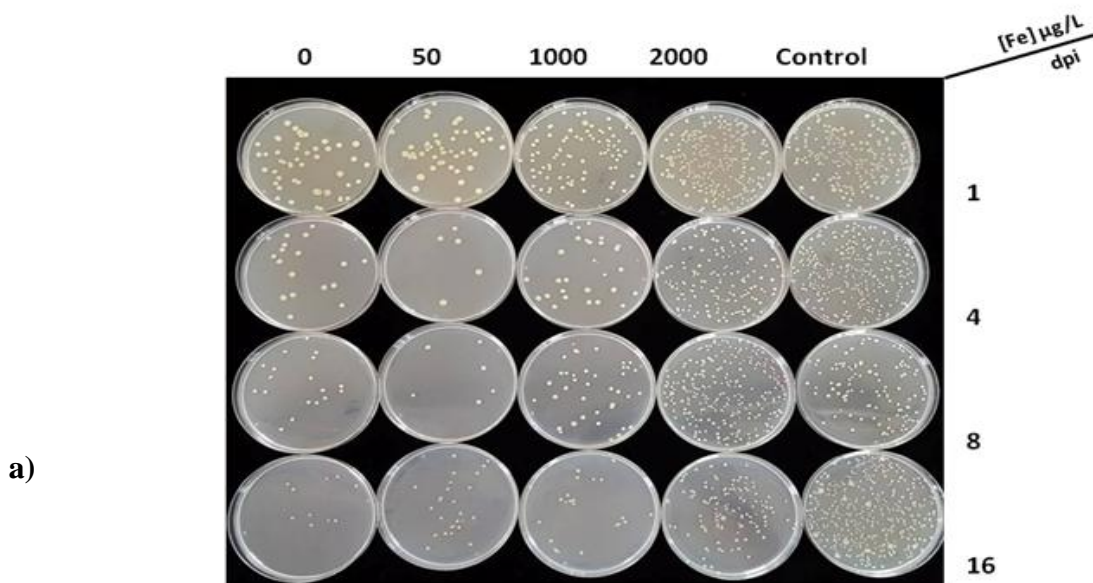
On both the first and fourth day post inoculation, CFCF treatments from MBI600 culture grown in 0 and 50 µg/L Fe treatments reduced *Pto* total leaflet population compared to CFCF MBI600 1000 µg/L Fe treatment, reference or control treatment and the differences were statistically significant (Figure 3.21).

Eight days post inoculation CFCF treatments of MBI600 culture grown in 0 or 50 µg/L Fe reduced *Pto* total population compared to reference and control treatments, differences were statistically significant. The CFCF MBI600 1000 µg/L Fe treatment also reduce *Pto* total population but differences were not statistically significant compared to the reference and control treatments (Figure 3.21).

Finally, sixteen days post inoculation, CFCF treatments from MBI600 culture grown in 0 or 50 µg/L Fe reduced *Pto* total population compared to the CFCF 2000 µg/L Fe treatment and control treatment, differences were statistically significant. CFCF from MBI600 culture grown in 1000 µg/L Fe differs significantly compared with control treatment but not with the reference treatment (Figure 3.21).



Figure 3.20: Bacterial speck disease symptoms.



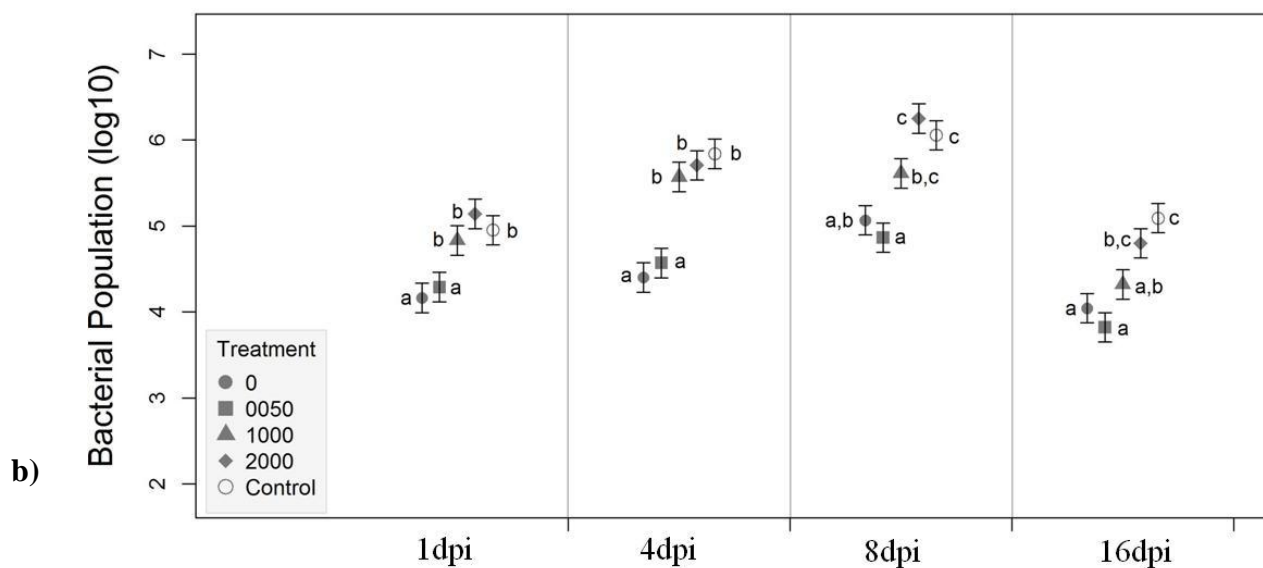
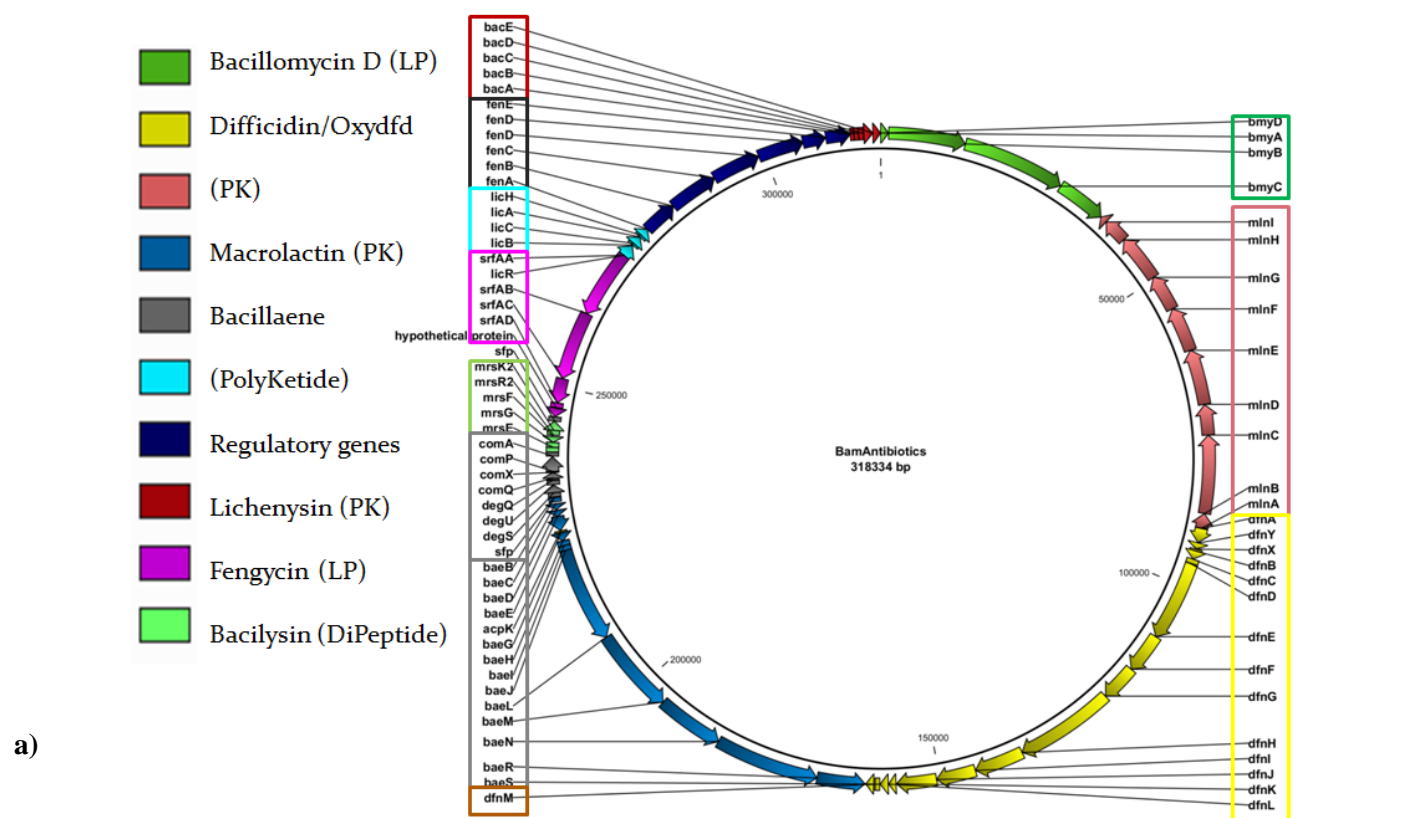


Figure 3.21: *Pto* total population growth, calculated in leaves over a period of 16 days post inoculation (dpi). a) Population in agar plates b) Results are the estimated means of the logarithm of the bacterial population from four samples with standard errors. Pooled samples of 6 leafs from 3 plants were used (2 leafs per plant) in a total number of 12 plants per treatment. Plants were treated with succinate medium (control), CFCF MBI600 0, 50, 1000 or 2000 $\mu\text{g/L}$ Fe treatment. Plants were spray-inoculated with a 10^6 cfu/mL bacterial suspension simultaneously to CFCF (or succinate medium) treatment. Pooled leaf samples were homogenized in a 10% glycerol solution in sterile distilled H_2O . Serial dilutions were plated on nutrient agar containing $5\mu\text{g/mL}$ rifampicin. Different letters represent statistically different data points at $P \leq 0.05$ according to Tukey post hoc comparisons.

3.5 Determination of *B. amyloliquefaciens* gene expression in different iron concentrations

The *B. amyloliquefaciens* genome encodes for a variety of biosynthetic gene clusters for secondary metabolites (Figure 3.22).



a)

Metabolite	Genes and gene cluster	Size	Function	Expression <i>in situ</i>	Effect against
Sfp-dependent non-ribosomal synthesis of lipopeptides					
Surfactin	<i>srfABCD</i>	32.0 kb	Biofilm, ISR	Strong, during root colonization	Virus
Bacillomycin D	<i>bmyCBAD</i>	39.7 kb	Direct suppression, ISR	Weak, during root colonization	Fungi
Fengycin	<i>fenABCDE</i>	38.2 kb	Direct suppression, ISR	Weak, during root colonization	Fungi
Bacillibactin	<i>dhbABCDEF</i>	12.8 kb	Siderophore	During iron deficiency in soil	Microbial competitors
Unknown	<i>nrsABCDEF</i>	17.5 kb	Unknown	Unknown	Unknown
Sfp-dependent non-ribosomal synthesis of polyketides					
Macrolactin	<i>mInABCDEFGHl</i>	53.9 kb	Direct suppression	Not shown	Bacteria
Bacillaene	<i>baeBCDE, acpK, baeGHIJLMNRS</i>	74.3 kb	Direct suppression	Not shown	Bacteria
Difficidin	<i>dfnAYXBCDEFGHIJKLM</i>	71.1 kb	Direct suppression	Not shown	Bacteria
Sfp-independent non-ribosomal synthesis					
Bacilysin	<i>bacABCDE, ywFG</i>	6.9 kb	Direct suppression	Not shown	Bacteria, cyanobacteria
Ribosomal synthesis of processed and modified peptides (bacteriocins)					
Plantazolicin	<i>pznFKGHIAJC DBEL</i>	9.96 kb	Direct suppression	Unknown	<i>B. anthrax</i> , nematodes
Amylocyclin	<i>acnBACDEF</i>	4.49 kb	Direct suppression	Unknown	Closely related bacteria
Synthesis of volatiles					
Acetoin/2,3-butandiol	<i>bdh, alsDRS</i>	3.6 kb	ISR	During root colonization	Plant pathogens

b)

Figure 3.22: a) Biosynthetic clusters of secondary metabolites on *B. amyloliquefaciens* MBI600 genome. b) Secondary metabolites and their effect against other microorganisms (Chowdhury *et al.* 2015).

RNA was isolated from *B. amyloliquefaciens* cells grown in succinate medium under different iron concentrations (0, 50, 1000, 2000 µg/L Fe) (§2.16). Expression levels of

selected genes and relative ratios were determined by competitive hybridization of fluorescently labeled cDNA samples as described in section 2.17. The first group of genes studied was related to the production of secondary metabolites such as siderophore synthase C (*dhbC*), bacillomycin (iturin) synthase C (*bmyC*), fengycin synthase C (*fenC*), surgactin synthase AC (*sfpAC*) and *yczE* a positive regulator of bacillomycin (iturin) synthesis (Figures 3.23 and 3.25). The second group of genes was related to *B. amyloliquefaciens* competition and included genes such as *comK*, *cheC*, *swrA*, *deqU* and *yusV* (Figures 3.24 and 3.26). *ComK* is a gene that is involved in competence and *cheC* encodes chemotaxis protein phosphatase CheC. *SwrA* gene encodes swarming motility protein SwrA. This protein up-regulates the expression of flagellar genes and increases swarming mobility. *DeqU* encodes for a response regulator DeqU. This regulator is involved in the control of extracellular macromolecule hydrolyzing enzyme synthesis and competence, regulates the expression of secondary metabolites bacillomycin D and bacilycin and is a positive regulator of genes involved in swarming mobility and biofilm formation in *B. amyloliquefaciens* FZB42. *YusV* protein is a ATP-binding protein and is involved in import of the iron-hydroxamate siderophores. The gyrase housekeeping gene *gyrA* was used as reference in all cases. Primers for qPCR were designed based on MBI600 annotated genome and are listed on Table 2.16.

At first, we compared RNA transcripts from *B. amyloliquefaciens* cells grown under treatments of 0, 50, 1000 µg/L Fe in succinate medium, 24 and 48 hpi (Figure 3.23 and 3.24). The maximum expression of *dhbC*, *bmyC*, *fenC* and *yczE* genes was observed at 50 µg/L Fe at both 24 and 48 hpi. In contrast, the maximum expression of *sfpAC* was observed at 0 µg/L Fe at both 24 and 48 hpi. The maximum expression of *comK*, *cheC* and *swrA* genes was also observed at 50 µg/L Fe at 24 hours. At 48 hours, expression levels of *comK* and *cheC* at 50 µg/L Fe remained higher compared to other treatments (Fe concentrations); however, expression levels at 0 and 1000 µg/L Fe increased considerably. In contrast, expression levels of *swrA* at 48 hpi correlated with Fe concentration and thus were higher in the case of 1000 µg/L Fe. Maximum expression of *yusV* and *deqU* was observed at 0 and 1000 µg/L Fe respectively and was time independent (Figure 3.24). Even if expression of all genes at 24 hpi is lower in the case of 1000 µg/L Fe concentration (treatment), this condition was reversed at 48 hpi. This suggests that cells in stationary phase, produce siderophores and up

regulated (selected) gene transcription in a manner similar to that of lower Fe concentration treatments, due to iron depletion of the medium (Figure 3.23 and 3.24). It was concluded that a concentration of 1000 µg/L Fe in succinate medium is not saturated at the late stages of the stationary phase of MBI600 cells. Consequently, a series of preliminary experiments defined the saturated -non toxic- Fe concentration for optimal growth at all stages of the MBI600 growth curve at 2000 µg/L Fe.

The afore mentioned experiments were repeated using 0, 50, 2000 µg/L Fe in succinate medium and sampling at 24 and 48 hpi (Figure 3.25 and 3.26). Indeed, expression levels at 2000 µg/L Fe were found to be significantly lower at both 24 and 48 hours for transcript of *dhbC*, *bmyC*, *yczE* and *fenC* genes compared with the 0 and 50 µg/L Fe. It is concluded that siderophore production is inhibited at 2000 µg/L Fe and thus this concentration is considered saturated and the reference concentration in this study. *SrfAC* expression level at 24 hpi was significantly higher at 0 µg/L Fe compared with 50 and 2000 µg/L but at 48 hpi levels were found to be similar in the case of 0 and 2000 µg/L (Figure 3.25). *YusV* transcription followed the same pattern with metabolite synthases and was higher at 0 µg/L Fe compared with 50 or 2000 µg/L at both 24 and 48 hpi (Figure 3.26). Concerning *comk*, *cheC* and *swrA* genes, a higher expression was observed at 50 and 2000 µg/L Fe compared with 0 µg/L Fe. In specific, expression of all genes was very low in the case of 0 µg/L Fe at 24 hpi but increased at 48 hpi. On the contrary, expression at 2000 µg/L Fe dramatically decreased during the late stages of stationary phase (48 hpi) (Figure 3.26). *DegU* expression levels were not changed in relation to the concentration of iron.

Finally, a statistical analysis was carried out by combining the above experiments in order to draw conclusions on whether and how the expression of genes of the two groups was affected in comparison with the reference (2000 µg/L Fe). Results suggest that at 24 hpi there is a statistical significant upregulation, compared to reference concentration in the case of *yusV* in all treatments. In addition, there is a two-fold upregulation of *srfAC*, though non significant in all treatments compared to reference. At 48 hpi, there is a statistically significant differentiation of all genes in all three different concentrations of iron relative to the control, other than *degU* and, *srfAC*. In the case of *yusV*, statistically significant differences compared with the control were found solely at the 0 µg/ L concentration (Figure 3.27).

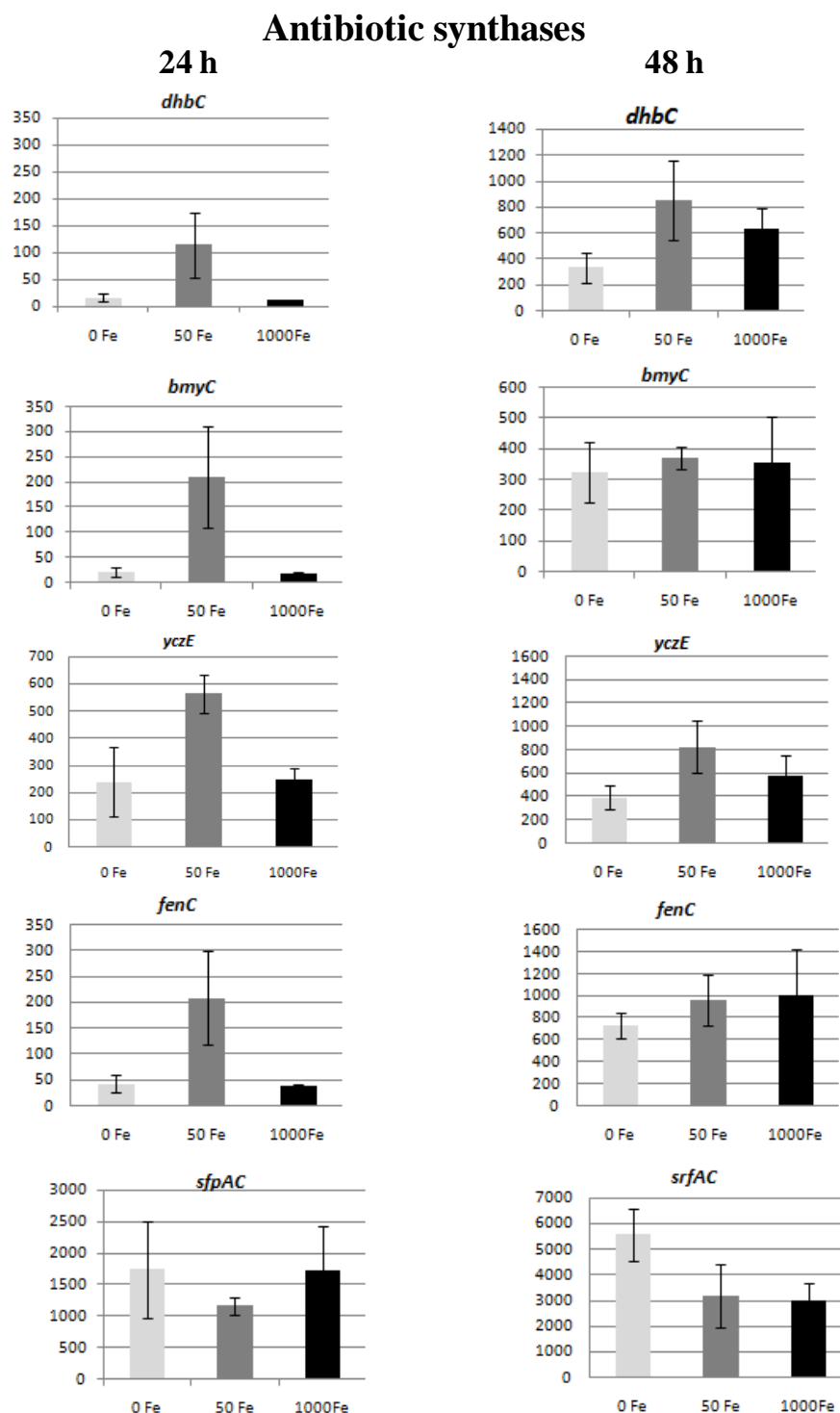


Figure 3.23: RT-qPCR results of differential genes expression of *B. amyloliquefaciens* grown for 24 and 48 hpi in succinate medium at different iron concentrations (0, 50, 1000 µg/L). The genes examined concern secondary metabolite synthesis (*dhbC* :siderophore synthase, *bmyC*: bacillomycin (iturin) synthase, *yczE*: positive regulator of bacillomycin (iturin) synthesis, *fenC*: fengycin synthase, *sfpAC* :surfactin synthase).

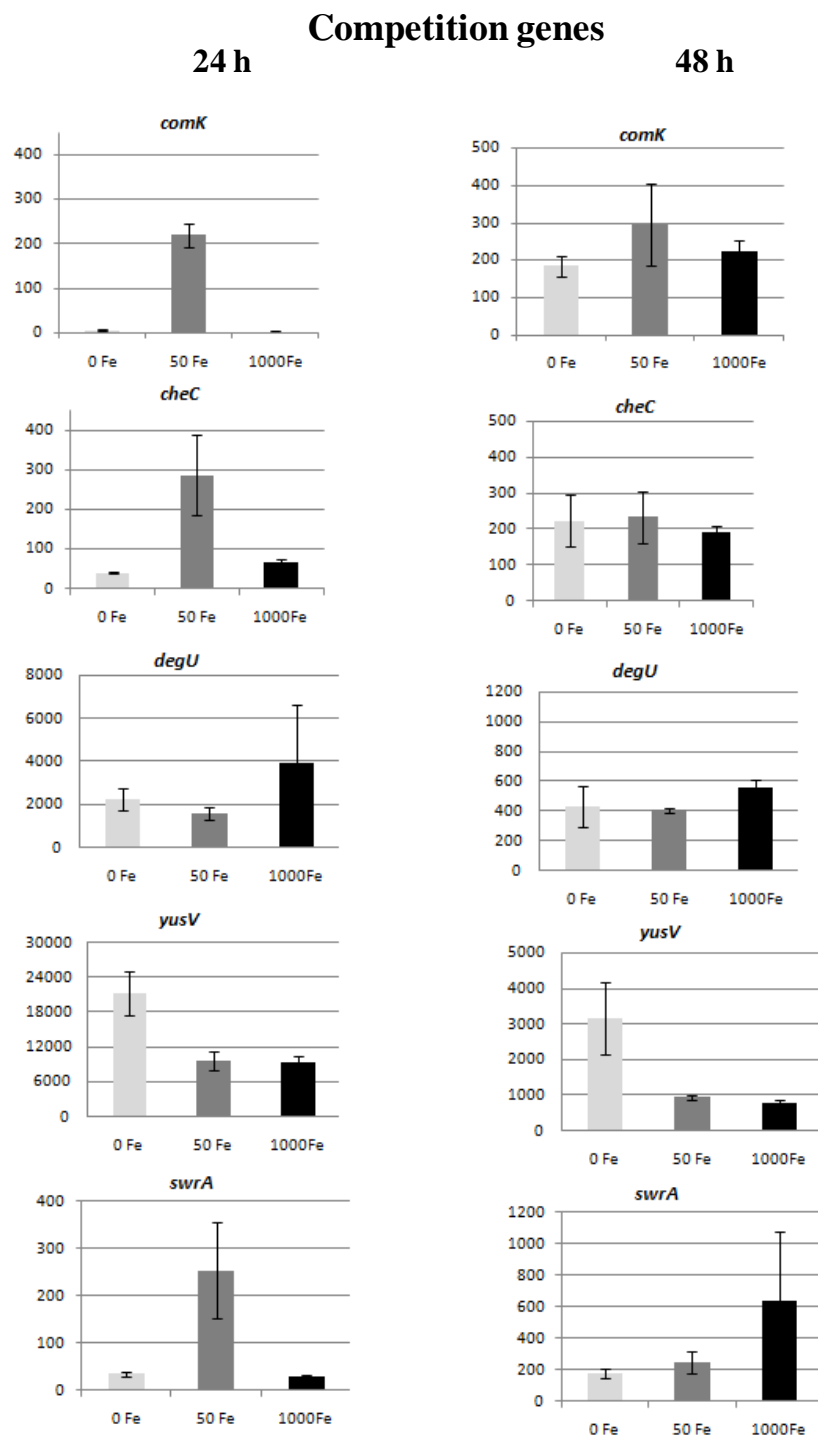


Figure 3.24: RT-qPCR results of differential genes expression of *B. amyloliquefaciens* grown for 24 and 48 hpi in succinate medium at different iron concentrations (0, 50, 1000 µg/L). The genes examined concern *B. amyloliquefaciens* competition. *comK*: competition; *cheC*: chemotaxis; *degU*: positive regulator of bacillomycin (iturin); *yusV*: Probable siderophore transport system; *swrA*: swarming.

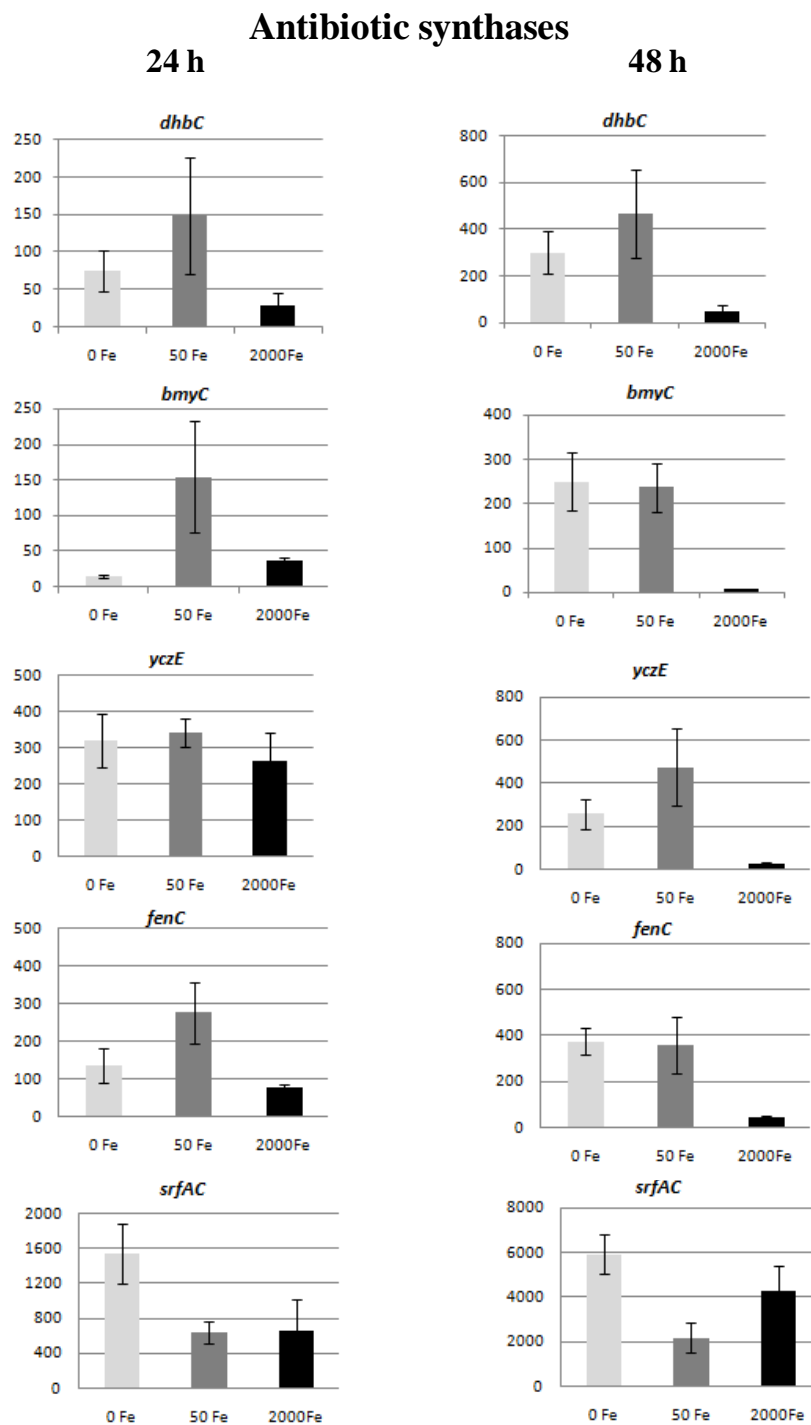


Figure 3.25: RT-qPCR results of differential genes expression of *B. amyloliquefaciens* grown for 24 and 48 hpi in succinate medium at different iron concentrations (0, 50, 2000 μ g/L). The genes examined concern secondary metabolite synthesis. *dhbC* :siderophore synthase; *bmyC*: bacillomycin (iturin) synthase; *yczE*: positive regulator of bacillomycin (iturin) synthase; *fenC*: fengycin synthase; *sfpAC* : surfactin synthase.

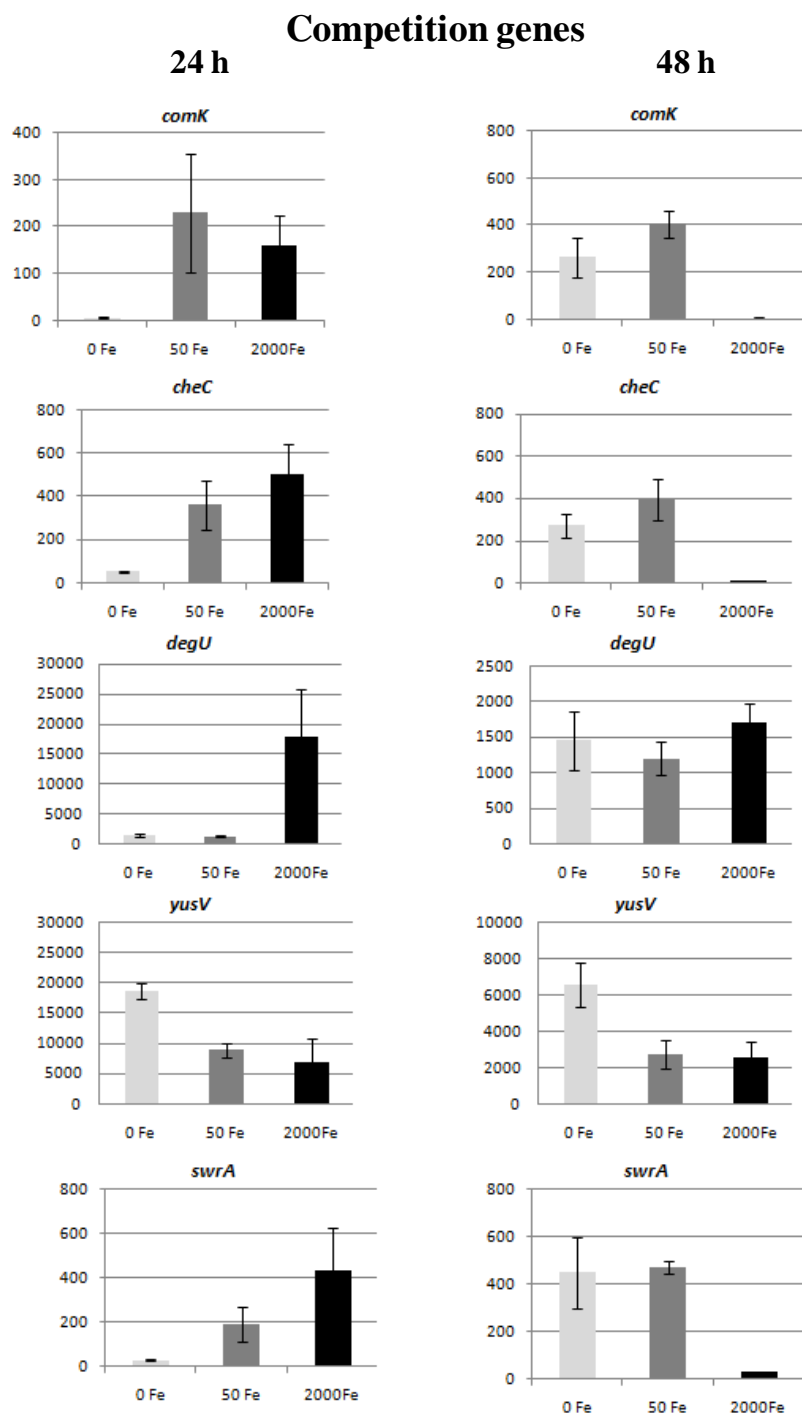
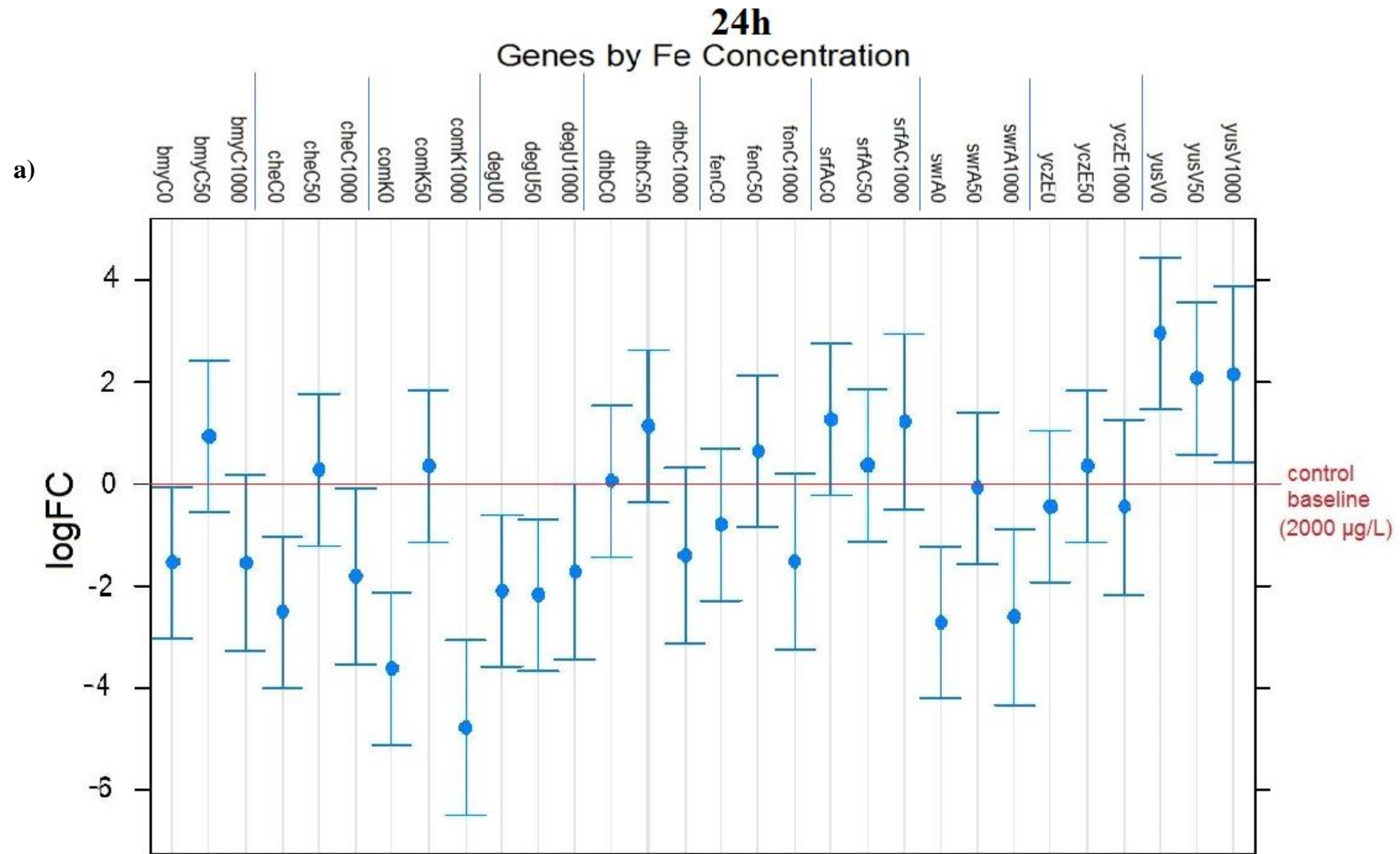


Figure 3.26: RT-qPCR results of differential genes expression of *B. amyloliquefaciens* grown for 24 and 48 hpi in succinate medium at different iron concentrations (0, 50, 2000 $\mu\text{g/L}$). The genes examined concern *B. amyloliquefaciens* competition *comK*: competition; *cheC*: chemotaxis; *degU*: positive regulator of bacillomycin (iturin); *yusV*: Probable siderophore transport system; *swrA*: swarming

Chapter 3: Results



Chapter 3: Results

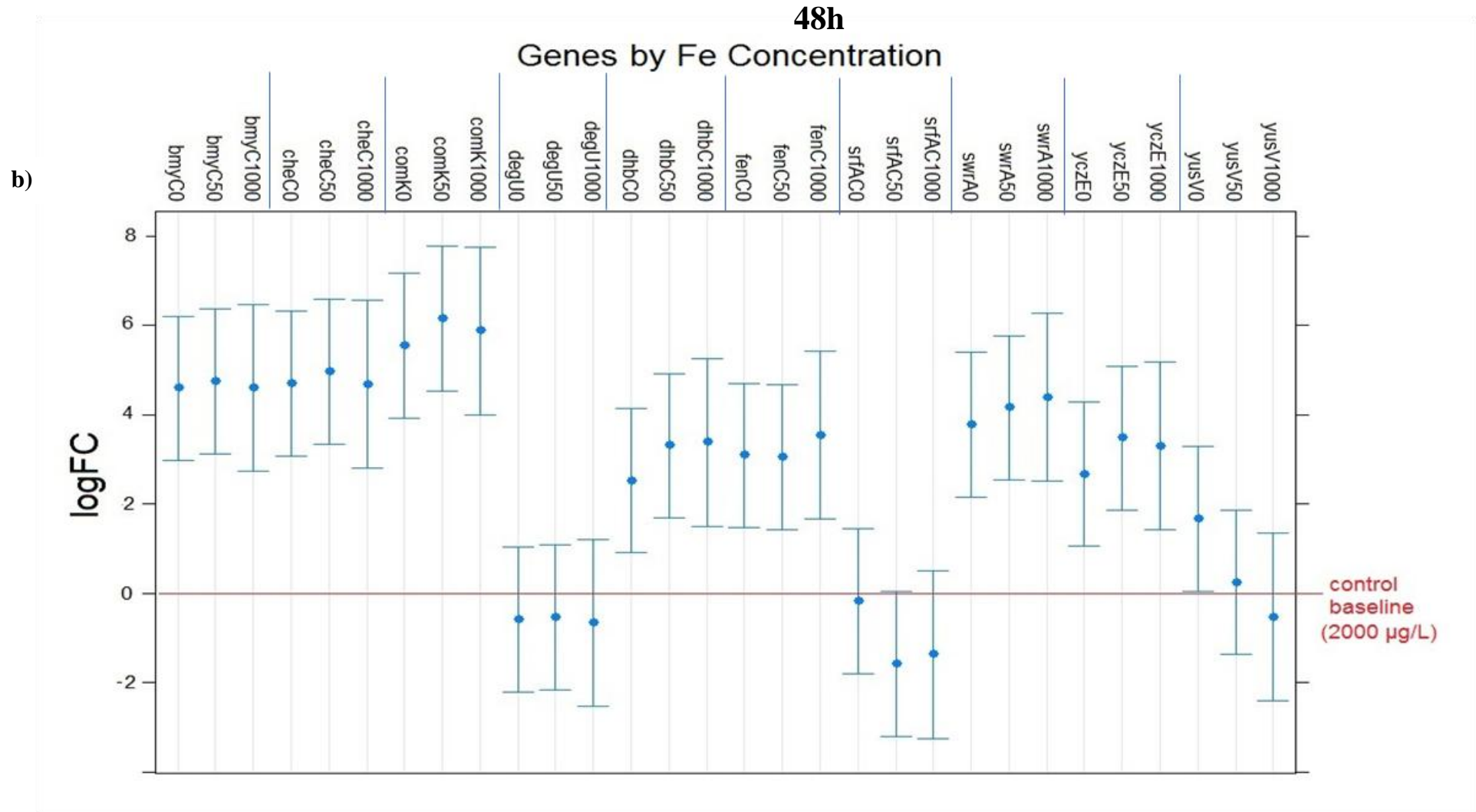


Figure 3.27: RT-qPCR results of differential gene expression of *B. amyloliquefaciens* grown for a) 24h b) 48 hpi in succinate medium at low iron concentrations (0, 50, 1000 µg/L) in comparison to *B. amyloliquefaciens* grown at 2000µg/L Fe. Log Fold Changes (logFC) between each treatment and the reference concentration of 2000 µg / L Fe (red line) were calculated by the implementation of Linear Mixed Models analysis in R using the housekeeping gene *gyrA* as control for normalization (Steibel *et al.* 2009). The genes examined concern a) secondary metabolite synthesis *dhbC*: siderophore synthase; *bmyC*: bacillomycin (iturin) synthase; *yczE*: positive regulator of bacillomycin (iturin) synthesis; *fenC*: fengycin synthase; *sfpAC*: surfactin and b) *B. amyloliquefaciens* competition; *comK*: competition; *cheC*: chemotaxis; *swrA*: swarming; *deqU*: positive regulator of bacillomycin (iturin); *yusV*: probable siderophore transport system. Bars indicate confidence intervals of logFC estimates at the level of 0.95.

DISCUSSION

Siderophores are small, high-affinity iron-chelating compounds synthesized and secreted by bacteria through short, well-defined metabolic pathways in response to iron restriction (Perez-Miranda *et al.* 2007). Many organisms have the ability to utilize siderophores produced by other organisms so called xenosiderophores (Crosa *et al.* 2004). *Bacillus subtilis* produce the catechol siderophore, bacillibactin (Raza *et al.* 2008). Siderophores have been suggested to be an environmentally friendly alternative to hazardous pesticides (Schenk *et al.* 2012). It has been reported that different *Pseudomonas* species can improve plant growth by producing siderophores (pyoverdines) and/or by protecting them from pathogens (Kloepper *et al.* 1980, Gamalero and Glick 2011). The significant role of siderophores in the biological control mechanism was firstly suggested by Kloepper (1980). This mechanism depends on the role of siderophores as competitors for Fe in order to reduce the Fe availability for the phytopathogens (Beneduzi *et al.* 2012). The role of siderophores in biocontrol *in planta* have been mentioned before. (Yu *et al.* 2011) stated that siderophores produced by *Bacillus subtilis* had a significant role in the biocontrol of *F. oxysporum*, which causes the *Fusarium* wilt of pepper. Also, (Verma *et al.* 2011) suggest that siderophores produced by *A. indica* had a high affinity to chelate Fe (III) from soil and thereby negatively affect the growth of several fungal pathogens.

- ***B. amyloliquefaciens* produce and secrete siderophores under iron limited conditions**

B. amyloliquefaciens subsp. *plantarum* UCMB5113 genome contains a gene cluster (*dhbABCDEF*) that is responsible for the synthesis of the iron-siderophore bacillibactin (Miethke *et al.* 2006). *B. amyloliquefaciens* MBI600 genome sequence, which is fully annotated, was found in this study to contain the same gene cluster. The ability to produce and secrete siderophores was confirmed by the CAS assay. The

whole genome has been searched for production of petrobactin, a siderophore that *B. anthracis* and *B. cereus* produce but the gene region *asbAB* was not found.

- ***B. amyloliquefaciens* MBI600 was found to inhibit growth of *Pseudomonas* in agar plates and broth tests under iron limited conditions.**

Inhibition zones formed by *B. amyloliquefaciens* were negatively correlated to iron concentration. Such a phenotype was more evident in the case of *Pto*, where statistically significant differences occurred between treatments of iron deficiency conditions and conditions of high iron concentration. This finding is important considering that MBI600 CFCF, extracted from cultures grown in rich medium, has no antibiotic activity against *Pseudomonas*. On the contrary, it boosts *Pseudomonas sp.* growth probably due to availability of nutrient, amino acids and other organic compounds that are synthesized during the MBI600 cell growth cycle and thus are available at the CFCF. Interestingly, addition of a high CFCF concentration, yielded from cultures grown under iron starvation, reduces in some cases the growth rate of pathogens, suggesting that siderophores might exhibit antibiotic properties. This effect occurred at 48 hpi in the case of *Pta* and 24 hpi in the case of *Pto* (§3.3.2). The combination of agar and broth test results *in vitro*, clearly indicate sensitivity of *Pseudomonas* to MBI600 under iron starvation condition. Since the MBI600 antibiotic arsenal, mainly consisting of lipopeptides, proved insufficient to inhibit *Pseudomonas* grow under antagonism experiments when using a rich iron diet, even when high concentration of crude extract rich in lipopeptides was used, it is concluded that siderophores are responsible for this gain of function. Thus, *in vitro* range of a biological control agent might vary under different nutrition conditions. In fact, since rhizosphere of phyllosphere niches that BCA need to colonize during commercial application often pose an abiotic stress, such as iron depletion. *In vitro* testing in rich medium conditions might undermine the potential of BCA against pathogens in plant inhabitants.

Data from experiments which carried out using a multi-detection microplate reader where optical densities at 600 nm were measured automatically every 30 min, it was found that up to 16 hpi, *Pseudomonas*' growth was not affected in the presence of CFCF. Interestingly, at 16 hpi or when pathogen population growth was deep into the stationary phase, a vertical drop occurred in OD estimates, which was analogous to the concentration of the CFCF. This result can be explained in two ways. One is that siderophores are products of secondary metabolism and thus begin to be produced and secreted in the static phase, and consequently their transport systems, which possibly import xenosiderophores, are also activated. On the other hand, siderophores and their transport system are expressed in low iron concentrations in the environment. Thus, after 16 hours, the available iron in the medium had been consumed, and only then siderophore production and transport systems were activated, again to import xenosiderophores that had an antibiotic effect. Both explanations converge to that *Pseudomonas* siderophores and its xenosiderophore transport system is activated upon

iron depletion and possibly absorbs MBI600 siderophores as xenosiderophores, which in turn can only act inside the cell to do the killing.

- **The effectiveness of CFCF riched under iron limited conditions is also evaluated *in planta***

The hypothesis that pathogen sensitivity to MBI600 might differ under stress conditions was confirmed *in planta*. Growth of MBI600 cultures under iron starvation probably led to a CFCF rich in siderophores that could affect *Pta* artificial inoculation of *N. benthamiana* plants. In specific, *Pta* leaf total population was lower in the case of low Fe concentration CFCF, especially at 0 µg/L one week post inoculation. This was probably due to a significant antibiotic effect upon *Pta* contact with CFCF, as indicated by the significantly lower *Pta* total leaf population 1 dpi. As expected, *Pta* finally recovered 14 dpi, since CFCF was only sprayed once and its effect is local rather than systemic, and thus could not affect pathogens cells that survived the first impact and enter the leaf apoplast. This phenomenon is reflected by the reduction of the severity of symptoms from the disease for a period of at least two weeks in the case of the 0 µg/L concentration and thus the delay in symptom development.

A similar trend was observed during the *in planta* efficacy evaluation of CFCF, yielded from MBI600 cultures grown in the presence of low iron concentration, against *Pto* inoculation of tomato plant. In specific, the strong bactericidal impact that was observed 1 and 4 dpi due to direct contact of *Pto* cells with low Fe CFCF treatments, led to a delay in infection and thus in *Pto* internal population, that was observed even 1 week post inoculation. Bactericidal effects of low Fe CFCF were stronger in the case of *Pto*, compared to *Pta*, and population at 16 dpi was still lower compared to control.

- **Determination of *B. amyloliquefaciens* gene expression in different iron concentrations**

To elucidate the interesting results obtained by *in vitro* and *in planta* experimentation and correlate them with key cell functions of MBI600 genetic competence, an extensive analysis was performed at the molecular level. In detail, modifications (up or down regulation) in levels of *dhbC*, *bmyC*, *fenC*, *sfpAC*, *yczE*, *comK*, *cheC*, *swrA*, *degU* and *yusV* genes involved in biosynthesis and regulation of siderophores or secondary metabolites (acting as antibiotics), as well as in mobility and chemotactism were examined using qPCR. A statistical analysis was carried out by combining all qPCR data from samples taken 24 and 48 hpi from MBI600 liquid medium cultures containing increasing concentrations of iron (Figure 3.27). Low iron diet treatments were compared with the reference concentration of 2000 µg/L Fe, which was found to inhibit transcription of the siderophore biosynthetic pathways. Results suggested that at 48 hpi statistically significant differences among iron treatments occurred in all cases but those of genes *degU* and *srfAC*. In specific, *dhbC*, an isochrorismate synthase of the siderophore synthase operon that was selected as a bacillibactin

synthesis marker gene, was found to be overexpressed in low-iron conditions. This is a reasonable fact, because siderophore synthases are upregulated under low iron concentrations by the ferric uptake regulator protein (Fur), which coordinates the expression of iron uptake and homeostasis pathways in response to available iron (Ollinger *et al.* 2006). In support, *yusV*, a gene involved in siderophore uptake (Baichoo *et al.* 2002) was also overexpressed at 24 hpi in the case of all treatments and at 48 hpi in the case of 0 µg/L Fe, compared to the reference treatment.

Moreover, it seemed that iron starvation co-regulates siderophore and secondary metabolite production. It has been previously shown that production of fengycin, iturin and bacillomycin is advantageous for *B. subtilis* to eliminate competitors in the same habitat, but their production is articulately delayed (late stationary phase) as compared with surfactin (transition between exponential and stationary growth) (Hofemeister *et al.* 2004, Stein 2005). Accordingly, it was found that iron starvation increased expression of surfactin biosynthetic genes at 24 hpi encodes while bacillomycin synthase C (*bmyC*) and fengycin synthase C (*fenC*) gene were overexpressed at 48 hpi.

Surfactin plays a key role in *B. amyloliquefaciens* competence and its activity is controlled by *sfp*. The *B. subtilis* 168 strain carrying a mutation in *sfp* was unable to grow in Fe-starvation medium (Ollinger *et al.* 2006). *Sfp* encodes a phosphopantepheini transferase and post translationally converts inactivate peptides synthetases (including surfactin and other NRPSs) to their active holoenzyme forms (Nakano *et al.* 1992, Finking and Marahiel 2004). Surfactin synthase is required for the cells of *B. subtilis* to become producers of the lipopeptide antibiotics surfactin and lipastatin. In addition, surfactin is necessary but not sufficient for swarming (Kearns *et al.* 2004) and enables biofilm formation in bacilli (Yan *et al.* 2003) and *Pseudomonas aeruginosa* (Davey *et al.* 2003) motility.

It also seems that in iron limited conditions, genes that encodes bacillomycin synthase C (*bmyC*) and fengycin synthase C (*fenC*) overexpressed in comparison to iron sufficient conditions. This suggests that MBI600 appears to induce its offense in order to prevail against other organism in a habitat depleted in iron. This hypothesis is boosted by the increase in iron-limited conditions of the *comK* gene which is also involved in competence. The expression of ComK is considered to boost competition but also enhance fitness (Yuksel *et al.* 2016). It has been proven that the expression of *comk* is extremely low during exponential growth and then rises as a culture approaches the stationary phase of growth (Miras and Dubnau 2016). This fact leads to the conclusion that the results of 48 hpi are the ones that should lead us to conclusions about expression of *comk* in variant iron concentrations and not that of 24 hpi.

The increase in the expression of *yczE* which is a positive regulator of bacillomycin is more likely to be responsible for the overexpression of *bmyC* as mentioned above. In parallel, iron depletion is detected by chemotactism and stimulates motility towards

more favorable conditions, as indicated by overexpression of *cheC* which interacts and regulates methylation of the chemoreceptors and is thought to fine tune the behavioural response in chemotaxis (Kirby *et al.* 2001). In addition overexpression of *swrA*, a gene controlling the number of flagella in liquid environments and the assembly of flagella in response to cell contact with solid surfaces, governing swarming motility, supports that iron depletion stimulates motility, surface or liquid, towards favorable conditions (Kearns *et al.* 2004, Calvio *et al.* 2005)

DegU plays a key role in regulating post-exponential-phase processes in *B. subtilis*, including motility, biofilm formation (Kobayashi 2007, Verhamme *et al.* 2007) and genetic competence (Ogura and Tanaka 1996). The DegS-DegU regulatory system is controlled by *degU* transcription, phosphorylation and DegU-P activity and is thought to function as a 'rheostat' that senses and responds to changes in the environment (Murray *et al.* 2009). Based on its transcription levels in the case for all treatments at 24 and 48 hpi we hypothesize that its function under low iron condition relies in its phosphorylation or DegU-P activity rather than its transcription since its expression has not affected significantly among different Fe treatments.

Future prospects

Important information is still lacking, including the role of siderophores in ISR antibiosis and competence. Because iron is central for many metabolic processes and not easily available, it is the focus of serious competition between organisms. In mammals, there are several examples in which the virulence of infectious bacteria has been correlated to their ability to assimilate host iron through their siderophores (Saha *et al.* 2013). In turn, the host fights back and develops strategies to avoid iron capture by bacteria, highlighting cross-regulatory interactions between iron homeostasis and immune responses (Ong *et al.* 2006, Nairz *et al.* 2014). Similar processes seem to operate in plants. The production of siderophores by pathogenic bacteria was shown to facilitate infection in their hosts, pointing out their role as virulence factors (Franza and Expert 2013). In previous studies treatment of plant tissues or cell suspensions by bacterial siderophores was reported to trigger defense responses in tobacco and *A. thaliana* (van Loon *et al.* 2008, Aznar *et al.* 2014). On the contrary, (Trapet *et al.* 2016) suggested that the physiological incidence and mode of action of pyoverdine from *P. fluorescens* C7R12 on *Arabidopsis thaliana* plants grown under iron-sufficient or -deficient conditions it was investigated. It was suggested that pyoverdine modulated the expression of around 2000 genes including expression of genes related to development and iron acquisition/redistribution while it repressed the expression of defense-related genes. The fact that *B. amyloliquefaciens* strains are important BCA and are thought to elicit plant defense, renders further studies on the role of siderophores on ISR/SAR, competence and antibiosis, necessary.

The antibiotic action of siderophores will be revealed with knock-out of siderophore biosynthetic operon and with the purification of siderophores. The knock out will be used to prove that the reduction in *Pseudomonas* growth both *in vitro* and *in planta* is

Chapter 4:Discussion

due to siderophores antibiotic activity and not a result of other antibiotics overproduction in iron deficient conditions. The purification of siderophores will be used to check the direct antibiotic activity. Finally, the hypothesis that siderophores have antibiotic activity will be tested also in BCA-pathogenic fungi systems.

BIBLIOGRAPHY

Ahmed, E. and S. J. Holmstrom (2014). "Siderophores in environmental research: roles and applications." Microb Biotechnol **7** (3): 196-208.

Anderson, L. M., V. O. Stockwell and J. E. Loper (2004). "An Extracellular Protease of *Pseudomonas fluorescens* Inactivates Antibiotics of *Pantoea agglomerans*." Phytopathology **94** (11): 1228-1234.

Andrews, S. C., A. K. Robinson and F. Rodriguez-Quinones (2003). "Bacterial iron homeostasis." FEMS Microbiol Rev **27** (2-3): 215-237.

Aznar, A., N. W. Chen, M. Rigault, N. Riache, D. Joseph, D. Desmaele, G. Mouille, S. Boutet, L. Soubigou-Taconnat, J. P. Renou, S. Thomine, D. Expert and A. Dellagi (2014). "Scavenging iron: a novel mechanism of plant immunity activation by microbial siderophores." Plant Physiol **164** (4): 2167-2183.

Aznar, A. and A. Dellagi (2015). "New insights into the role of siderophores as triggers of plant immunity: what can we learn from animals?" Journal of Experimental Botany **66** (11): 3001-3010.

Baichoo, N., T. Wang, R. Ye and J. D. Helmann (2002). "Global analysis of the *Bacillus subtilis* Fur regulon and the iron starvation stimulon." Mol Microbiol **45** (6): 1613-1629.

Baker, K. F. (1987). "Evolving concepts of biological control of plant pathogens." Annual Review of Phytopathology **25**: 67-85.

Bartlett, J. M. and D. Stirling (2003). "A short history of the polymerase chain reaction." Methods Mol Biol **226**: 3-6.

Beneduzi, A., A. Ambrosini and L. M. P. Passaglia (2012). "Plant growth-promoting rhizobacteria (PGPR): Their potential as antagonists and biocontrol agents." Genetics and Molecular Biology **35** (4 Suppl): 1044-1051.

Bodilis, J., B. Ghysels, J. Osayande, S. Matthijs, J. P. Pirnay, S. Denayer, D. De Vos and P. Cornelis (2009). "Distribution and evolution of ferripyoverdine receptors in *Pseudomonas aeruginosa*." Environ Microbiol **11** (8): 2123-2135.

Chapter 5: Bibliography

- Branda, S. S., F. Chu, D. B. Kearns, R. Losick and R. Kolter (2006). "A major protein component of the *Bacillus subtilis* biofilm matrix." Mol Microbiol **59** (4): 1229-1238.
- Braun, V. and M. Braun (2002). "Iron transport and signaling in *Escherichia coli*." FEBS Letters **529** (1): 78-85.
- Calvio, C., F. Celandroni, E. Ghelardi, G. Amati, S. Salvetti, F. Cecilian, A. Galizzi and S. Senesi (2005). "Swarming Differentiation and Swimming Motility in *Bacillus subtilis* Are Controlled by *swrA*, a Newly Identified Dicistronic Operon." Journal of Bacteriology **187** (15): 5356-5366.
- Chen, X. H., A. Koumoutsis, R. Scholz, A. Eisenreich, K. Schneider, I. Heinemeyer, B. Morgenstern, B. Voss, W. R. Hess, O. Reva, H. Junge, B. Voigt, P. R. Jungblut, J. Vater, R. Sussmuth, H. Liesegang, A. Strittmatter, G. Gottschalk and R. Borriss (2007). "Comparative analysis of the complete genome sequence of the plant growth-promoting bacterium *Bacillus amyloliquefaciens* FZB42." Nat Biotech **25** (9): 1007-1014.
- Chen, X. H., A. Koumoutsis, R. Scholz, K. Schneider, J. Vater, R. Sussmuth, J. Piel and R. Borriss (2009). "Genome analysis of *Bacillus amyloliquefaciens* FZB42 reveals its potential for biocontrol of plant pathogens." J Biotechnol **140** (1-2): 27-37.
- Choudhary, D. K. and B. N. Johri (2009). "Interactions of *Bacillus* spp. and plants – With special reference to induced systemic resistance (ISR)." Microbiological Research **164** (5): 493-513.
- Choudhary, D. K., A. Prakash and B. N. Johri (2007). "Induced systemic resistance (ISR) in plants: mechanism of action." Indian Journal of Microbiology **47** (4): 289-297.
- Chowdhury, S. P., A. Hartmann, X. Gao and R. Borriss (2015). "Biocontrol mechanism by root-associated *Bacillus amyloliquefaciens* FZB42 – a review." Frontiers in Microbiology **6** (780).
- Cornelis, P. (2010). "Iron uptake and metabolism in pseudomonads." Appl Microbiol Biotechnol **86** (6): 1637-1645.
- Cornelis, P. and J. Bodilis (2009). "A survey of TonB-dependent receptors in fluorescent pseudomonads." Environ Microbiol Rep **1** (4): 256-262.
- Crosa, J. H., A. R. Mey and S. M. Payne (2004). Iron Transport in Bacteria, American Society of Microbiology.
- Cuiv, P. O., P. Clarke and M. O'Connell (2006). "Identification and characterization of an iron-regulated gene, *chtA*, required for the utilization of the xenosiderophores aerobactin, rhizobactin 1021 and schizokinen by *Pseudomonas aeruginosa*." Microbiology **152** (Pt 4): 945-954.
- Das, A., R. Prasad, A. Srivastava, P. H. Giang, K. Bhatnagar and A. Varma (2007). Fungal Siderophores: Structure, Functions and Regulation. Microbial Siderophores. A. Varma and S. B. Chincholkar. Berlin, Heidelberg, Springer Berlin Heidelberg: 1-42.
- Davey, M. E., N. C. Caiazza and A. O'Toole (2003). "Rhamnolipid surfactant production affects biofilm architecture in *Pseudomonas aeruginosa* PAO1." J Bacteriol **185** (3): 1027-1036.

- Davey, M. E. and G. O'Toole, A. (2000). "Microbial biofilms: from ecology to molecular genetics." Microbiol Mol Biol Rev **64** (4): 847-867.
- De Vleeschauwer, D., M. Djavaheri, P. A. Bakker and M. Hofte (2008). "Pseudomonas fluorescens WCS374r-induced systemic resistance in rice against Magnaporthe oryzae is based on pseudobactin-mediated priming for a salicylic acid-repressible multifaceted defense response." Plant Physiol **148** (4): 1996-2012.
- Dean, C. R. and K. Poole (1993). "Cloning and characterization of the ferric enterobactin receptor gene (pfeA) of Pseudomonas aeruginosa." J Bacteriol **175** (2): 317-324.
- Desai, A. and G. Archana (2011). Role of Siderophores in Crop Improvement. Bacteria in Agrobiolgy: Plant Nutrient Management. D. K. Maheshwari. Berlin, Heidelberg, Springer Berlin Heidelberg: 109-139.
- Eisenhauer, H. A., S. Shames, P. D. Pawelek and J. W. Coulton (2005). "Siderophore Transport through Escherichia coli Outer Membrane Receptor FhuA with Disulfide-tethered Cork and Barrel Domains." Journal of Biological Chemistry **280** (34): 30574-30580.
- Elias, S., E. Degtyar and E. Banin (2011). "FvbA is required for vibriobactin utilization in Pseudomonas aeruginosa." Microbiology **157** (Pt 7): 2172-2180.
- Farag, M. A., H. Zhang and C.-M. Ryu (2013). "Dynamic Chemical Communication between Plants and Bacteria through Airborne Signals: Induced Resistance by Bacterial Volatiles." Journal of Chemical Ecology **39** (7): 1007-1018.
- Finking, R. and M. A. Marahiel (2004). "Biosynthesis of nonribosomal peptides1." Annu Rev Microbiol **58**: 453-488.
- Franza, T. and D. Expert (2013). "Role of iron homeostasis in the virulence of phytopathogenic bacteria: an 'a la carte' menu." Mol Plant Pathol **14** (4): 429-438.
- Fukushima, T., B. E. Allred and K. N. Raymond (2014). "Direct Evidence of Iron Uptake by the Gram-Positive Siderophore-Shuttle Mechanism without Iron Reduction." ACS Chemical Biology **9** (9): 2092-2100.
- Fukushima, T., B. E. Allred, A. K. Sia, R. Nichiporuk, U. N. Andersen and K. N. Raymond (2013). "Gram-positive siderophore-shuttle with iron-exchange from Fe-siderophore to apo-siderophore by Bacillus cereus YxeB." Proc Natl Acad Sci U S A **110** (34): 13821-13826.
- Gamalero, E. and B. R. Glick (2011). Mechanisms Used by Plant Growth-Promoting Bacteria. Bacteria in Agrobiolgy: Plant Nutrient Management. D. K. Maheshwari. Berlin, Heidelberg, Springer Berlin Heidelberg: 17-46.
- Ghelardi, E., S. Salvetti, M. Ceragioli, S. A. Gueye, F. Celandroni and S. Senesi (2012). "Contribution of Surfactin and SwrA to Flagellin Expression, Swimming, and Surface Motility in Bacillus subtilis." Applied and Environmental Microbiology **78** (18): 6540-6544.
- Ghysels, B., B. T. Dieu, S. A. Beatson, J. P. Pirnay, U. A. Ochsner, M. L. Vasil and P. Cornelis (2004). "FpvB, an alternative type I ferripyoverdine receptor of Pseudomonas aeruginosa." Microbiology **150** (Pt 6): 1671-1680.
- Ghysels, B., U. Ochsner, U. Mollman, L. Heinisch, M. Vasil, P. Cornelis and S. Matthijs (2005). "The Pseudomonas aeruginosa pirA gene encodes a second receptor

for ferrienterobactin and synthetic catecholates analogues." FEMS Microbiol Lett **246** (2): 167-174.

Gomez-Vasquez, R., R. Day, H. Buschmann, S. Randles, J. R. Beeching and R. M. Cooper (2004). "Phenylpropanoids, phenylalanine ammonia lyase and peroxidases in elicitor-challenged cassava (*Manihot esculenta*) suspension cells and leaves." Ann Bot **94** (1): 87-97.

Haggag, W. M. E. (1999). "Enhancement of suppressive metabolites from *Pseudomonas fluorescens* against tomato damping-off pathogens." AGRIS **2** (1): 1-14.

Hannauer, M., Y. Barda, G. L. Mislin, A. Shanzer and I. J. Schalk (2010). "The ferrichrome uptake pathway in *Pseudomonas aeruginosa* involves an iron release mechanism with acylation of the siderophore and recycling of the modified desferrichrome." J Bacteriol **192** (5): 1212-1220.

Hartney, S. L., S. Mazurier, T. A. Kidarsa, M. C. Quecine, P. Lemanceau and J. E. Loper (2011). "TonB-dependent outer-membrane proteins and siderophore utilization in *Pseudomonas fluorescens* Pf-5." Biometals **24** (2): 193-213.

Heydari, A. and M. Pessarakli (2010). "A review on biological control of fungal plant pathogens using microbial antagonists." Journal of Biological Sciences **10** (4): 273-290.

Hofemeister, J., B. Conrad, B. Adler, B. Hofemeister, J. Feesche, N. Kucheryava, G. Steinborn, P. Franke, N. Grammel, A. Zwintscher, F. Leenders, G. Hitzeroth and J. Vater (2004). "Genetic analysis of the biosynthesis of non-ribosomal peptide- and polyketide-like antibiotics, iron uptake and biofilm formation by *Bacillus subtilis* A1/3." Mol Genet Genomics **272** (4): 363-378.

Hotta, K., C. Y. Kim, D. T. Fox and A. T. Koppisch (2010). "Siderophore-mediated iron acquisition in *Bacillus anthracis* and related strains." Microbiology **156** (Pt 7): 1918-1925.

Hsieh, E. J. and B. M. Waters (2016). "Alkaline stress and iron deficiency regulate iron uptake and riboflavin synthesis gene expression differently in root and leaf tissue: implications for iron deficiency chlorosis." J Exp Bot **67** (19): 5671-5685.

Ippolito, A. and F. Nigro (2000). "Impact of preharvest application of biological control agents on postharvest diseases of fresh fruits and vegetables." Crop Protection **19** (8-10): 715-723.

Kearns, D. B., F. Chu, R. Rudner and R. Losick (2004). "Genes governing swarming in *Bacillus subtilis* and evidence for a phase variation mechanism controlling surface motility." Mol Microbiol **52** (2): 357-369.

Kessmann, H., T. Staub, C. Hofmann, T. Maetzke, J. Herzog, E. Ward, S. Uknes and J. Ryals (1994). "Induction of systemic acquired disease resistance in plants by chemicals." Annu Rev Phytopathol **32**: 439-459.

Kirby, J. R., C. J. Kristich, M. M. Saulmon, M. A. Zimmer, L. F. Garrity, I. B. Zhulin and G. W. Ordal (2001). "CheC is related to the family of flagellar switch proteins and acts independently from CheD to control chemotaxis in *Bacillus subtilis*." Mol Microbiol **42** (3): 573-585.

- Kloepper, J. W., J. Leong, M. Teintze and M. N. Schroth (1980). "Enhanced plant growth by siderophores produced by plant growth-promoting rhizobacteria." Nature **286** (5776): 885-886.
- Kobayashi, K. (2007). "Gradual activation of the response regulator DegU controls serial expression of genes for flagellum formation and biofilm formation in *Bacillus subtilis*." Mol Microbiol **66** (2): 395-409.
- Koebnik, R. (2005). "TonB-dependent trans-envelope signalling: the exception or the rule?" Trends Microbiol **13** (8): 343-347.
- Koumoutsis, A., X.-H. Chen, A. Henne, H. Liesegang, G. Hitzeroth, P. Franke, J. Vater and R. Borriss (2004). "Structural and Functional Characterization of Gene Clusters Directing Nonribosomal Synthesis of Bioactive Cyclic Lipopeptides in *Bacillus amyloliquefaciens* Strain FZB42." Journal of Bacteriology **186** (4): 1084-1096.
- Krewulak, K. D. and H. J. Vogel (2008). "Structural biology of bacterial iron uptake." Biochim Biophys Acta **1778** (9): 1781-1804.
- Kumar, A., A. Prakash and B. N. Johri (2011). *Bacillus as PGPR in Crop Ecosystem. Bacteria in Agrobiolgy: Crop Ecosystems*. D. K. Maheshwari. Berlin, Heidelberg, Springer Berlin Heidelberg: 37-59.
- Llamas, M. A., F. Imperi, P. Visca and I. L. Lamont (2014). "Cell-surface signaling in *Pseudomonas*: stress responses, iron transport, and pathogenicity." FEMS Microbiol Rev **38** (4): 569-597.
- Llamas, M. A., M. J. Mooij, M. Sparrius, C. M. Vandenbroucke-Grauls, C. Ratledge and W. Bitter (2008). "Characterization of five novel *Pseudomonas aeruginosa* cell-surface signalling systems." Mol Microbiol **67** (2): 458-472.
- Llamas, M. A., M. Sparrius, R. Kloet, C. R. Jimenez, C. Vandenbroucke-Grauls and W. Bitter (2006). "The heterologous siderophores ferrioxamine B and ferrichrome activate signaling pathways in *Pseudomonas aeruginosa*." J Bacteriol **188** (5): 1882-1891.
- Logan, N. A. and P. D. Vos (2015). *Bergey's Manual of Systematics of Archaea and Bacteria*, John Wiley & Sons, Ltd.
- Ma, J. F. (2005). "Plant Root Responses to Three Abundant Soil Minerals: Silicon, Aluminum and Iron." Critical Reviews in Plant Sciences **24** (4): 267-281.
- Marshall, B., A. Stintzi, C. Gilmour, J. M. Meyer and K. Poole (2009). "Citrate-mediated iron uptake in *Pseudomonas aeruginosa*: involvement of the citrate-inducible FecA receptor and the FeoB ferrous iron transporter." Microbiology **155** (Pt 1): 305-315.
- May, J. J., T. M. Wendrich and M. A. Marahiel (2001). "The *dhb* operon of *Bacillus subtilis* encodes the biosynthetic template for the catecholic siderophore 2,3-dihydroxybenzoate-glycine-threonine trimeric ester bacillibactin." J Biol Chem **276** (10): 7209-7217.
- Mettrick, K. A. and I. L. Lamont (2009). "Different roles for anti-sigma factors in siderophore signalling pathways of *Pseudomonas aeruginosa*." Mol Microbiol **74** (5): 1257-1271.

Chapter 5: Bibliography

- Meziane, H., V. D. S. I, V. A. N. L. LC, M. Hofte and P. A. Bakker (2005). "Determinants of *Pseudomonas putida* WCS358 involved in inducing systemic resistance in plants." Mol Plant Pathol **6** (2): 177-185.
- Miethke, M., O. Klotz, U. Linne, J. J. May, C. L. Beckering and M. A. Marahiel (2006). "Ferri-bacillibactin uptake and hydrolysis in *Bacillus subtilis*." Mol Microbiol **61** (6): 1413-1427.
- Miethke, M. and M. A. Marahiel (2007). "Siderophore-Based Iron Acquisition and Pathogen Control." Microbiology and Molecular Biology Reviews **71** (3): 413-451.
- Miras, M. and D. Dubnau (2016). "A DegU-P and DegQ-Dependent Regulatory Pathway for the K-state in *Bacillus subtilis*." Frontiers in Microbiology **7** (1868).
- Moyne, A. L., T. E. Cleveland and S. Tuzun (2004). "Molecular characterization and analysis of the operon encoding the antifungal lipopeptide bacillomycin D." FEMS Microbiol Lett **234** (1): 43-49.
- Murray, E. J., T. B. Kiley and N. R. Stanley-Wall (2009). "A pivotal role for the response regulator DegU in controlling multicellular behaviour." Microbiology **155** (Pt 1): 1-8.
- Nairz, M., D. Haschka, E. Demetz and G. Weiss (2014). "Iron at the interface of immunity and infection." Front Pharmacol **5**: 152.
- Nakano, M. M., N. Corbell, J. Besson and P. Zuber (1992). "Isolation and characterization of *sfp*: a gene that functions in the production of the lipopeptide biosurfactant, surfactin, in *Bacillus subtilis*." Molecular and General Genetics MGG **232** (2): 313-321.
- Neilands, J. B. (1995). "Siderophores: structure and function of microbial iron transport compounds." J Biol Chem **270** (45): 26723-26726.
- Niazi, A., S. Manzoor, S. Asari, S. Bejai, J. Meijer and E. Bongcam-Rudloff (2014). "Genome Analysis of *Bacillus amyloliquefaciens* Subsp. *plantarum* UCMB5113: A Rhizobacterium That Improves Plant Growth and Stress Management." PLOS ONE **9** (8): e104651.
- Nishikiori, T., H. Naganawa, Y. Muraoka, T. Aoyagi and H. Umezawa (1986). "Plipastatins: new inhibitors of phospholipase A2, produced by *Bacillus cereus* BMG302-ff67. III. Structural elucidation of plipastatins." J Antibiot (Tokyo) **39** (6): 755-761.
- Ogura, M. and T. Tanaka (1996). "*Bacillus subtilis* DegU acts as a positive regulator for *comK* expression." FEBS Lett **397** (2-3): 173-176.
- Ollinger, J., K.-B. Song, H. Antelmann, M. Hecker and J. D. Helmann (2006). "Role of the Fur Regulon in Iron Transport in *Bacillus subtilis*." Journal of Bacteriology **188** (10): 3664-3673.
- Ong, S. T., J. Z. Ho, B. Ho and J. L. Ding (2006). "Iron-withholding strategy in innate immunity." Immunobiology **211** (4): 295-314.
- Pal B and M. Gardener (2006). Biological Control of Plant Pathogens.
- Perez-Miranda, S., N. Cabirol, R. George-Tellez, L. S. Zamudio-Rivera and F. J. Fernandez (2007). "O-CAS, a fast and universal method for siderophore detection." J Microbiol Methods **70** (1): 127-131.

- Pieterse, C. M. J., J. A. Van Pelt, S. C. M. Van Wees, J. Ton, K. M. Léon-Kloosterziel, J. J. B. Keurentjes, B. W. M. Verhagen, M. Knoester, I. Van der Sluis, P. A. H. M. Bakker and L. C. Van Loon (2001). "Rhizobacteria-mediated Induced Systemic Resistance: Triggering, Signalling and Expression." European Journal of Plant Pathology **107** (1): 51-61.
- Priest, F. G., M. Goodfellow, L. A. Shute and R. C. W. Berkeley (1987). "Bacillus amyloliquefaciens sp. nov., nom. rev." International Journal of Systematic and Evolutionary Microbiology **37** (1): 69-71.
- Quadri, L. E. N. (2000). "Assembly of aryl-capped siderophores by modular peptide synthetases and polyketide synthases." Molecular Microbiology **37** (1): 1-12.
- Raaska, L., L. Viikari and T. Mattila-Sandholm (1993). "Detection of siderophores in growing cultures of Pseudomonas spp." Journal of Industrial Microbiology **11** (3): 181-186.
- Raymond, K. N. and E. A. Dertz (2004). Biochemical and Physical Properties of Siderophores. Iron Transport in Bacteria, American Society of Microbiology.
- Raza, W., H. Wu, M. A. A. Shah and Q. Shen (2008). "Retracted: A catechol type siderophore, bacillibactin: biosynthesis, regulation and transport in Bacillus subtilis." Journal of Basic Microbiology **48** (2): n/a-n/a.
- Reva, O. N., C. Dixelius, J. Meijer and F. G. Priest (2004). "Taxonomic characterization and plant colonizing abilities of some bacteria related to Bacillus amyloliquefaciens and Bacillus subtilis." FEMS Microbiol Ecol **48** (2): 249-259.
- Romero, D., A. Perez-Garcia, J. W. Veening, A. de Vicente and O. P. Kuipers (2006). "Transformation of undomesticated strains of Bacillus subtilis by protoplast electroporation." J Microbiol Methods **66** (3): 556-559.
- Romero, D., H. Vlamakis, R. Losick and R. Kolter (2011). "An Accessory Protein Required for Anchoring and Assembly of Amyloid Fibers in B. subtilis Biofilms." Molecular microbiology **80** (5): 1155-1168.
- Rowland, B. M. and H. W. Taber (1996). "Duplicate isochorismate synthase genes of Bacillus subtilis: regulation and involvement in the biosyntheses of menaquinone and 2,3-dihydroxybenzoate." Journal of Bacteriology **178** (3): 854-861.
- Ryu, C.-M., M. A. Farag, C.-H. Hu, M. S. Reddy, J. W. Kloepper and P. W. Paré (2004). "Bacterial Volatiles Induce Systemic Resistance in Arabidopsis." Plant Physiology **134** (3): 1017-1026.
- Saha, R., N. Saha, R. S. Donofrio and L. L. Bestervelt (2013). "Microbial siderophores: a mini review." J Basic Microbiol **53** (4): 303-317.
- Sahoo, R. a. (2015). "Iron is an essential micronutrient for plant growth. ." Reviews in Agricultural Science, **3**: 1-24.
- Sbailhat, L., K. Takeyama, T. Koga, D. Takemoto and K. Kawakita (2015). "Induced Resistance in Solanum lycopersicum by Algal Elicitor Extracted from Sargassum fusiforme." The Scientific World Journal **2015**: 870520.
- Schenk, P. M., L. C. Carvalhais and K. Kazan (2012). "Unraveling plant-microbe interactions: can multi-species transcriptomics help?" Trends Biotechnol **30** (3): 177-184.

- Schwyn, B. and J. B. Neilands (1987). "Universal chemical assay for the detection and determination of siderophores." Anal Biochem **160** (1): 47-56.
- Shanahan, P., D. J. O'Sullivan, P. Simpson, J. D. Glennon and F. O'Gara (1992). "Isolation of 2,4-Diacetylphloroglucinol from a Fluorescent Pseudomonad and Investigation of Physiological Parameters Influencing Its Production." Applied and Environmental Microbiology **58** (1): 353-358.
- Sharma, R. R., D. Singh and R. Singh (2009). "Biological control of postharvest diseases of fruits and vegetables by microbial antagonists: A review." Biological Control **50** (3): 205-221.
- Steibel, J. P., R. Poletto, P. M. Coussens and G. J. M. Rosa (2009). "A powerful and flexible linear mixed model framework for the analysis of relative quantification RT-PCR data." Genomics **94** (2): 146-152.
- Stein, T. (2005). "Bacillus subtilis antibiotics: structures, syntheses and specific functions." Mol Microbiol **56** (4): 845-857.
- Sticher, L., B. Mauch-Mani and J. P. Metraux (1997). "Systemic acquired resistance." Annu Rev Phytopathol **35**: 235-270.
- Thimon, L., F. Peypoux, J. Wallach and G. Michel (1995). "Effect of the lipopeptide antibiotic, iturin A, on morphology and membrane ultrastructure of yeast cells." FEMS Microbiol Lett **128** (2): 101-106.
- Thomashow, L. S., D. M. Weller, R. F. Bonsall and L. S. Pierson (1990). "Production of the antibiotic phenazine-1-carboxylic Acid by fluorescent pseudomonas species in the rhizosphere of wheat." Appl Environ Microbiol **56** (4): 908-912.
- Trapet, P., L. Avoscan, A. Klinguer, S. Pateyron and S. Citerne (2016). "The Pseudomonas fluorescens Siderophore Pyoverdine Weakens Arabidopsis thaliana Defense in Favor of Growth in Iron-Deficient Conditions." **171** (1): 675-693.
- Traxler, M. F., M. R. Seyedsayamdost, J. Clardy and R. Kolter (2012). "Interspecies modulation of bacterial development through iron competition and siderophore piracy." Mol Microbiol **86** (3): 628-644.
- Uknes, S., B. Mauch-Mani, M. Moyer, S. Potter, S. Williams, S. Dincher, D. Chandler, A. Slusarenko, E. Ward and J. Ryals (1992). "Acquired resistance in Arabidopsis." Plant Cell **4** (6): 645-656.
- van Loon, L. C., P. A. Bakker, W. H. van der Heijdt, D. Wendehenne and A. Pugin (2008). "Early responses of tobacco suspension cells to rhizobacterial elicitors of induced systemic resistance." Mol Plant Microbe Interact **21** (12): 1609-1621.
- Verhamme, D. T., T. B. Kiley and N. R. Stanley-Wall (2007). "DegU co-ordinates multicellular behaviour exhibited by Bacillus subtilis." Mol Microbiol **65** (2): 554-568.
- Verma, V. C., S. K. Singh and S. Prakash (2011). "Bio-control and plant growth promotion potential of siderophore producing endophytic Streptomyces from Azadirachta indica A. Juss." J Basic Microbiol **51** (5): 550-556.
- Yakoby, N., R. Zhou, I. Kobiler, A. Dinoor and D. Prusky (2001). "Development of Colletotrichum gloeosporioides Restriction Enzyme-Mediated Integration Mutants as Biocontrol Agents Against Anthracnose Disease in Avocado Fruits." Phytopathology **91** (2): 143-148.

Yan, L., K. G. Boyd, D. R. Adams and J. G. Burgess (2003). "Biofilm-Specific Cross-Species Induction of Antimicrobial Compounds in Bacilli." Applied and Environmental Microbiology **69** (7): 3719-3727.

Yan, Z., M. S. Reddy, C. M. Ryu, J. A. McInroy, M. Wilson and J. W. Kloepper (2002). "Induced systemic protection against tomato late blight elicited by plant growth-promoting rhizobacteria." Phytopathology **92** (12): 1329-1333.

Yu, X., C. Ai, L. Xin and G. Zhou (2011). "The siderophore-producing bacterium, *Bacillus subtilis* CAS15, has a biocontrol effect on *Fusarium* wilt and promotes the growth of pepper." European Journal of Soil Biology **47** (2): 138-145.

Yue, W. W., S. Grizot and S. K. Buchanan (2003). "Structural evidence for iron-free citrate and ferric citrate binding to the TonB-dependent outer membrane transporter FecA." J Mol Biol **332** (2): 353-368.

Yuksel, M., J. J. Power, J. Ribbe, T. Volkmann and B. Maier (2016). "Fitness Trade-Offs in Competence Differentiation of *Bacillus subtilis*." Front Microbiol **7**: 888.

Zawadzka, A. M., R. J. Abergel, R. Nichiporuk, U. N. Andersen and K. N. Raymond (2009). "Siderophore-mediated iron acquisition systems in *Bacillus cereus*: Identification of receptors for anthrax virulence-associated petrobactin." Biochemistry **48** (16): 3645-3657.

Zhang, N., D. Yang, D. Wang, Y. Miao, J. Shao, X. Zhou, Z. Xu, Q. Li, H. Feng, S. Li, Q. Shen and R. Zhang (2015). "Whole transcriptomic analysis of the plant-beneficial rhizobacterium *Bacillus amyloliquefaciens* SQR9 during enhanced biofilm formation regulated by maize root exudates." BMC Genomics **16**: 685.

Zhang, Z., Z. T. Ding, D. Shu, D. Luo and H. Tan (2015). "Development of an efficient electroporation method for iturin A-producing *Bacillus subtilis* ZK." Int J Mol Sci **16** (4): 7334-7351.